University of California

Santa Barbara

The Basic Attractor of the Viscous Moore-Greitzer Equation

A Dissertation submitted in partial satisfaction

of the requirement for the degree of

Doctor of Philosophy

in

Mathematics

by

Höskuldur Ari Hauksson

Committee in charge:

Professor Björn Birnir, Chairperson

Professor Xu-Dong Liu

Professor Igor Mezić

Professor Gustavo Ponce

Professor Thomas C. Sideris

December 1998

The dissertation of Höskuldur Ari Hauksson is approved

Committee Chairperson

December 1998

Acknowledgements

There are many people to whom I am greatly endebted after my four years at the University of California, Santa Barbara. First I would like to thank my thesis advisor, Björn Birnir, for his guidence and help throughout my whole stay here. I feel that I have benefited from his vision and his fearless way of thinking about new problems. I thank Igor Mezić for guiding me through the literature on jet engines and for many fruitful discussions about our subject and the world. I owe much to my discussions with him and Andrzej Banaszuk, who also has taught me the value of stubbornness in rockclimbing. I want to thank Petar Kokotović for his guidence and support and for his efforts to keeping me honest with respect to his field. It is due to him that I have been able to catch a glimpse into the world of control theory. I thank Zari Rachev for guiding me into the new field of financial mathematics. I feel that I have been infected by his enthusiasm for this exciting subject.

There are many more who have influenced me and of those I would like to mention Tom Sideris, Gustavo Ponce, Mike Crandall, Xu-dong Liu, Trent Walker and John Hauser, all of whom were willing to sit down with me and ponder various problems I had on my mind. I would further like to thank the staff of the math department, in particular Karen Whitney and Mike Tucker, for their help and support.

Lastly I would like to thank my family for their encouragements and support which has been valuable to me. I want to thank my friends, in particular, Holger and Jenny, Frank, Mike and Asa, Volkan, the guys in the CCEC lab and my friends in the math department for being there and be willing to lend a sympathetic ear when I needed it. Thank you all.

Acknowledgement of Support

I would like to acknowledge the financial support that I have received from a number of institutions during my studies. I want to thank the support of AFSOR under grant number F49620-95-1-0409. This work has also been supported by Nýsköpunarsjódur Námsmanna, by a LACOR grant number 4157U0015-3A from Los Alamos National Laboratory and by NSF under grant number DMS-9704874. Equipment were funded by NSF under grants number DMS-9628606 and PHY-9601954. Lastly I would like to thank the University of California at Santa Barbara for giving me teaching assistant positions and tuition waivers when those were needed.

Vita

June 17, 1969: Born - Reykjavik, Iceland

1992: Carpenter, Fjölbrautarskólinn í Breidholti

1994: B.S. Physics, University of Iceland

1994: B.S. Mathematics, University of Iceland

1996: M.S. Mathematics, University of California, Santa Barbara

1998: Ph.D. Mathematics, University of California, Santa Barbara

Publications

- A. Banaszuk, H.A. Hauksson and I. Mezić. A backstepping controller for a nonlinear partial differential equation model of compression system instabilities. *SIAM Journal of Control and Optimization, 1998.*

- B. Birnir and H.A. Hauksson. Finite dimensional attractor of the Moore-Greitzer equation. *SIAM Journal of Applied Mathematics, 1998.*

- B. Birnir and H.A. Hauksson. The basic attractor of the viscous Moore-Greitzer equation. *Submitted, 1998.*

- B. Birnir and H.A. Hauksson. The low-dimensional flow on the basic attractor of the viscous Moore-Greitzer equation. *Submitted, 1998.*

- B. Birnir and H.A. Hauksson. The basic control for the viscous Moore-Greitzer equation. *Submitted, 1998.*

- H.A. Hauksson and S.T. Rachev. The GARCH-stable option pricing model. *Preprint, 1998.*

- H.A. Hauksson and S.T. Rachev. On the smile, mispricing and valuation at risk in the context of the GARCH-stable asset return model. *Preprint, 1998.*

Abstract

The Basic Attractor of the Viscous Moore-Greitzer Equation

by

Höskuldur Ari Hauksson

The operation of a jet engine is described and a number of current research areas outlined. An equation for the three dimensional air flow through jet engine compression systems is derived. This equation is reduced to a parabolic nonlinear nonlocal equation on the unit circle coupled with two ordinary differential equations. It is proven that this evolution equation, called the viscous Moore Greitzer (vMG) equation, has a unique solution.

The existence of a global attractor for the vMG equation is proven and a bound for the Hausdorff and fractal dimensions of the attractor established. The basic attractor is defined and it is shown that the basic attractor of the vMG equation consists of design flow, surge and stall. Explicit solutions for stall are found and their stability analyzed analytically as well as numerically. The global attractor is constructed for a certain parameter range.

A low order model which captures the flow on the basic attractor is constructed and simulations of this model compared with simulations of the vMG equation. Numerical results indicate that this model captures quantitatively as well as qualitatively the essential dynamics of the PDE model. Some extensions of this low order model are discussed.

Attractor controllability and basic controllability are defined. It is confirmed that in the linearized viscous Moore-Greitzer model stall disturbances are uncontrollable by throttle control. Basic control is defined and a basic throttle control is constructed for the vMG equation. The performance of this control is compared numerically to a backstepping control construction by A. Banaszuk, the author and I. Mezić. These numerical results indicate clearly that the basic control, by utilizing the asymptotic dynamics of the equation, requires much less control effort. It is shown that the vMG equation is not basically controllable with throttle control, but if one in addition has nonaxisymmetric control, then it is basically controllable.

Contents

List of Figures

Chapter 1

Introduction

In recent years a lot of attention has been devoted to the study of air flow through turbomachines. These machines have a wide range of applications, but are most common as jet engines, propelling the majority of modern day aircrafts. Other applications include tanks, submarines and natural gas pumps in pipelines. The main reason for this interest in turbomachines is due to the fact that when the machine operates close to its optimal operating parameter values, the flow can become unstable. These instabilities put a large stress on the engine and in some cases the engine needs to be turned off in order to recover original operation. For this reason turbomachines are currently operated away from their optimal operating parameter values. We will in what follows focus our attention on jet engines.

A jet engine, see Figure 1.1, is composed of four main parts. First there is the *compressor*, where the incoming air is compressed by alternating rings of rotating blades and stationary blades. On Figure 1.1 this is marked as LPC group or low pressure compressor group and HPC or high pressure compressor group. The second main part is the combustion chamber or the *plenum*, marked diffuser and combustor group on Figure 1.1. There the air is mixed with fuel and this compressed mixture

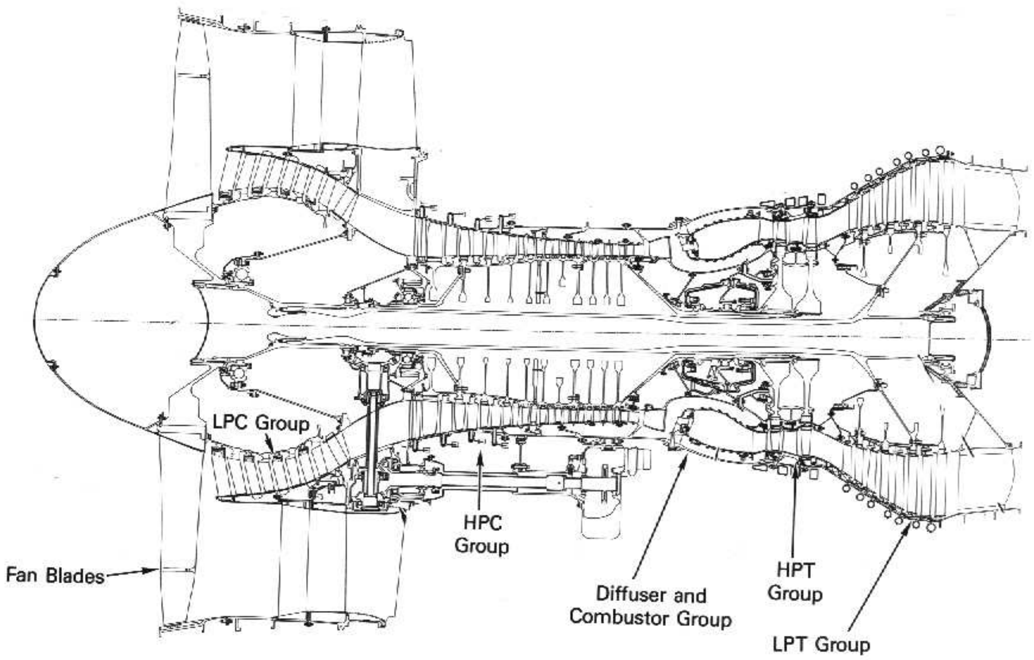

Figure 1.1: *The inside of a jet engine.*

ignited. As a result the pressure rises dramatically and the air rushes through the third main part, which is the *turbine*, marked HPT group or high pressure turbine group and LPT or low pressure turbine group on Figure 1.1. These three parts are refered to as the *compression system.* The turbine extracts energy from the flow which is used to drive the compressor and also to turn the *fan* at the front. The fan is the fourth main part of the engine. In commercial aircraft jet engines the fan generates most of the thrust that the engine produces.

In a complex machine like a jet engine there are many things that must be kept under control. The airflow can exhibit various undesirable behaviors, components of the engine can start to vibrate and overheat and the burning of the fuel in the plenum can become unstable. Ever since the first jet engine was made, scientists have been trying improve the performace of the engines by increasing fuel efficiency, making lighter engines, increasing the thrust it delivers and improving their stability and safety. Current jet engine research is focused on a number of different areas, most notably on stall and surge suppression, flutter suppression and improving the efficiency and stability of the combustion. These areas are described briefly here below.

1.0.1 Surge and Stall

There are primarily two types of instabilities that occur in the airflow through the compression system. They are called *surge* and *stall*. Surge is characterized by large oscillations of the mean mass flow through the compression system. During part of the cycle, the mean mass flow may become reversed, thrusting air out the front of the compressor. This puts a large stress on the components of the engine and seriously impairs its performance. When stall occurs, there are regions of relatively low air flow that form at isolated locations around the rim of the compressor. Here too, the phenomenon can be so pronounced that the flow in these isolated regions is reversed. Again this causes a large stress on the components of the engine and reduces its performance. Both of these instabilities are very severe and have caused aircrafts to crash. They can be triggered by a number of things, this includes birds that can get sucked into the engine and turbulent or distorted flow that can enter the engine when the airplane flies through the turbulent wake of another aircraft or the angle of attack of the air into the engine becomes too large.

When the engine is operating close to its optimal parameter values it is more sensitive to disturbances and prone to going into surge and stall. Many modern day jet engines operate far away from their optimal parameter values for the added stability and security. Much effort has been put into trying to stabilize the flow closer to the optimal parameter values. Surge and stall do, however, still occur and consequently a good mechanism for recovering original operation of the engine, after such a disturbance has set in, is needed. To facilitate this, a better understanding of the behaviour of the air flow during stall and surge is necessary. The purpose of this thesis is to analyze the flow during surge and stall and to invent ways of recovering original operation in an efficient way.

Moore and Greitzer [59] published in 1986 a PDE model for two dimensional airflow disturbances in turbomachines which has been very successful at predicting qualitatively the behavior of the airflow during surge and stall. A substantial amount of work has been done on finite Galerkin approximations of that model since, see e.g. [56] [38] [53] and references therein. Good quantitative description of stall has, however, until now not been given. In 1993 Adomaitis and Abed [2] suggested to include a viscosity term in the model of Moore and Greitzer. They did, however, not offer any justification for including this term.

Currently Mezić [57] has derived a model of the three dimensional flow in jet engine compressors. His model reduces to a special case of the model considered by Adomaitis and Abed when one assumes that the dependence of the flow on the radial direction is negligable. Among other things, Mezić proves that under certain assumptions the flow through the compression system is indeed two dimensional as was assumed by Moore and Greitzer. He also gave the viscous term a new and better interpretation. The term is not due to the viscosity of the air, but rather, it is a diffusion term due to the inviscid process of turbulent momentum transport via Reynolds stresses.

Much research effort has been focused on constructing control methods for recovering normal operation of the engine after a large disturbance occurs. The majority of this effort, see [5] [7] [26] [35] [43] [44] [45] [48] [68], has been focused on low order Galerkin projections of the Moore-Greitzer model. One exception is Banaszuk, Hauksson and Mezić [4] where they constructed a backstepping control law for the Moore-Greitzer partial differential equation.

1.0.2 Flutter

Flutter is characterized by the vibration of the blades in the compressor or in the fan and the interaction of this vibration with the air flow. This is a very complex phenomenon because modern fan and compressor blades resemble twisted and bent plate-like objects whose cross sections vary from root to tip. The blades are mounted on a structure which can be elastic and this structure must therefore be included in the analysis of the vibration. The aerodynamic loading of the blades and centrifugal forces play a large role and to complicate things even further, small beams, called shrouds, are fixed on the blades to push against neighboring blades to impede the oscillation. The motion of individual blades is coupled to the other blades through the elastic structure and through the induced unsteady motion of the air flow.

Earlier results assumed that more than one vibrational mode needed to be included in the analysis of flutter [8] [9] [71] [72]. In particular, they assumed that torsional and bending vibrations needed to be included in the analysis. Later research has made the simplifying assumption that there is only one vibrational mode important for the blades and this mode may include both rotation and bending of the blade. Experimental results tend to support this assumption [27].

A second simplification many authors have made, is to represent the blade by a "typical" section and hence arrive at a two dimensional cascade model [1]. Furthermore, most of the analytical results on flutter have used a linear theory for the air flow. More recently some progress has been made in implementing fully nonlinear models on computers to predict flutter behavior. Experimental support of these models is still insufficient and analytical results remain scarce. For a comprehensive overview of contemporary flutter research see Försching [27] and the two volumes of the AGARD Manual on Aeroelasticity in Axial-Flow Turbomachines [60].

For completeness, we include here the equations of a flutter model derived by Gysling, Myers and Nett [32]. They used the typical section assumption and considered engines with rigid stators and flexible rotors. Furthermore, they assumed that there exist two smooth functions $q(t,\theta)$ and $\alpha(t,\theta)$ that measure the bend and twist respectively of a rotor blade located at angle θ. The aerodynamic forces acting on the blade F and the momentum transfer to the blade M influence q and α in the following way

$$\begin{aligned} F &= \frac{\partial^2 q}{\partial \tau^2} + (\xi_{ea} - \xi_{cg}) c \frac{\partial^2 \alpha}{\partial \tau^2} + k_{11} \frac{\partial q}{\partial \tau} + k_{12} q \\ M &= \frac{\partial^2 \alpha}{\partial \tau^2} + \frac{c(\xi_{ea} - \xi_{cg})}{c^2(\xi_{ea} - \xi_{cg})^2 + \epsilon^2 c^2} \frac{\partial^2 q}{\partial \tau^2} + k_{21} \frac{\partial \alpha}{\partial \tau} + k_{12} \alpha. \end{aligned}$$

Here k_{ij}, ϵ and c are constants, ξ_{ea} and ξ_{cg} measure the position of the elastic axis and the center of gravity respectively and τ is a normalized time.

The force and momentum couple the unsteady blade motion with the motion of the air flow

$$F = f_1(\phi) + f_2(\phi) \frac{\partial q}{\partial \theta}$$

where f_1 and f_2 depend only on the flow which is denoted by ϕ and

$$M = c(\xi_{ea} - \xi_{cg})F.$$

The air flow through the engine is then modeled by the Moore-Greitzer model which will be described in Chapter 2.

1.0.3 Combustion Instabilities

The term combustion instability, although descriptive, is rather misleading. What it refers to is not an instability of the burning process itself, but rather of the whole combustion system. The combustion process is the largest source of energy for the system, but the instabilities involve the combusting agents and the combustion products which form the medium that supports the unsteady motions. The fluctuations in the plenum can often reach sufficient amplitudes to cause excessive rates of heat transfer to exposed surfaces and unacceptable structural vibrations. This can in extreme cases lead to the failure of the engine.

The majority of the research effort to date has been focused on experimental and analytical work. A large part of the experimental work has involved determining quantities that, due to the complex processes involved, cannot be determined from first principles. The analytical work has primarily been focused on the linear behavior of the system. This work has been able to predict stability of the system with respect to small disturbances to some extent. Recently increased effort has been put into analyzing nonlinear models of combustions systems. This effort has primarily been focused on numerical simulations.

There are two phases involved in the combustion process. The equations for the mass averaged properties of the two phases are

$$
\begin{aligned}
\frac{D\rho}{Dt} &= \mathcal{W} \\
\rho\frac{D\mathbf{u}}{Dt} &= -\nabla p + \mathcal{F} \\
\rho\bar{C}_\nu\frac{DT}{Dt} &= -p\nabla\cdot\mathbf{u} + \mathcal{L} \\
\frac{Dp}{Dt} &= -\bar{\gamma}p\nabla\cdot\mathbf{u} + \mathcal{P}
\end{aligned}
$$

where

$$
\begin{aligned}
\mathcal{W} &= -\rho\nabla\cdot\mathbf{u} - \nabla\cdot(\rho_p\delta\mathbf{u}_p) \\
\mathcal{F} &= \nabla\cdot\hat{\tau}_\nu + \delta\mathcal{F}_p + \delta\mathbf{u}_p w_p \\
\mathcal{L} &= Q + \delta Q_p + \delta\mathbf{u}_p\cdot\mathcal{F}_p + \delta e_{p0}w_p - \mathbf{u}\cdot\nabla\cdot\hat{\tau}_\nu \\
\mathcal{P} &= (\bar{R}/\bar{C}_\nu)(\mathcal{L} - \bar{C}_\nu T\nabla\cdot(\rho_p\delta\mathbf{u}_p) \\
\frac{D}{Dt} &= \frac{\partial}{\partial t} + \mathbf{u}\cdot\nabla.
\end{aligned}
$$

This is a first order hyperbolic system. Here ρ is the average density, $\mathbf{u}$ is the average velocity and p is the average pressure of the two phases. w_p is the rate at which condensed material is converted into gas, the viscous stress tensor for the gases is $\hat{\tau}_\nu$ and Q represents both heat released in chemical reactions and heat transferred by conduction. The subscript p refers to the condensed phase. The coupling between the gaseous and condensed phases is modeled by

$$
\begin{aligned}
\mathbf{F}_p &= -\rho_p\left[\frac{\partial\mathbf{u}_p}{\partial t} + \mathbf{u}_p\cdot\nabla\mathbf{u}_p\right] \\
Q_p &= -\rho_p C\left[\frac{\partial T_p}{\partial t} + \mathbf{u}_p\cdot\nabla T_p\right] \\
\delta\mathbf{F}_p &= -\rho_p\left[\frac{\partial\delta\mathbf{u}_p}{\partial t} + \delta\mathbf{u}_p\cdot\nabla\delta\mathbf{u}_p + \delta\mathbf{u}_p\cdot\nabla\mathbf{u} + \mathbf{u}\cdot\nabla\delta\mathbf{u}_p\right] \\
\delta Q_p &= -\rho_p C\left[\frac{\partial\delta T_p}{\partial t} + \delta\mathbf{u}_p\cdot\nabla\delta T_p + \delta\mathbf{u}_p\cdot\nabla T + \mathbf{u}\cdot\nabla\delta T_p\right]
\end{aligned}
$$

and $\delta \mathbf{u}_p = \mathbf{u}_p - \mathbf{u}, \delta T_p = T_p - T$.

The notation here is the same as in Culick [22]. For an overview of contemporary combustion research see his paper and references therein.

Chapter 2

The Equations of Motion

2.1 Derivation of Equations

Here we derive the equations of motion for the air flow through the compression system. This derivation is mostly due to Mezić [57] and in part due to Moore and Greitzer [59]. These references can be consulted for a more detailed discussion about modeling the airflow through the compression system.

Some simplifying assumptions about the geometry of the compression system will be needed. We assume that the inlet duct is a straight channel which upstream ends in an infinite reservoir at constant atmospheric pressure p_a. The compressor is also straight and at its exit there is an immediate expansion into the plenum or the combustion chamber which is a large volume where the pressure is uniform p_p and velocity components can be ignored. In the inlet duct and compressor the air will be modeled by the incompressible Navier-Stokes equation. It is, however, necessary to treat the air in the plenum as compressible. We will also make the assumptions that the compression system has no guide vanes.

The compressor and the inlet duct can be thought of as two concentric cylinders and the air flows in between them. The inner one represents the hub and the outer one the casing. The angular variable is denoted by θ, the radial one by r and the axial variable, measuring the depth into the compressor, by z.

It will prove fruitful to put ourselves into a rotating frame of reference. If we consider a frame of reference that rotates with the angular velocity $\beta\mathbf{z}$, where $\mathbf{z}$ is a unit vector along the compressor axis, then the incompressible Navier-Stokes equation can be written in cylindrical coordinates as

$$\rho(\frac{\partial \mathbf{u}}{\partial t} + (\omega + 2\beta\mathbf{z}) \times \mathbf{u}) = -\nabla p_T + \rho\beta r\mathbf{r} + \mathbf{f} + \mu\Delta\mathbf{u}. \tag{2.1}$$

Here $\mathbf{u} = (u_r, u_\theta, u_z)$ represents the three dimensional velocity of the flow, ρ is the density of the fluid, ω the vorticity, $\mathbf{f}$ is the force by which the blades act on the fluid and $p_T = p + \rho\mathbf{u}^2/2$ is the stagnation pressure. The terms $(\omega + 2\beta\mathbf{z}) \times \mathbf{u}$ and $\rho\beta r\mathbf{r}$ come from the rewriting of the $\mathbf{u}_I \cdot \nabla\mathbf{u}_I$ term in the Navier-Stokes equation in an inertial frame of reference. Here $\mathbf{u}_I$ represents the flow velocity in the inertial frame of reference. We assume no-slip boundary conditions at the hub and the casing, but the boundary conditions at the blades have been replaced by the force term.

By applying the method of homogenization, one can considerably simplify this equation. We average the flow over the box shown in Figure 2.1 and a time τ and obtain the following equation

$$\rho(\frac{\partial \bar{\mathbf{u}}}{\partial t} + (\bar{\omega} + 2\beta\mathbf{z}) \times \bar{\mathbf{u}}) = -\nabla\bar{p}_T + \rho\beta r\mathbf{r} + \bar{\mathbf{f}} + \mu\Delta\bar{\mathbf{u}} - \rho\nabla\overline{\mathbf{u}'\mathbf{u}'}$$

where the overlines denote the averaged quantities, the primes denote the fluctuations from the mean and $\bar{p}_T = \bar{p} + \rho\bar{\mathbf{u}}^2/2$.

These equations are not closed, in that they depend on the fluctuations from the mean of the velocity. To remedy this the Reynolds stresses $\rho\nabla\overline{\mathbf{u}'\mathbf{u}'}$ will be replaced

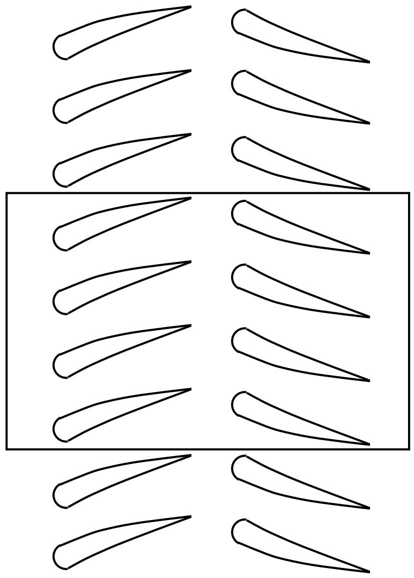

Figure 2.1: *The volume over which we average.*

by the eddy diffusivity $-\mu_{eddy}\Delta\bar{\mathbf{u}}$. The average force term could potentially also depend on the fluctuations from the mean of the variables. Following Mezić we make the assumption that it only depends on $\bar{\mathbf{u}}_z$ and the radius r and that its cross sectional components are small enough to be ignored, i.e. $\mathbf{f} = (0, 0, f_z(u_z, r))$. Furthermore, by redefining the static pressure we can make it absorb the centrifugal term $\rho\beta r\mathbf{r}$. The averaged equations are now closed and from now on we shall only concern ourselves with the averaged quantities. For simplifying the notation, we drop the overlines and the equations can then be written as

$$\rho(\frac{\partial \mathbf{u}}{\partial t} + (\omega + 2\beta\mathbf{z}) \times \mathbf{u}) = -\nabla p_T + \mathbf{f} + \nu\Delta\mathbf{u}$$

where we have defined $\nu = \mu + \mu_{eddy}$. Since the viscosity of air is very small, we will from now on refer to ν as the eddy viscosity coefficient, which we will assume to be a constant.

We will choose β to be the induced rotation of the fluid in the averaging volume.

The rotation is induced by the rotors, and for compressors with high solidity the induced rotation will be close to half of the rotor speed. For simplicity we will assume that the induced rotation is exactly half the rotor speed.

It would certainly simplify the equations considerably if we could show that ω is negligable, i.e. that $\|\omega\| \ll |\beta|$. Indeed, one can show that to a leading order this is true [57] in the steady state case. Here the methods of homogenization theory are used under the assumptions that the cross sectional Rossby number and the axial Rossby number are small as well as a certain parameter related to the design of the compressor microstructure. These assumptions will hold under the following conditions.

- The typical pitch, i.e. the distance between adjacent blades in a rotor or a stator, is much smaller than the typical radius.
- The averaging volume, which contains just one stage, i.e. one rotor and one stator, is large enough to contain many blades, but small compared with the whole disc.
- The scale of variation in the cross sectional average flow multiplied by β is much greater than the angle of the pitch multiplied by the typical size of cross sectional velocity components.
- The rotor speed is much smaller than the scale of axial motion multiplied by β.
- The rotor speed multiplied by the pitch is much smaller than the typical size of the cross sectional velocity components multiplied by the cross sectional scale of variation.

- The time scale of evolution multiplied by the rotor speed is much greater than the distance from hub to casing.

The approximate averaged equations are

$$\rho(\frac{\partial \mathbf{u}}{\partial t} + 2\beta\mathbf{z}\times\mathbf{u}) = -\nabla p_T + \mathbf{f} + \nu\Delta\mathbf{u}. \tag{2.2}$$

One can of course not hope that this approximation be true in the unsteady case for all initial conditions. We shall, however, see later that both design flow and stall fall under the steady solution case and we will therefore make the assumption that $\|\omega\| \ll |\beta|$.

Under the above assumption it also follows that the partial time derivatives of the cross sectional components of the velocity vector can be ignored. Furthermore, it follows that the axial velocity component is independent of the axial coordinate, i.e. $u_z = u_z(r,\theta)$. Equation (2.2) can thus be written in coordinate form as

$$\begin{aligned}
2\beta u_\theta &= \frac{1}{\rho}\frac{\partial p}{\partial r} \\
2\beta u_r &= -\frac{1}{\rho r}\frac{\partial p}{\partial \theta} \\
\frac{\partial u_z}{\partial t} &= -\frac{1}{\rho}\frac{\partial p}{\partial z} + \frac{f_z(u_z,r)}{\rho} + \nu\left(\frac{\partial^2 u_z}{\partial r^2} + \frac{\partial^2 u_z}{\partial \theta^2}\right).
\end{aligned} \tag{2.3}$$

Note that the equations (2.3) do not only describe the fluid flow through the compressor, but also in the inlet duct. This can be shown by the same type of scaling as before. In the inlet duct the force term is zero.

Let us consider the inlet duct and, for now, ignore the eddy viscosity term in equation (2.3). Due to continuity, the total pressure at the inlet must be equal to the atmospheric pressure p_a, i.e.

$$p_a = p(r,\theta,0,t) + \frac{\rho}{2}u_z^2(r,\theta,t)$$

where $z = 0$ at the entrance into the inlet duct. We now integrate the last equation in (2.3) over the length of the inlet duct, which we denote by L_i, to obtain

$$\frac{1}{\rho} p(r, \theta, L_i, t) = \frac{1}{\rho} p_a - L_i \frac{\partial u_z}{\partial t}(r, \theta, t) - \frac{1}{2} u_z^2(r, \theta, t).$$

Consider now the compressor and let us include the eddy viscosity terms again. In the same manner as above we can integrate the last equation of (2.3) over the length of the compressor, denoted by L, to obtain

$$\frac{1}{\rho} p_e = \frac{1}{\rho} p(r, \theta, L_i, t) - L \frac{\partial u_z}{\partial t}(r, \theta, t) + L \left(\frac{1}{\rho} f_z(u_z, r) + \nu \left(\frac{\partial^2 u_z}{\partial r^2} + \frac{\partial^2 u_z}{\partial \theta^2} \right) \right)$$

where p_e is the pressure at the exit from the compressor. We assume that there is an immediate expansion after the compressor into the plenum and that the pressure in the plenum is uniform. Due to continuity, the plenum pressure must be equal to the exit pressure, i.e. $p_p = p_e$. Combining the above we have

$$\begin{aligned} 2\beta u_\theta &= \frac{1}{\rho} \frac{\partial p}{\partial r} \\ 2\beta u_r &= -\frac{1}{\rho r} \frac{\partial p}{\partial \theta} \\ \frac{\partial u_z}{\partial t} &= -\Psi + \psi_c(u_z, r) + \nu \left(\frac{\partial^2 u_z}{\partial r^2} + \frac{\partial^2 u_z}{\partial \theta^2} \right) \end{aligned} \tag{2.4}$$

where we have defined

$$\begin{aligned} \Psi &= \frac{p_p - p_a}{(L + L_i)\rho}, \\ \psi_c(u_z, r) &= \frac{1}{L + L_i} \left(\frac{L}{\rho} f_z(u_z, r) - \frac{1}{2} u_z^2 \right) \end{aligned}$$

and redefine ν as

$$\nu = \frac{(\mu + \mu_{eddy})L}{L + L_i}.$$

The above model is known as Mezić's model. In his treatment [57] he assumed that the plenum pressure and hence Ψ was constant. We do not make that assumption here, but instead we use an argument presented by Moore and Greitzer [59] to derive an equation for the evolution of Ψ.

Recall that to the leading order the plenum eliminates all spatial variations. The plenum receives mass at the rate $\rho C_1 \Phi$ and it discharges mass at the rate $\rho C_1 \Phi_T$. Here Φ is the angular average of u_z, C_1 is a constant and Φ_T is the velocity of the air leaving the plenum through the throttle. Φ_T is scaled to account for the difference in the throttle area and the exit duct area. If we write the volume of the plenum as V_p and the plenum density as ρ_p, then by conservation of mass we have

$$\rho_p C_1(\Phi - \Phi_T) = V_p \frac{d\rho_p}{dt}$$

We assume that the process in the plenum is polytropic, that is, $\rho_p = C_2 p_p^{1/k}$ where C_2 is some constant and thus

$$\frac{d\rho_p}{dt} = \frac{\rho_p}{k p_p}\frac{dp_p}{dt} = \frac{\rho_p}{k p_p}\frac{d(p_p - p_a)}{dt},$$

where the second equality holds because p_a does not depend on time. If we assume that the gas behaves similarly to perfect gas then p_p/ρ_p can be approximated by p_a/ρ_a. Putting the two equations above together we get

$$\frac{d}{dt}\Psi = C(\Phi - \Phi_T).$$

If we assume thet Bernoulli's equation holds for the flow over the throttle, that the length of the throttle is small and the throttle discharges air to an infinite reservoir which is at atmospheric pressure, then it follows that

$$\Psi = F_T(\Phi_T, \gamma) = \frac{\Phi_T^2}{\gamma^2}$$

where γ is a constant called the throttle coefficient. This constant determines how much of the energy of the flow is extracted by the turbine. Inverting this equation and combining with the above will yield an evolution equation for Ψ

$$\frac{d}{dt}\Psi = C(\Phi - \gamma F_T^{-1}(\Psi)).$$

To simplify the equations even further, we can assume that the axial velocity u_z and the forcing on the blades f_z do not depend on the radial direction r. This violates the no slip boundary conditions, but away from the boundary this is a good approximation. With this assumption the last equation in (2.4) decouples from the other two. In other words, the system

$$\begin{aligned} \frac{d}{dt}\Psi &= C(\Phi - \gamma F_T^{-1}(\Psi)) \\ \frac{\partial u_z}{\partial t} &= -\Psi + \psi_c(u_z) + \nu \frac{\partial^2 u_z}{\partial \theta^2} \end{aligned}$$

can be solved independently and then the angular and radial velocity components can be found as functions of this solution.

We write the axial velocity as $u_z = \Phi + \varphi$ where Φ is the angular averaged velocity and φ the deviation from the average. The second equation in the above system can be split into two parts, one which describes the evolution of the average flow Φ and one which describes the evolution of the deviation from the average φ. The system becomes

$$\begin{aligned} \frac{\partial \varphi}{\partial t} &= \nu \frac{\partial^2 \varphi}{\partial \theta^2} + \psi_c(\Phi + \varphi) - \overline{\psi_c} \\ \frac{d}{dt}\Phi &= \overline{\psi_c} - \Psi \\ \frac{d}{dt}\Psi &= C(\Phi - \gamma F_T^{-1}(\Psi)) \end{aligned} \tag{2.5}$$

where $\overline{\psi_c}$ denotes the angular average of $\psi_c(\Phi + \varphi)$.

The original Moore-Greitzer equation was derived under a different set of assumptions, in particular, they assumed that the flow through the compression system is two dimensional and that the flow in the inlet duct is irrotational. Furthermore, they included inlet and outlet guide vanes in their analysis. The Moore-Greitzer equation, with the additional viscosity term suggested by Adomaitis and Abed [2], is the same as the equation derived above, except for that the PDE equation has one additional term in the Moore-Greitzer setting. This term can be incorporated by introducing the operator K, see Banaszuk *et al.* [4],

$$K(\Phi + \sum_{n\in\mathbf{Z}\setminus\{0\}} \varphi_n \mathrm{e}^{in\theta}) = \Phi + \sum_{n\in\mathbf{Z}\setminus\{0\}} (1 + \frac{am}{|n|})\varphi_n \mathrm{e}^{in\theta}$$

and then the well known viscous Moore-Greitzer (vMG) equation can be written as

$$\frac{\partial}{\partial t}\varphi = K^{-1}\left(\nu\frac{\partial^2\varphi}{\partial\theta^2} - \frac{1}{2}\frac{\partial\varphi}{\partial\theta} + \psi_c(\Phi+\varphi) - \overline{\psi_c}\right) \tag{2.6}$$

$$\frac{d\Phi}{dt} = \frac{1}{l_c}(\overline{\psi_c} - \Psi) \tag{2.7}$$

$$\frac{d\Psi}{dt} = \frac{1}{4l_cB^2}(\Phi - \gamma F_T^{-1}(\Psi)) \tag{2.8}$$

When the constant am is zero, the operator K is just the identity operator and then by rescaling the variables, the vMG equation is exactly the same as the equation derived above (2.5). The constant am is indeed small in all practical applications, and as we shall see later, the operator K plays only a minor role. The solutions of the vMG equation behave in essentially the same way, with or without the K operator. For the sake of completeness, we include the K operator in our analysis where it is convenient and we show by perturbation analysis that where it has been neglected its influence is small. The other constants appearing in the system are l_c which represents the effective lenght of the ducting in the compression system and B which can be thought of as representing the size of the plenum. Compressors with a large B parameter have a tendency to surge while compressors with a small B parameter tend to go into stall.

2.2 Existence of Solutions

In proving the existence of a unique solution of the vMG equation, we take the traditional path of first proving local existence and uniqueness as well as obtaining regularity results for the local solution via the contraction mapping principle. By obtaining a priori bounds on the solution one can then extend its existence for all positive time. Before we begin, let us establish the notation.

2.2.1 Notation and Prerequisites

The first step is to determine a good function space for the solutions of (2.6-2.8). The variable φ describes the variation of the axial flow velocity from the average flow velocity. Hence φ must have zero average and indeed this property is preserved by the equations. The natural choice is to let φ live in a space of functions of zero mean.

We denote by $|\cdot|_p$, $1 \leq p \leq \infty$, and $\|\cdot\|_k$, $k = 1, 2, \ldots$ the norms on the spaces $\bar{L}^p(S^1)$ and the Sobolev spaces $\bar{H}^k(S^1)$ of functions with zero mean. The norm $\|\cdot\|_k$ is given by

$$\|x\|_k^2 = \int_0^{2\pi} |\frac{\partial^k}{\partial\theta^k} x(\theta)|^2 d\theta$$

and the norm $|\cdot|_p$ is just the usual L^p norm.

We let $X^k = \bar{H}^k \times \mathbb{R}^2$, which is a Hilbert space when equipped with the norm

$$\|(\varphi, z)\|^2_{X^k} = \gamma_0 \|\varphi\|_k^2 + \sum_{i=1}^{2} \gamma_i |z_i|^2$$

and with the corresponding inner product. Here $\gamma_0, \gamma_1, \gamma_2 > 0$ are constants to be specified later, k is an integer and $\varphi \in \bar{H}^k, z \in \mathbb{R}^2$.

The system (2.6-2.8) can be written more compactly as an abstract evolution equation in X^k

$$\frac{dx}{dt} = Ax + f(x), \qquad x(0) = x_0, \tag{2.9}$$

where

$$A(\varphi, \Phi, \Psi) = (K^{-1}(\frac{\nu}{2}\frac{\partial^2 \varphi}{\partial \theta^2} - \frac{1}{2}\frac{\partial \varphi}{\partial \theta}), 0, 0) \tag{2.10}$$

$$f(\varphi, \Phi, \Psi) = (K^{-1}(\psi_c(\Phi + \varphi) - \overline{\psi_c}), \frac{1}{l_c}(\overline{\psi_c} - \Psi), \frac{1}{4 l_c B^2}(\Phi - F_T^{-1}(\Psi)). \tag{2.11}$$

The domain of A is $D(A) = X^2$. One easily verifies that A has a complete set of eigenvectors χ_n and we denote the corresponding eigenvalues by λ_n. These are given by

$$\lambda_n = (-\frac{\nu}{2}[\frac{n}{2}]^2 - i[\frac{n}{2}]\frac{1}{2})(1 - \frac{am}{[\frac{n}{2}] + am})$$

$$\chi_n(\theta) = \begin{cases} (0, e_n) & : \text{ if } \quad n = 0, 1 \\ (\mathrm{e}^{i[\frac{n}{2}]\theta}, 0) & : \text{ if } \quad n \quad \text{odd} \\ (\mathrm{e}^{-i[\frac{n}{2}]\theta}, 0) & : \text{ if } \quad n \quad \text{even} \end{cases}$$

where $[s]$ denotes the integer part of s and $\{e_0, e_1\}$ is the standard basis in $\mathbb{R}^2$.

We will need the following three lemmas.

Lemma 2.1. *The operators $K, \frac{\partial}{\partial t}$ and $\frac{\partial}{\partial \theta}$ commute on $C^1(0,T;H^1)$. K and K^{-1} are bounded and positive operators.*

Proof: First note that K and $\frac{\partial}{\partial \theta}$ are mutually diagonalizable in the Sobolev space H^1 with the basis $\{e^{in\theta}\}_{n\in\mathbf{Z}}$ and hence they commute. Representing an element $x \in C^1(0,T;H^1)$ by

$$x = \sum_{n\in\mathbf{Z}} c_n(t)e^{in\theta}$$

we can differentiate under the sum with respect to t and hence K commutes with $\frac{\partial}{\partial t}$. The spectrum $\sigma(K)$ lies in $[1, 1+am]$ so clearly K is a positive bounded operator. It is straight forward to verify that the same holds for K^{-1} and $\sigma(K^{-1}) \subset [1-\frac{am}{1+am}, 1]$.

$\square$

Lemma 2.2. *The linear operator A generates a continuous semigroup $S(t)$ on X^0.*

Proof: We first need to verify that A is a closable operator. To this end, it suffices to show that the domain of the adjoint, $D(A^*)$, is dense in X^0. We can formally calculate A^*

$$A^*(\varphi, \Phi, \Psi) := (K^{-1}(\frac{\nu}{2}\frac{\partial^2\varphi}{\partial\theta^2} + \frac{1}{2}\frac{\partial\varphi}{\partial\theta}), 0, 0)$$

by integration by parts. This operator is well defined on X^2 which is dense in X^0 and thus A is closable.

If $d(\lambda)$ denotes the distance of λ from the spectrum of $A, \sigma(A)$, then $\|\lambda I - A\| \geq d(\lambda)$ from which one can conclude that $\|(\lambda I - A)^{-1}\| \leq d(\lambda)^{-1}$. Since $\sigma(A)$ lies in the left half of the complex plane we have that the resolvent is bounded for all positive λ

$$\|(\lambda I - A)^{-1}\| \leq d(\lambda)^{-1} \leq \lambda^{-1}$$

and thus

$$\|(\lambda I - A)^{-m}\| \leq \|(\lambda I - A)^{-1}\|^m \leq \lambda^{-m}.$$

It now follows from the Hille-Yosida Theorem that A generates a C^0-semigroup $S(t)$. $\square$

An arbitrary $x \in X^k$ can be expanded in the basis of eigenvectors of A

$$x = \sum_{n=0}^{\infty} \beta_n \chi_n$$

and the norm of $x = (\varphi, z)$ is then given by

$$\|x\|_{X^k}^2 = \gamma_0 \sum_{n=2}^{\infty} ([\frac{n}{2}]^k |\beta_n|)^2 + \gamma_1 |z_1|^2 + \gamma_2 |z_2|^2.$$

We will in what follows use the notation K for both the operator as defined above as well as for the operator (K, I) where I is the identity in $\mathbb{R}^2$.

Lemma 2.3. *For $x = (\varphi, z) \in X^k$ the following inequalities hold*

$$\begin{aligned} \mathrm{Re}\langle x, KAx\rangle_{X^k} &\leq -\delta\|\varphi\|_{k+1}^2 \\ \|S(t)x\|_{X^{k+1}} &\leq t^{-3/4} C \|x\|_{X^k} \\ \|S(t)x\|_{X^k} &\leq \|x\|_{X^k} \\ \|(S(t) - I)x\|_{X^k} &\leq t^{1/4} C \|x\|_{X^{k+1}} \end{aligned}$$

for $t > 0$ small and some positive constants δ, C.

Proof: Without loss of generality we may assume that the constants in the norm as defined above are $\gamma_i = 1$ for $i = 0, 1, 2$. For the first inequality observe that

$$\begin{aligned}
\mathrm{Re}\langle x, KAx\rangle_{X^k} &= \sum_{n=2}^{\infty}(1+\frac{am}{[\frac{n}{2}]})\mathrm{Re}\lambda_n([\frac{n}{2}]^k|\beta_n|)^2 \\
&= \sum_{n=2}^{\infty}(1+\frac{am}{[\frac{n}{2}]})(\frac{\mathrm{Re}\lambda_n}{[n/2]^2})([\frac{n}{2}]^{k+1}|\beta_n|)^2 \\
&\leq -\delta\|\varphi\|_{k+1}^2
\end{aligned}$$

and

$$\delta = \min_n \frac{-\mathrm{Re}\lambda_n}{[n/2]^2}(1+\frac{am}{[\frac{n}{2}]}) \geq \frac{\nu}{4}(1-\frac{am}{1+am}).$$

The action of the semigroup can be written in the following way

$$S(t)x = \sum_{n=0}^{\infty} \mathrm{e}^{\lambda_n t}\langle\chi_n, x\rangle\chi_n$$

and we can proceed to get

$$\begin{aligned}
\|S(t)x\|_{X^{k+1}}^2 &= \sum_{n=2}^{\infty}([\frac{n}{2}]^{k+1}\mathrm{e}^{\mathrm{Re}\lambda_n t}|\beta_n|)^2 + |z_1|^2 + |z_2|^2 \\
&\leq (\sum_{n=2}^{\infty}[\frac{n}{2}]^2\mathrm{e}^{2\mathrm{Re}\lambda_n t})(\sum_{n=2}^{\infty}([\frac{n}{2}]^k|\beta_n|)^2) + |z_1|^2 + |z_2|^2 \\
&\leq \sum_{n=2}^{\infty}([\frac{n}{2}]^2\mathrm{e}^{-\nu[\frac{n}{2}]^2 t})\|\varphi\|_k^2 + |z_1|^2 + |z_2|^2.
\end{aligned}$$

By estimating

$$\begin{aligned}
\sum_{n=2}^{\infty}[\frac{n}{2}]^2\mathrm{e}^{-\nu[\frac{n}{2}]^2 t} &= \frac{2}{t\nu}\sum_{n=1}^{\infty}\nu t n^2\mathrm{e}^{-\nu[\frac{n}{2}]^2 t} \\
&\leq \frac{2}{t\nu}\int_0^{\infty} t\nu s^2\mathrm{e}^{-t\nu s^2}ds \\
&= \frac{2}{(t\nu)^{3/2}}\int_0^{\infty} r^2\mathrm{e}^{-r^2}dr \\
&= t^{-3/2}C
\end{aligned}$$

where C is a constant, we get for $t \leq C^{2/3}$

$$\|S(t)x\|^2_{X^{k+1}} \leq t^{-3/2}C\|x\|^2_{X^k}.$$

Taking the square root of both sides will give the second inequality.

The third inequality follows from the fact that the real part of the spectrum of A lies on the negative real axis and from the simple representation of the semigroup that we have.

Let x be represented as a linear combination of eigenfunctions as before. We now get

$$\begin{aligned}
\|(S(t)-I)x\|^2_{X^k} &= \sum_{n=2}^{\infty}([\frac{n}{2}]^k(\mathrm{e}^{\mathrm{Re}\lambda_n t}-1)|\beta_n|)^2 \\
&\leq \sum_{n=2}^{\infty}(\frac{\mathrm{e}^{\mathrm{Re}\lambda_n t}-1}{[\frac{n}{2}]})^2\sum_{n=2}^{\infty}([\frac{n}{2}]^{k+1}|\beta_n|)^2 \\
&\leq \sum_{n=2}^{\infty}(\frac{\mathrm{e}^{-\frac{\nu}{2}[\frac{n}{2}]^2 t}-1}{[\frac{n}{2}]})^2\|x\|^2_{X^{k+1}}.
\end{aligned}$$

By estimating

$$\begin{aligned}
\sum_{n=2}^{\infty}(\frac{\mathrm{e}^{-\frac{\nu}{2}[\frac{n}{2}]^2 t}-1}{[\frac{n}{2}]})^2 &= \frac{t\nu}{2}\sum_{n=1}^{\infty}(\frac{\mathrm{e}^{-t\frac{\nu}{2}n^2}-1}{n\sqrt{\frac{t\nu}{2}}})^2 \\
&\leq \frac{t\nu}{2}\int_0^{\infty}(\frac{\mathrm{e}^{-t\frac{\nu}{2}s^2}-1}{s\sqrt{\frac{t\nu}{2}}})^2 ds \\
&= \sqrt{\frac{t\nu}{2}}\int_0^{\infty}(\frac{\mathrm{e}^{-r^2}-1}{r})^2 dr \\
&= \sqrt{t}C
\end{aligned}$$

where C is a constant, we get

$$\|(S(t)-I)x\|^2_{X^k} \leq \sqrt{t}C\|x\|^2_{X^{k+1}}$$

which gives us the last inequality. $\square$

2.2.2 Existence and Regularity of Local Solutions

The local problem 2.9 is well posed and the solutions are smooth functions. This follows from Henry [36] since the operator A is sectorial and $f \in C^{\infty}$. For completeness we include here the proof of local existence of smooth solutions.

Theorem 2.4. *For any $x_0 \in X^1$, there exists a unique solution of (2.9) $x(t) \in C([0,T]; X^1)$, for some $T > 0$, such that $x(0) = x_0$. Furthermore, x is smooth in its arguments.*

Proof: We will prove the existence by using the contraction principle. We use that f is a C^1 function from X^k to X^k for $k > \frac{1}{2}$.

Define the set B by

$$B_M = \{u \in C([0,T]; X^1) | \sup_{0 \leq t \leq T} \|u(t) - u_0\|_{X^1} \leq M\}$$

where $T > 0$ is to be specified later and $M > 3\|x_0\|_{X^1}$ is a finite constant. Let us also define a mapping

$$\mathcal{F}u = S(t)u_0 + \int_0^t S(t-\tau) f(u(\tau)) d\tau.$$

For $u \in B_M$ we have

$$\begin{aligned} \|\mathcal{F}u - u_0\|_{X^1} &\leq \|(S(t) - I)u_0\|_{X^1} + \int_0^t \|S(t-\tau) f(u(\tau))\|_{X^1} d\tau \\ &\leq \|S(t)u_0\|_{X^1} + \|u_0\|_{X^1} + \int_0^t \|f(u(\tau))\|_{X^1} d\tau \end{aligned}$$

by Lemma 2.3. Since f is C^1, it is locally bounded. We conclude that

$$\begin{aligned} &\leq 2\|u_0\|_{X^1} + Ct\|u\|_{C([0,T];X^1)} \\ &\leq M, \end{aligned}$$

for small enough t. Let $T > 0$ be small enough so that this holds for all t such that $0 \leq t \leq T$. Then $\mathcal{F}$ maps B_M into itself. B_M is a closed subset of a complete metric space, therefore it is a complete metric space.

Now consider for $u, v \in B_M$

$$\begin{aligned}
\|\mathcal{F}u - \mathcal{F}v\|_{X^1} &= \|\int_0^t S(t-\tau)(f(u(\tau)) - f(v(\tau)))d\tau\|_{X^1} \\
&\leq \int_0^t \|S(t-\tau)(f(u(\tau)) - f(v(\tau)))\|_{X^1} d\tau \\
&\leq C\int_0^t (t-\tau)^{-3/4}\|f(u(\tau)) - f(v(\tau))\|_{X^1} d\tau \\
&\leq C'\int_0^t (t-\tau)^{-3/4}\|u(\tau) - v(\tau)\|_{X^1} d\tau \\
&\leq 4C'\|u - v\|_{C([0,T];X^1)} t^{1/4} \\
&\leq \frac{1}{2}\|u - v\|_{C([0,T];X^1)}
\end{aligned}$$

if we make T small enough. Here we used that f is locally bounded and we used Lemma 2.3. Hence

$$\|\mathcal{F}u - \mathcal{F}v\|_{C([0,T];X^1)} \leq \frac{1}{2}\|u - v\|_{C([0,T];X^1)}$$

and $\mathcal{F}$ is a strict contraction on B_M and hence it has a unique fixed point. The constant M is arbitrary so there exists a unique mild solution of equation (2.9) with initial condition in X^1.

To prove the regularity of u let us now assume that $u \in C([0,T]; X^k)$, $k \geq 1$ is a mild solution of (2.9), i.e. a fixed point of $\mathcal{F}$. For $t > 0$ we have

$$
\begin{aligned}
\|\mathcal{F}u\|_{k+1}(t) &\leq \|S(t)u_0\|_{k+1} + \|\int_0^t S(t-\tau)f(u(\tau))d\tau\|_{k+1} \\
&\leq Ct^{-3/4}\|u_0\|_k + \int_0^t \|S(t-\tau)f(u(\tau))\|_{k+1}d\tau \\
&\leq Ct^{-3/4}\|u_0\|_k + C\int_0^t (t-\tau)^{-3/4}\|f(u(\tau))\|_k d\tau \\
&\leq Ct^{-3/4}\|u_0\|_k + C'\int_0^t (t-\tau)^{-3/4}\|u(\tau)\|_k d\tau \\
&\leq Ct^{-3/4}\|u_0\|_k + 4C't^{1/4}\|u\|_{C([0,T];X^k)}.
\end{aligned}
$$

Here we used Lemma 2.3 and the fact that f is locally bounded. This shows that the X^{k+1} norm of u is bounded for all t such that $0 < t < T$. If we consider the initial value problem with initial value $u(t) \in X^k$, then the solution will be in $C((t,T];X^{k+1})$. This too holds for any $0 < t \leq T$ and thus $u \in C((0,T];X^{k+1})$. By induction and Sobolev Embedding Theorem we get that u is smooth in the space variable. Furthermore, we see from equation (2.9) that the time derivative of u is continuous and smooth in space. Iterated differentiation of the equation with respect to time and substituting the result back into equation (2.9) to get rid of the mixed derivatives one concludes that u is smooth in the time variable as well. $\square$

Remark 2.5 In the case when the nonlinear function f depends smoothly on some parameters and is smooth for all parameter values in question, then one can verify that the solution also depends smoothly on these parameters. This follows from the continuous dependence of the solution on initial data (and parameters). Thus the local initial value problem is well posed.

2.2.3 A Priori Bounds and Global Existence

To get global existence it suffices to show that the solutions stay bounded for all time. Our goal is however to prove the existence of a global attractor, which we will define shortly. We therefore need to get more than just existence for all time, we need to show that there exist absorbing sets in the appropriate spaces.

Definition 2.6. *A bounded set D is said to be an* absorbing set *for an evolution equation, if for all bounded sets R there exists a time t_R such that for all $t > t_R$ we have $S(t)R \subset D$.*

It is clear that if an evolution equation has an absorbing set in the same space that its initial value problem is well posed in, then the solutions will stay bounded for all time and global existence follows.

We now state two lemmas which will give us *a priori* bounds in X^0 and X^1, respectively. The first one gives us the existence of an absorbing set in X^0. The second one gives us that the flow disturbance φ decays exponentially into a bounded set in $\bar{H}^1$. From this we conclude that we have absorbing set in X^1.

Lemma 2.7. *There exists an absorbing set D for equation (2.9) in X^0.*

Proof: We want to start by estimating $\langle x, Kf(x)\rangle_{X^0}$. First we specify the constants in the norm, $\gamma_0 = \frac{1}{a}, \gamma_1 = l_c$ and $\gamma_2 = 4l_cB^2$. With this choice we get cancellation of some cross terms.

In the inner product on X^0 which corresponds to this norm we get

$$\begin{aligned}\langle x, Kf(x)\rangle_{X^0} &= \langle \varphi, \psi_c(\varphi+\Phi)\rangle_{\bar{L}^2} + \langle \Phi, \psi_c(\varphi+\Phi)\rangle_{\bar{L}^2} - F_T^{-1}(\Psi)\Psi \\ &= \langle (\varphi+\Phi), \psi_c(\varphi+\Phi)\rangle_{\bar{L}^2} - F_T^{-1}(\Psi)\Psi.\end{aligned}$$

Here we have included the operator K to cancel the action of its inverse.

Since ψ_c is a cubic polynomial with a negative leading coefficients there exist positive constants, C_1, C_2, such that $y\psi_c(y) \leq -C_1 y^2 + C_2$. Using this we get

$$\begin{aligned}
\langle x, Kf(x)\rangle &\leq -C_1|\varphi + \Phi|_2^2 + C_2 - F_T^{-1}(\Psi)\Psi \\
&= -C_1|\varphi|_2^2 - C_1|\Phi|^2 - \gamma|\Psi|^{3/2} + C_2 \\
&\leq -C'\|x\|_{X^0}^{3/2} + C_2.
\end{aligned}$$

Here we used the fact that φ has zero average and we estimated the function F_T^{-1}. Furthermore, we assumed that $|\varphi|_2^2, |\Phi|^2 \geq 1$. If this is not the case, one can increase the constant C_2 and the estimate still holds.

We differentiate the following norm to get

$$\begin{aligned}
\frac{1}{2}\frac{d}{dt}\|K^{\frac{1}{2}}x\|_{X^0}^2 &= \mathrm{Re}\langle x, KAx\rangle + \langle x, Kf(x)\rangle \\
&\leq -\delta\|x\|_{X^1}^2 - C'\|x\|_{X^0}^{3/2} + C_2
\end{aligned}$$

by Lemma 2.3. The inequality

$$\|K^{\frac{1}{2}}\|^{-1}\|K^{\frac{1}{2}}x\|_{X^0} \leq \|x\|_{X^0} \leq \|K^{\frac{1}{2}}x\|_{X^0}$$

now enables us to get the follwing estimate

$$\frac{1}{2}\frac{d}{dt}\|K^{\frac{1}{2}}x\|_{X^0}^2 \leq -C'\|K^{\frac{1}{2}}\|^{-3/2}\|K^{\frac{1}{2}}x\|_{X^0}^{3/2} + C_2$$

where we have ignored the first term in the above estimate. For $\epsilon > 0$ let $D_\epsilon = \{x \in X^0 | \|K^{\frac{1}{2}}x\|_{X^0} \leq (\frac{C_2+\epsilon}{C'})^{2/3}\|K^{\frac{1}{2}}\|\}$. Then D_ϵ is a bounded closed set and for $x \in X^0 \backslash D_\epsilon$ we have

$$\frac{1}{2}\frac{d}{dt}\|K^{\frac{1}{2}}x\|_{X^0}^2 \leq -\epsilon$$

and $\|K^{\frac{1}{2}}x\|_{X^0}^2$ decays at least linearly outside D_ϵ. Since $\|x\|_{X^0} \leq \|K^{\frac{1}{2}}x\|_{X^0}$ we conclude that D_ϵ is an absorbing set. $\square$

The existence of an absorbing set in X^0 implies that the ODE variable z will be absorbed in a bounded set in $\mathbb{R}^2$ in finite time. To get an absorbing set in $X^k, k \geq 1$ it therefore suffices to show that the flow disturbance φ is absorbed into some bounded ball in finite time for all bounded z.

Lemma 2.8. *There exists an absorbing set for equation (2.9) in $X^k, k = 1, 2$. Furthermore, the solutions $x = (\varphi, z)$ satisfy the* a priori *bound*

$$\|\varphi\|_k^2(t) \leq \|K^{\frac{1}{2}}\|^2 \|\varphi\|_k^2(0) \mathrm{e}^{-t} + (1 - \mathrm{e}^{-t})C \tag{2.12}$$

where the constant C is independent of the initial conditions.

Proof: Let us denote the first coordinate of f in equation (2.9) by f_1.

Consider the case $k = 1$. Without loss of generality we may assume that $x(t)$ lies in an absorbing set D_ϵ in X^0 for $t \geq 0$. If not, we find a time t_0 so that it does for $t \geq t_0$ and then take $x(t_0)$ as our new initial condition.

Since ψ_c is a cubic polynomial with a negative leading coefficient, $\sup_{\phi \in \mathbb{R}} \psi_c'(\phi)$ is a finite constant. We define $M = \sup_{\phi \in \mathbb{R}} \psi_c'(\phi)$, then

$$\begin{aligned} \langle \varphi, K f_1(x) \rangle_{\bar{H}^1} &= \int_0^{2\pi} \psi_c'(\varphi + \Phi) \varphi_\theta^2 d\theta \\ &\leq M \|\varphi\|_1^2 \end{aligned}$$

where φ_θ denotes $\frac{\partial}{\partial \theta}$.

As before we differentiate the following norm

$$\begin{aligned}
\frac{1}{2}\frac{d}{dt}\|K^{\frac{1}{2}}\varphi\|_1^2 &= \mathrm{Re}\langle\varphi, KA\varphi\rangle_{\bar{H}^1} + \langle\varphi, Kf_1(x)\rangle_{\bar{H}^1} \\
&\leq -\delta\|\varphi\|_2^2 + M\|\varphi\|_1^2 \\
&\leq -\delta\|K^{\frac{1}{2}}\|^{-2}\|K^{\frac{1}{2}}\varphi\|_2^2 + M\|K^{\frac{1}{2}}\|^{-2}\|K^{\frac{1}{2}}\varphi\|_1^2
\end{aligned}$$

using Lemma 2.3.

We can bound the $\bar{H}^1$ norm by an interpolation of the form

$$\|\cdot\|_1^2 \leq \frac{1}{2\sigma}\|\cdot\|_0^2 + \frac{\sigma}{2}\|\cdot\|_2^2.$$

So if we choose $\sigma = \frac{\delta\|K^{\frac{1}{2}}\|^{-2}}{(M\|K^{\frac{1}{2}}\|^{-2}+1)}$, then

$$\frac{d}{dt}\|K^{\frac{1}{2}}\varphi\|_1^2 \leq -\|K^{\frac{1}{2}}\varphi\|_1^2 + C - \frac{\delta}{2}\|K^{\frac{1}{2}}\|^{-2}\|K^{\frac{1}{2}}\varphi\|_2^2$$

where

$$C = \sup_{x\in D_\epsilon}\frac{1}{2\sigma}M\|K^{\frac{1}{2}}\|^{-2}\|K^{\frac{1}{2}}\varphi\|_0^2(s).$$

Neglecting the last term we get the following estimate

$$\frac{d}{dt}\|K^{\frac{1}{2}}\varphi\|_1^2 \leq -\|K^{\frac{1}{2}}\varphi\|_1^2 + C.$$

Solving this ODE inequality yields

$$\|K^{\frac{1}{2}}\varphi\|_1^2(t) \leq \|K^{\frac{1}{2}}\varphi\|_1^2(0)\mathrm{e}^{-t} + C(1-\mathrm{e}^{-t})$$

and thus

$$\|\varphi\|_1^2(t) \leq \|K^{\frac{1}{2}}\|^2\|\varphi\|_1^2(0)\mathrm{e}^{-t} + C(1-\mathrm{e}^{-t}).$$

It follows that for $\epsilon > 0$, the ball in X^1 of radius $C+\epsilon$ is an absorbing set in X^1.

The key estimate in this proof was the bound

$$\langle \varphi, K f_1(x) \rangle_{\bar{H}^1} \leq M \|\varphi\|_1^2.$$

Once we have obtained the same type of bound for the case $k = 2$, we can proceed in exactly the same way as before to get an absorbing set in X^2. To this end consider the following estimate

$$\begin{aligned}
\langle \varphi, K f_1(x) \rangle_{\bar{H}^2} &= \langle \varphi_{\theta\theta}, \psi_c'(\Phi + \varphi)\varphi_{\theta\theta} \rangle_{\bar{L}^2} + \langle \varphi_{\theta\theta}, \psi_c''(\Phi + \varphi)\varphi_\theta^2 \rangle_{\bar{L}^2} \\
&\leq |\psi_c'(\Phi + \varphi)|_\infty^2 \|\varphi\|_2^2 + \frac{1}{2}(\|\varphi\|_2^2 + |\psi_c''(\Phi + \varphi)\varphi_\theta^2|_2^2) \\
&\leq |\psi_c'(\Phi + \varphi)|_\infty^2 \|\varphi\|_2^2 + \frac{1}{2}(\|\varphi\|_2^2 + |\psi_c''(\Phi + \varphi)|_\infty^2 |\varphi_\theta|_2^2 |\varphi_\theta|_\infty^2) \\
&\leq |\psi_c'(\Phi + \varphi)|_\infty^2 \|\varphi\|_2^2 + \frac{1}{2}(\|\varphi\|_2^2 + |\psi_c''(\Phi + \varphi)|_\infty^2 \|\varphi\|_1^2 \|\varphi\|_2^2) \\
&\leq M(\|\varphi\|_1)\|\varphi\|_2^2.
\end{aligned}$$

Here we have made extensive use of the Sobolev Imbedding theorem. The function M is bounded on bounded sets, so if D_ϵ is a bounded absorbing set in X^1 then

$$\tilde{M} = \sup_{x \in D_\epsilon} M(\|\varphi\|_1)$$

is a finite constant and the estimate

$$\langle \varphi, K f_1(x) \rangle_{\bar{H}^2} \leq \tilde{M} \|\varphi\|_2^2$$

will allow us to proceed as before, with X^2 in the place of X^1 and X^1 in the place of X^0, to obtain a bounded absorbing set in X^2. $\square$

The local existence of solutions together with the a priori bounds give us global existence and we can now state the following theorem

Theorem 2.9. *The initial value problem (2.9) has a unique solution in* $C([0,\infty);X^1)$. *Furthermore, the solution is smooth in both space and time variables for* $t > 0$.

Remark 2.10 The existence of a global solution in X^1 and the smoothness of the local solution guarantees that the solution is smooth for all time. Absorbing sets in X^1 and X^2 do not imply the existence of an absorbing set in X^k in general. This can however be proven by induction. The essential estimate one needs is of the type

$$\langle \varphi, Kf_1(x)\rangle_{\bar{H}^k} \leq M(\|\varphi\|_{k-1})\|\varphi\|_k^2$$

where the function M is bounded on bounded sets. This argument is the same as in Lemma 2.8.

Remark 2.11 Although we have assumed that ψ_c is a cubic polynomial with a negative leading coefficient, the above analysis goes through for a more general ψ_c. In fact, all we needed was that ψ_c was smooth, $\sup \psi_c' < \infty$ and $\psi_c(y)y \leq -C_1y^2+C_2$ for some positive constants C_1, C_2.

Chapter 3

The Attractor

3.1 The Global Attractor

In the last few decades much progress has been made in the study of the long time behavior of nonlinear partial differential equations. The central theme in many of these results is that for all or almost all initial conditions, the solution will converge to a certain set of solutions called the attractor. This attractor is usually much smaller than the phase space and in many cases it has been shown that it is finite dimensional. One of the first results in this area were by Ladyzhenskaya [46] who proved the existence of a global attractor for the Navier-Stokes equation in three spatial dimensions and that the solutions in the attractor were strong solutions.

Many authors have visited this subject and to name but a few we mention Henry [36], Hale [34], Temam [69], Babin and Vishik [3] and Raugel and Sell [63] [64] [62].

In the previous chapter we proved that the vMG equation has a unique solution and hence there exists a family of evolution operators $\{T(t)\}_{t\geq 0}$ which form a nonlinear semigroup such that, $T(0)x_0 = x_0$, $T(t)T(s) = T(t+s)$ and $T(t)x_0 = x(t)$ where $x(t)$ is the solution of equation (2.9) with initial value $x(0) = x_0$. We now want to prove the existence of an attractor for the vMG equation, but before we do so, let us put our language on a firm footing by making a few definitions.

Definition 3.1. *Let $\{T(t)\}_{t\geq 0}$ be a continuous semi-group on a Banach space X. The* ω-limit set *of a set B is defined by*

$$\omega(B) = \cap_{s\geq 0}\overline{\cup_{t\geq s}T(s)B}$$

A set $\mathcal{M}$ is said to be invariant *if $T(t)\mathcal{M} = \mathcal{M}$ for all $t \geq 0$.*

An invariant set $\mathcal{A}$ is said to be an attractor *if there exists a neighborhood U of $\mathcal{A}$ such that for every neighborhood V of $\mathcal{A}$ we have $\cap_{t\geq 0}T(t)U \subset V$. The largest such U is called the* basin of attraction *of $\mathcal{A}$. If $\mathcal{A}$ is compact and its basin of attraction contains all bounded sets in X, then we say that $\mathcal{A}$ is a* global attractor.

Observe that if $\mathcal{A}$ is the global attractor then $\omega(B) \subset \mathcal{A}$ for all bounded sets B.

Before we prove the existence of a global attractor for the vMG equation we recall a theorem which can be found in Hale [34].

Theorem 3.2. *If $T(t)$ has a compact absorbing set D, then $\mathcal{A} = \omega(D)$ is a global attractor. If D is convex, then the global attractor $\mathcal{A}$ is connected.*

A more general theorem on the existence of global attractors can be found in Birnir and Grauer [12]. The existence of a global attractor for the vMG equation now follows.

Corollary 3.3. *The vMG equation (2.9) has a global attractor $\mathcal{A}$ which is connected and consists of spatially smooth functions.*

Proof: By Lemma 2.8, there exists an absorbing set D_1 in X^1. Let C be a bounded set in X^1 and find a time T_C such that $T(t)C \subset D_1$ for all $t \geq T_C$. Because all solutions are smooth in positive time we have $T(1)D_1 \subset X^k$, for $k \geq 1$. By the

Sobolev embedding theorem we know that $D = T(1)D_1$ is compact in X^1, hence $T(t)C \subset D$ for $t \geq T_C + 1$ and D is a compact absorbing set. D can be chosen to be convex and thus by Theorem 3.2 we have a connected global attractor $\mathcal{A}$.

Since the attractor is invariant we know that $T(1)\mathcal{A} = \mathcal{A}$, but then by Theorem 2.9, $\mathcal{A} \subset X^k$ for all $k \geq 1$ and thus by the Sobolev embedding theorem, $\mathcal{A}$ consists of spatially smooth functions. □

Remark 3.4 Note that although $\mathcal{A}$ consists of smooth functions, it may not be smooth as a set.

3.1.1 Dimension of the Attractor

Methods for estimating the dimension of the attractor $\mathcal{A}$ were invented by Manẽ [52] developed by Ruelle [65, 66] and later by Lieb [49] and Temam [69]. One typically studies the first variation of the evolution equation, i.e. analyzing the linearized equation, linearized about a solution to the nonlinear equation (2.9). If one can show that for all n large enough the n-dimensional volume element will decay strongly enough in the linearized flow, one can conclude that the dimension of the attractor is finite.

Before we dive into finding bounds for the dimension of the attractor, let us clarify what we mean by a dimension of an abstract set.

Definition 3.5. *Let $U \subset X$ be compact, where X is a Hilbert space. Let $l \in \mathbb{R}, \epsilon > 0$ and define*

$$\mu_H(U, l, \epsilon) = \inf \sum_{i \in I} r_i^l$$

where the infimum is taken over all coverings $\{B_i\}_{i\in I}$ *of the set* U*,* B_i *are the balls in* X *of radius* $r_i \leq \epsilon$*. We define*

$$\mu_H(U,l) = \lim_{\epsilon\to 0} \mu_H(U,l,\epsilon).$$

$\mu_H(U,l)$ *is called the* l-dimensional Hausdorff measure *of the set* U*. The* Hausdorff dimension *of the set* U *is the unique number* l' *such that*

$$\mu_H(U,l) = \begin{cases} \infty & : \quad l < l' \\ 0 & : \quad l > l' \end{cases}$$

The Hausdorff dimension of a set U *is denoted by* $d_H(U)$*.*

Definition 3.6. *Let* $N_\epsilon(U)$ *be the smallest number of balls of radius* ϵ *which can cover* U*. The fractal dimension of* U*, denoted by* $d_F(U)$*, is defined as*

$$d_F(U) = \inf\{l > 0, \mu_F(U,l) = 0\}$$

where

$$\mu_F(U,l) = \limsup_{\epsilon\to 0} \epsilon^l N_\epsilon(U).$$

Thus the difference between the Hausdorff dimension and the fractal dimension is that the radii of the balls are fixed for the fractal dimension whereas they are allowed to vary for the Hausdorff dimension, before we let ϵ tend to zero. From the fact that $\mu_F(U,l) \geq \mu_H(U,l)$ we can deduce that the fractal dimension of a set is always greater or equal to its Hausdorff dimension. In general they are not equal.

The Hausdorff and fractal dimensions have a number of nice properties. Let U, V be compact subsets of X.

- If U is a smooth m-dimensional submanifold of X then $d_H(U) = m = d_F(U)$.

- The dimensions are monotonic, i.e. if $U \subset V$ then $d_H(U) \leq d_H(V)$ and $d_F(U) \leq d_F(V)$.

- For two sets U, V,

$$\begin{aligned} d_H(U \cup V) &= max\{d_H(U), d_H(V)\} \\ d_F(U \cup V) &= max\{d_F(U), d_F(V)\}. \end{aligned}$$

Let x denote a solution of the nonlinear evolution equation (2.9) with initial conditions $x(0) = x_0$ and assume that this solution lies in the attractor, $x \in \mathcal{A}$. We linearize the equation about this solution and denote this linearization by

$$\frac{d}{dt} y = Ay + B(x)y, \qquad y(0) = y_0 \tag{3.1}$$

where $B(x)$ is the Fréchet derivative of f.

Let us now consider the n-dimensional volume element $\|y_1 \wedge ... \wedge y_n\|$, see Ruelle [65]. The time evolution of an n-dimensional volume element is governed by the equation

$$\frac{d}{dt} \ln \|y_1 \wedge ... \wedge y_n\|_{X^1} = \sum_{j=1}^{n} \mathrm{Re}\langle u_j, (A + B(x))u_j \rangle$$

where $u_1(t), ..., u_n(t)$ is an orthonormal basis that spans span$[y_1(t), ..., y_n(t)]$. If we can show that all n-dimensional volume elements decay in time we can conclude that the Hausdorff dimension and the fractal dimension of the global attractor $\mathcal{A}$ is bounded, see Temam [69] and Constantin *et al.* [20].

Theorem 3.7. *The global attractor of equation (2.9) has a finite fractal dimension d_F and a finite Hausdorff dimension d_H. The dimensions are bounded by*

$$d_H \leq n_0 \qquad d_F \leq 2n_0$$

where n_0 is the smallest odd integer such that

$$2^{1/3}\sqrt{\frac{24L(1+am)}{\nu}}+1 \le n_0.$$

$L < \infty$ is a constant.

Proof: It is straight forward to verify that the linear equation (3.1) is well posed in X^1. It is known that $f : X^1 \to X^1$ is a C^1 function and thus $B(x)$ is a continuous linear operator from X^1 to X^1. The global attractor $\mathcal{A}$ is compact and thus we can bound the norm of $B(x)$ uniformly with a finite constant L

$$\sup_{x\in\mathcal{A}} \|B(x)\| = L < \infty.$$

Now consider the evolution of the n-dimensional volume element

$$\begin{aligned}\frac{d}{dt}\ln\|y_1\wedge\ldots\wedge y_n\|_{X^1} &= \sum_{j=1}^{n}\mathrm{Re}\langle u_j,(A+B(x))u_j\rangle \\ &\le \sum_{j=1}^{n}(\mathrm{Re}\lambda_{j-1}+L)\end{aligned}$$

It then becomes clear that all n-dimensional volume elements decay whenever n is large enough to make the sum

$$\sum_{j=1}^{n}(\mathrm{Re}\lambda_{j-1}+L) = -\sum_{j=0}^{n-1}\frac{\nu}{2}[\frac{j}{2}]^2(1-\frac{am}{[\frac{j}{2}]+am})+nL$$

negative. Let us assume that n is odd, then we can estimate the sum

$$
\begin{aligned}
& -\sum_{j=0}^{n-1} \frac{\nu}{2}[\frac{j}{2}]^2(1-\frac{am}{[\frac{j}{2}]+am})+nL \\
\leq & -\frac{\nu}{2}\frac{1}{1+am}\sum_{j=2}^{n-1}[\frac{j}{2}]^2+nL \\
= & -\nu\frac{1}{1+am}\sum_{j=1}^{\frac{n-1}{2}} j^2+nL \\
= & -\nu\frac{1}{1+am}\frac{1}{6}\frac{n-1}{2}(\frac{n-1}{2}+1)(2\frac{n-1}{2}+1)+nL \\
= & -\frac{\nu}{24(1+am)}n(n-\sqrt{\frac{24L(1+am)}{\nu}+1})(n+\sqrt{\frac{24L(1+am)}{\nu}+1}).
\end{aligned}
$$

Using the inequality

$$-cz(z-d)(z+d) \leq -\frac{2c}{3}z^3+\frac{2c}{3}d^3$$

which follows from Young's inequality, we finally obtain the estimate

$$\sum_{j=1}^{n}(\mathrm{Re}\lambda_{j-1}+L) \leq -\frac{\nu}{36(1+am)}n^3+\frac{\nu}{36(1+am)}\left(\frac{24L(1+am)}{\nu}+1\right)^{3/2}.$$

By Temam, Theorem VI.2.1 [69], if we let n_0 be the smallest positive odd integer such that

$$2^{1/3}\sqrt{\frac{24L(1+am)}{\nu}+1} \leq n_0$$

then the Hausdorff dimension of $\mathcal{A}$ is bounded by n_0 and the fractal dimension is bounded by $2n_0$. $\square$

3.2 The Basic Attractor

Once the existence of the finite dimensional global attractor has been established, the natural question arises: How can one construct the global attractor and can one obtain a system of ODEs that describe the evolution on the attractor? There are, for the most part, two main approaches that researchers have taken here.

The first one, and the more popular one, is to think of the attractor as a set embedded in a larger manifold, often called intertial manifold, see e.g. [21] and [24]. The problem of finding ODEs that describe the flow on this manifold or an approximate manifold, is then solved by using a Galerkin projection onto a basis, see e.g. [61] and [54]. The number of basis vectors needed is often quite large. This can be due to either that the bounds on the dimension of the attractors found by current methods tend to be rather conservative, or that the asymptotic dynamics of the system in question are in fact high dimensional. Hence the system of ODEs is not tractable for analytical analysis, but may lend itself better to numerical work.

The second approach is to consider only the core of the attractor called the basic attractor (see below). Here one constructs the particular solutions in the attractor which attract "almost all" of the phase space. For some systems, the asymptotic dynamics in this "almost every" sense are low dimensional and one can completely determine the flow on the basic attractor *analytically*.

Eventually one would like to see these two approaches merge, so that one would be able to say something about the flow on the global attractor analytically. The current state of the theory of nonlinear infinite dimensional dynamical systems does, however, not allow for this. In what follows we will therefore focus our attention on the basic attractor. We begin by clarifying what we mean by "almost every" in an infinite dimensional space and defining the basic attractor.

3.2.1 Prevalence and Basic Attractors

Before we can define the basic attractor, we need to extend the measure theoretic terms measure zero and almost every to infinite dimensional Banach spaces. Furthermore, we want to do it in such a way that these definitions behave well under the operations of the vector space. It turns out that it suffices that they behave well under translations of sets. The problem here lies in that there do not exist any nontrivial translation invariant measures in infinite dimensional spaces. If a subset $U \subset X$ in an infinite dimensional Banach space is nonempty and μ is a translation invariant measure on X, then either $\mu(U) = 0$ or $\mu(U) = \infty$. Following Hunt *et al.* [39] the notions of measure zero and almost every can be replaced by shy and prevalent respectively.

Definition 3.8. *Let X denote a separable Banach space. We denote by $S + v$ the translate of the set $S \subset X$ by a vector v. A measure μ is said to be* transverse *to a Borel set $S \subset X$ if the following two conditions hold:*

- *There exists a compact set $U \subset X$ for which $0 < \mu(U) < \infty$.*
- *$\mu(S + v) = 0$ for every $v \in X$.*

A Borel set $S \subset X$ is called shy *if there exists a compactly supported measure transverse to S. More generally, a subset of X is called shy if it is contained in a shy Borel set. The complement of a shy set is said to be a* prevalent *set.*

The basic attractor should be the smallest part of the global attractor $\mathcal{A}$ which attracts a prevalent set. This can be made precise.

Definition 3.9. *An attractor $\mathcal{B}$ is a* basic attractor *if it satisfies the two conditions*

1. *The basin of attraction of $\mathcal{B}$ is prevalent.*

2. *$\mathcal{B}$ is minimal with respect to property (1), i.e. there exists no strictly smaller $\mathcal{B}' \subset \mathcal{B}$ with* basin($\mathcal{B}$) $\subset$ basin*($\mathcal{B}'$), up to shy sets.*

This means that every point of $\mathcal{B}$ is essential, no point can be removed without removing a portion of the basin that is not shy. In numerical simulations or in physical experiments one would therefore only expect to observe the basic attractor after a long enough settling period.

In general, the basic attractor will be disconnected although the global attractor is connected. We can therefore speak of components of the basic attractor.

The following theorem, which is an extension of a finite dimensional version by Milnor [58], was proven in Birnir [11].

Theorem 3.10. *Let $\mathcal{A}$ be the compact attractor of a continuous map $T(t)$ on a separable Banach space X. Then $\mathcal{A}$ can be decomposed into a basic attractor $\mathcal{B}$ and a remainder $\mathcal{C}$,*

$$\mathcal{A} = \mathcal{B} \cup \mathcal{C}$$

such that basin($\mathcal{B}$) is prevalent and basin($\mathcal{C} \backslash \mathcal{B}$) is shy.

The basic attractor $\mathcal{B}$ for the vMG equation depends on the parameters in the equation, in particular, it depends on the throttle parameter $\mathcal{B} = \mathcal{B}(\gamma)$. It will prove useful later to have the following definition.

Definition 3.11. *Let $\tilde{\gamma} > 0$. The* union attractor *is the union*

$$\cup_{\gamma \geq \tilde{\gamma}} \mathcal{B}(\gamma).$$

It turns out that in the cases where an explicit description of $\mathcal{B}$ has been given, see [12] and [17], that the dimension of $\mathcal{B}$ is small, whereas the dimension of $\mathcal{C}$ can be quite large. As we shall see later, this is also the case for the basic attractor of the vMG equation.

3.3 Constructing the Basic Attractor

Experimental and numerical evidence indicate that the basic attractor in axial compression systems is low dimensional [23] [25] [30] [73]. It can consist of a combination of axisymmetric design flow, surge and stall. The design flow is a stationary solution and surge is a periodic cycle which has been well studied (see [59] and [56]). It only involves the two ODEs in the system (2.6-2.8). Stall has been studied in low order Galerkin truncations of the Moore-Greitzer equations [56] [53].

In this section we will briefly outline how one obtains solutions for design flow and surge. We then construct explicit stall solutions and analyze their stability as well as constructing their connection with design flow. For stall solutions we will initially assume that the operator K^{-1}, which is the sum of the identity I and a compact operator, is just the identity. Furthermore, we will assume that the throttle parameter γ has been chosen in a special way. We conclude this section by relaxing these assumptions.

3.3.1 Design Flow

Under normal conditions the engine operates in design flow. There the flow through the compressor is uniform in space and time, in particular, $\varphi = 0$ and Φ and Ψ are constant.

Figure 3.1 shows the (Φ, Ψ) plane. The parabola starting at the origin represents all stationary solutions for equation (2.8) and is called the throttle characteristic. The cubic curve represents all stationary solutions for equation (2.7), given that $\varphi = 0$, and is called the compressor characteristic. Since $\varphi = 0$ is a stationary solution for equation (2.6) we can conclude that the intersection of the two curves in Figure 3.1 is a stationary solution for the full system (2.6-2.8). This stationary solution is called design flow.

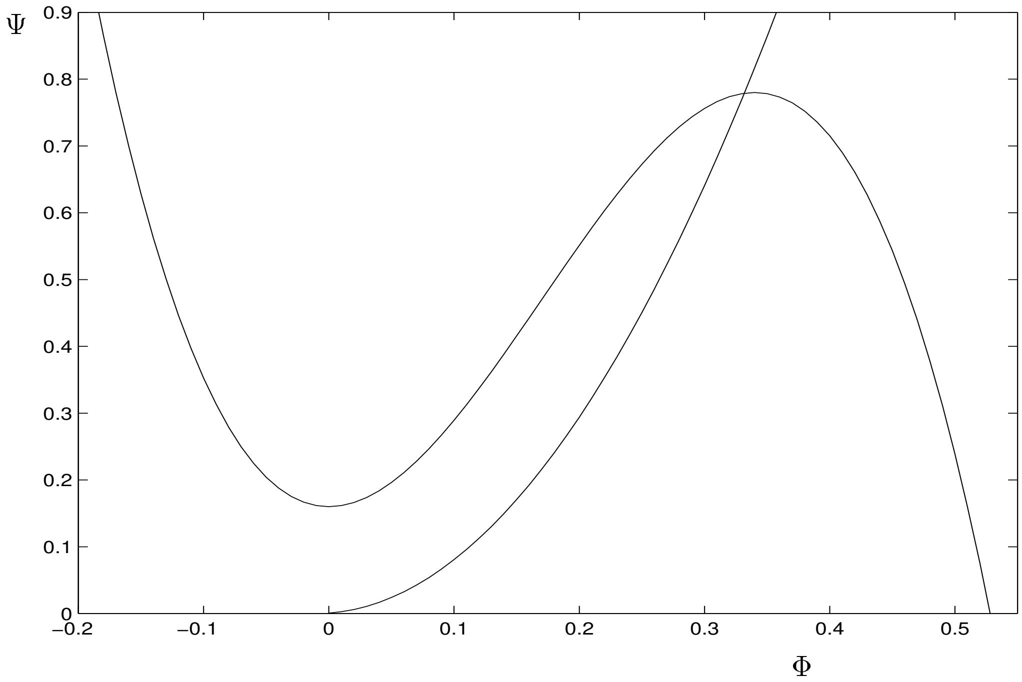

Figure 3.1: *Two characteristics: the cubic compressor characteristic and the parabolic throttle characteristic. The intersection of these curves is a stationary solution for* $\varphi = 0$. *They are stable to the right of the peak.*

To analyze the stability of the design flow $(0, \Phi_0, \Psi_0)$ we linearize the system about this solution. Let us define the variable $y = (y_1, y_2, y_3) = (\varphi, \Phi - \Phi_0, \Psi - \Psi_0)$. The linearized system is

$$\frac{d}{dt} y = Ay \tag{3.2}$$

where

$$A = \begin{bmatrix} K^{-1}(\nu\partial_\theta^2 + \psi_c'(\Phi_0)) & 0 & 0 \\ 0 & \frac{1}{l_c}\psi'(\Phi_0) & -\frac{1}{l_c} \\ 0 & \frac{1}{4l_cB^2} & \frac{-\gamma}{4l_cB^2}(F_T^{-1})'(\Psi_0) \end{bmatrix}. \tag{3.3}$$

This is a block diagonal system and its stability and bifurcations have been analyzed completely, see [56] and [19]. When the throttle parameter γ is decreased, the average flow Φ decreases as well and the design flow undergoes a series of subcritical Hopf bifurcations. If the parameter B is large enough, there will be one Hopf bifurcation originating from the two dimensional block related to the two ODEs (2.7-2.8). This bifurcation gives rise to surge. Furthermore, when $\psi_c'(\Phi) = \nu n^2$, then the n-th Fourier harmonic will become unstable and another subcritical Hopf bifurcation occurs. The number of these Hopf bifurcations, which give rise to stall, is bounded by

$$n_{max} \leq \sqrt{\frac{1}{\nu}\max_{\Phi}\psi_c'(\Phi)}. \tag{3.4}$$

Figure 3.2 shows how the amplitude of the periodic orbits originating from the subcritical Hopf bifurcations varies with the bifurcation parameter.

Design flow is stable to the right of the peak of the compressor characteristic. It is desirable to operate the engine on the right side of the peak with as high pressure rise as possible without risking the system being thrown into surge or stall by disturbances.

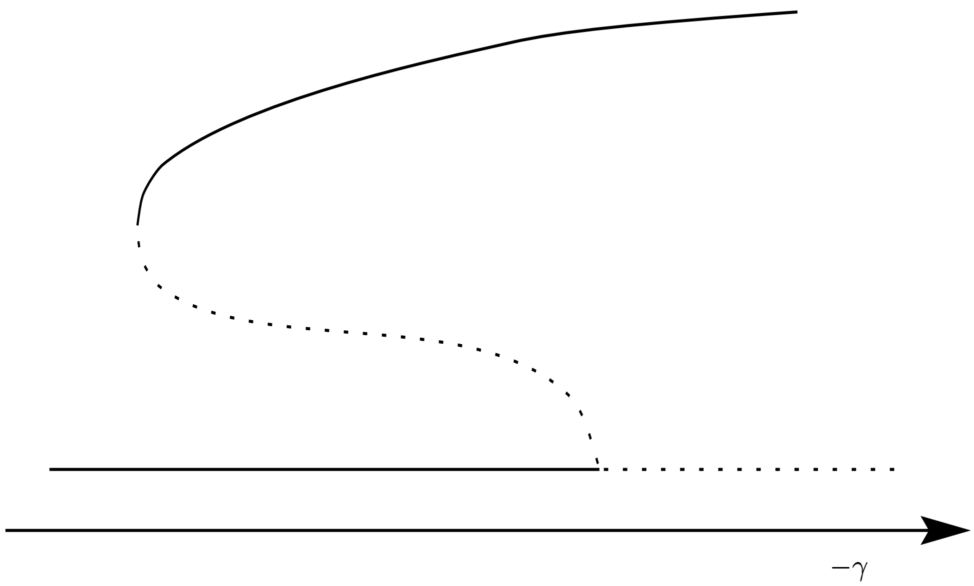

Figure 3.2: *The design flow undergoes a series of subcritical Hopf bifurcation to surge and stall. The amplitude of the periodic orbits is plotted as a function of the bifurcation parameter.*

3.3.2 Surge

Surge is a limit cycle in the two ODEs (2.7-2.8) where the nonaxisymmetric disturbance is zero, $\varphi = 0$. It has been studied by many authors, among them Greitzer [30] and McCaughan [55] [56]. It arises as a subcritical Hopf bifurcation in the system

$$\begin{aligned} \frac{d}{dt}\Phi &= \frac{1}{l_c}(\psi_c(\Phi) - \Psi) \\ \frac{d}{dt}\Psi &= \frac{1}{4B^2 l_c}(\Phi - \gamma F_T^{-1}(\Psi)) \end{aligned}$$

which occurs when the throttle parameter γ is decreased. Since the bifurcation is subcritical, we have a one parameter family of unstable surge cycles that originate from the bifurcation point. This branch bends on itself and the cycles become stable [56] [19], see Figure 3.2. These stable cycles are fairly large and a simulation of one is shown in Figure 3.3

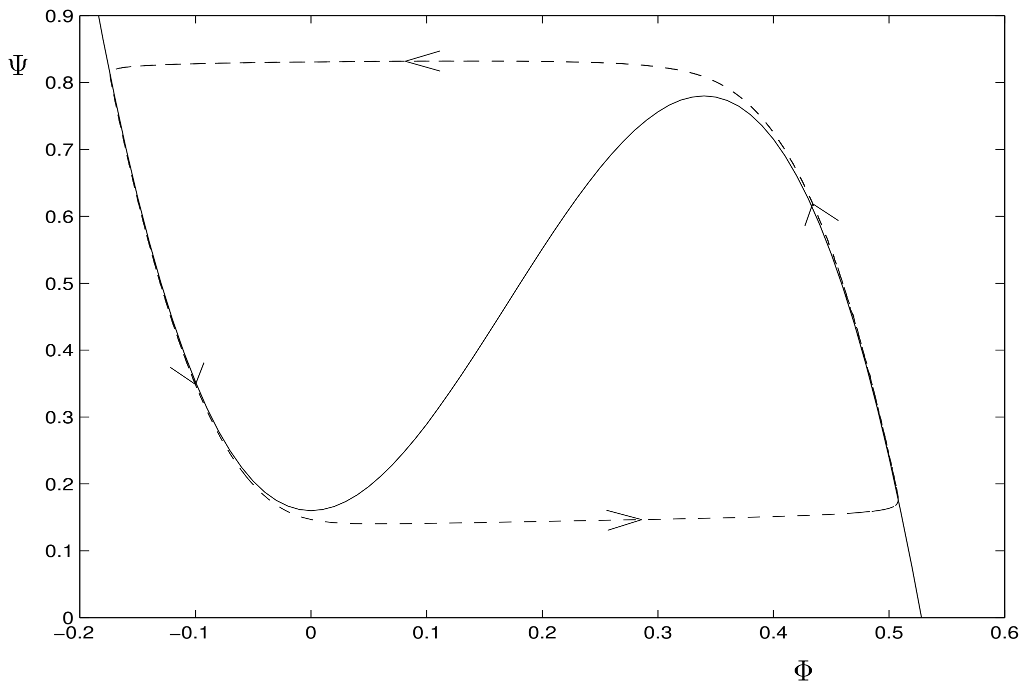

Figure 3.3: *The surge instability is a periodic orbit in the* (Φ, Ψ)*-plane.*

The solution spends most of its time on the sides of the cycle. There the slope of the compressor characteristic is negative so all nonaxisymmetric disturbances are damped.

3.3.3 Explicit Stall Solutions

Experimental and numerical evidence indicate that the two ODE variables Φ and Ψ are independent of time during stall and that we have a traveling wave solution

$$\varphi(t, \theta) = \varphi(\eta), \quad \eta = \theta - \alpha t$$

where α is the constant propagation speed of the wave around the annulus. We will therefore look for solutions of this form. We refer to the (t, η)-plane as the rotating reference frame and the (t,θ)-plane as the fixed reference frame. Let us for now neglect the operator K^{-1}. We will relax this assumption later.

Observe that when φ is a traveling wave that has a fixed profile and the mean flow Φ is constant, then the angular averaged pressure rise $\overline{\psi_c}$ is constant. With the above assumptions the system (2.6-2.8) reduces to a single ODE with periodic boundary conditions coupled to two algebraic equations

$$\begin{aligned} 0 &= \nu\varphi'' + (\alpha - \tfrac{1}{2})\varphi' + \psi_c(\Phi+\varphi) - \overline{\psi_c} \\ \begin{bmatrix} 0 \\ 0 \end{bmatrix} &= \begin{bmatrix} \frac{1}{l_c}(\overline{\psi_c} - \Psi) \\ \frac{1}{4l_cB^2}\Phi - \gamma F_T^{-1}(\Psi)) \end{bmatrix} = G_\gamma(\Phi,\Psi,\varphi). \end{aligned}$$

Here the prime denotes differentiation with respect to η.

In general the ODE and the algebraic equations will have to be solved simultaneously, but as we shall see in Lemma 3.12, there exists a special solution of the algebraic equations which places only small restrictions on the solution φ. We can therefore seek a solution of the ODE in a large class without regard for the algebraic equations.

Lemma 3.12. *There exist γ_*, Φ_*, Ψ_* such that*

1. *For $\Phi = \Phi_*$ we have*

$$\psi_c(\Phi+\varphi) - \psi_c(\Phi) = -b\varphi^3 + c\varphi$$

   for some constants b, c.

2. *For all $\varphi \in \bar{H}^1$ such that $\int_0^{2\pi} \varphi^3(\theta)d\theta = 0$, we have*

$$G_{\gamma_*}(\Phi_*,\Psi_*,\varphi) = 0.$$

Proof: The compressor characteristic ψ_c is a cubic polynomial with a negative leading coefficient. If we define

$$h_\Phi(x) = \psi_c(\Phi + x) - \psi_c(\Phi)$$

then $h_\Phi(0) = 0$ and h_Φ is also a cubic polynomial with a negative leading coefficient. Let Φ_* be the unique number such that h_{Φ_*} is an odd function. Then

$$h_{\Phi_*}(x) = -bx^3 + cx$$

and the first part of the Lemma is complete.

Now set $\Psi_* = \psi_c(\Phi_*)$ and $\gamma_* = \frac{\Phi_*}{F_T^{-1}(\Psi_*)}$, then

$$G_{\gamma_*}(\Phi_*, \Psi_*, 0) = 0.$$

Let φ satisfy the assumptions in the Lemma. Recall that since $\varphi \in \bar{H}^1$, it has zero average. We have

$$\begin{aligned} \int_0^{2\pi} h_{\Phi_*}(\varphi(\theta))d\theta &= -b\int_0^{2\pi} \varphi^3(\theta)d\theta + c\int_0^{2\pi} \varphi(\theta)d\theta \\ &= 0 \end{aligned}$$

and thus

$$\overline{\psi_c} = \psi_c(\Phi_*) = \Psi_*.$$

We conclude that

$$G_{\gamma_*}(\Phi_*, \Psi_*, \varphi) = 0$$

and the Lemma is proven. □

For now we shall assume that γ, Φ, Ψ have been chose as the specific values given by Lemma 3.12. This assumption is rather restrictive, but in section 3.3.6 we show that it can be relaxed. With this choice, our problem is reduced to finding a solution of the equation

$$0 = \nu\varphi'' + (\alpha - \frac{1}{2})\varphi' - b\varphi^3 + c\varphi$$

on the unit circle, subject to the constraints $\int_0^{2\pi} \varphi^3(\theta)d\theta = 0$ and $\varphi \in \bar{H}^1$.

Applying Hamiltonian methods, we consider this equation as an evolution equation and look for a periodic solution with the correct period to satisfy the periodic boundary conditions in the boundary value problem. The correct periods are $T = \frac{2\pi}{n}$ where n is a positive integer. This equation is the well known Duffing's equation. The constant $\alpha - \frac{1}{2}$ appears as damping which can be either positive, negative or zero. It is a known fact that for nonzero damping, the Duffing's equation has no periodic solutions. We must therefore restrict ourselves to the case when $\alpha = \frac{1}{2}$. The reader is refered to Guckenheimer and Holmes [31] and Lawden [47] for a further discussion of Duffing's equation.

Proposition 3.13. *For $\alpha = \frac{1}{2}$ there exist N solutions of equation (3.3.3) given by (Φ, Ψ, φ_j), $j = 1, ..., N$, where*

$$\varphi_j(\eta) = \sqrt{\mu_j}ns(\omega_j\eta + i\hat{\omega}_2, k_j)$$

and

$$\mu_j = 2\frac{c}{b}(1 + \sqrt{1 - (\frac{b}{c})^2\bar{c}_j}), \quad \omega_j = \sqrt{\frac{b\mu_j}{2\nu}}, \quad k_j = \frac{1 - \sqrt{1 - (\frac{b}{c})^2\bar{c}_j}}{1 + \sqrt{1 - (\frac{b}{c})^2\bar{c}_j}}, \quad N \leq [\sqrt{\frac{c}{\nu}}]$$

where $[\cdot]$ denotes the integer part, $\bar{c}_j$ are constants of integration, ns is the Jacobi elliptic function, see [70], and $i\hat{\omega}_2$ is half the imaginary period of ns.

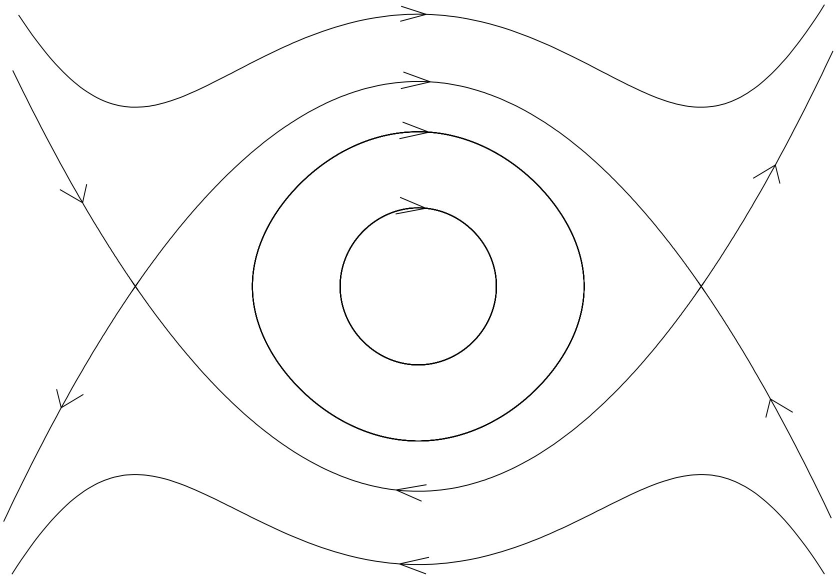

Figure 3.4: *The phase portrait for the Duffing's equation.*

Proof: Writing the ODE in (3.3.3) as a first order system one gets

$$\begin{aligned} \dot{x} &= y \\ \dot{y} &= \tfrac{1}{\nu}(bx^3 - cx). \end{aligned}$$

The only periodic cycles lie inside the heteroclinic orbit, see Figure 3.4. The period of these cycles is bounded below by the period of the linearized system T_{lin}, linearized about the center. The period then tends monotonically to infinity as we pick cycles closer to the heteroclinic orbit. The period of the system linearized about the origin (harmonic oscillator) is

$$T_{lin} = 2\pi\sqrt{\frac{\nu}{c}}.$$

We are looking for periodic orbits which have periods $T_j = \frac{2\pi}{j}$ and due to the lower bound on the periods offered by the linear system we can bound their number by

$$N \leq [\sqrt{\frac{c}{\nu}}].$$

This is exactly the same bound we arrived at earlier in equation (3.4). Multiplying through Duffing's equation with $\frac{d\varphi}{d\eta}$ and integrating once we obtain

$$\left(\frac{d\varphi}{d\eta}\right)^2 = \frac{b}{2\nu}(\varphi^4 - \frac{2c}{b}\varphi^2 + \bar{c})$$

where $\bar{c}$ is a constant of integration. One can use quadratures to integrate this equation. By recalling that the Jacobi elliptic function ns satisfies the differential equation

$$(ns')^2 = (ns^2 - 1)(ns^2 - k^2)$$

where k is the modulus, one quickly verifies that the solution is given by

$$\varphi(\eta) = \sqrt{\mu} ns(\omega\eta + i\hat{\omega}_2, k),$$

where the argument of the Jacobi elliptic function ns is shifted half way up its period parallelogram by $i\hat{\omega}_2$, compare [10], to make it real and non-singular. What remains is to pick out the correct orbits and that is done by choosing the correct constants of integration. Since ns is an odd function, it is trivial to verify that it satisfies the conditions in Lemma 3.12. □

The constants of integration can be determined by using an identity relating the period of ns to the modulus

$$T = 4\int_0^1 \frac{dt}{\sqrt{(1-t^2)(1-k^2t^2)}}.$$

In our case this becomes

$$T_j = \frac{2\pi}{j} = \frac{4}{\omega_j}\int_0^1 \frac{dt}{\sqrt{(1-t^2)(1-k_j^2t^2)}} \tag{3.5}$$

which can now be solved to give $\bar{c}_j$. The constants of integration lie on the interval $\bar{c}_j \in [0, (\frac{c}{b})^2]$.

3.3.4 Stability of Stall Solutions

We have now constructed special solutions which describe stall. The next step is to analyze their stability. As we shall see, once one has analyzed the stability for the first stall solution, one has in effect analyzed the stability of all of them. We will therefore focus our attention only on the first stall solution (Φ, Ψ, φ_1) and drop the subscript 1.

The stall solutions given by Proposition 3.13 are periodic in both space and time. We will in the sequel prove that these solutions are asymptotically orbitally stable. When proving asymptotic orbital stability of periodic orbits, one typically considers the Poincaré map associated with the orbit. To be more specific, one proves that the spectrum of the linearized Poincaré map lies in a closed subset of the open unit disk. To find the spectrum of the linearized Poincaré map, we study the full linearized system, i.e. the system (2.6-2.8) linearized about a stall solution, in the rotating reference frame. The stall solutions are stationary solutions in the rotating reference frame. It turns out that the spectrum of the full linearized system is related to the spectrum of the Lamé potential, which was studied by Hermite [37] early this century. Due to this connection to the Lamé potential, we are able to find analytically the eigenvalues and eigenvectors of the full linearized system, which in turn gives us the eigenvalues and eigenvectors of the linearized Poincaré map.

We begin by studying equation (2.6) linearized in about the stall solution. When the average term, $\overline{\psi_c}$, is neglected, the linearized equation can be written as

$$\frac{\partial u}{\partial \xi} = \nu \frac{\partial^2 u}{\partial \eta^2} - 3b\varphi^2 u + cu. \tag{3.6}$$

Before we substitute in the stall solution we found in last section, we can utilize a relationship between the Jacobi elliptic function ns and the Weierstrass $\wp$-function (see Du Val [70]), namely

$$ns^2 = \wp - e_2$$

where $e_1 \geq e_3 \geq e_2$ are the stationary values of $\wp$. Here we are following the convention in [70] for the ordering of the stationary values. The right hand side of equation (3.6) now becomes

$$\nu \frac{\partial^2}{\partial \eta^2} - 3b\mu(\wp(\omega\eta + i\hat{\omega}_2) - e_2) + c.$$

By making the substitution $s = \omega\eta$, we can rewrite this as

$$\frac{b\mu}{2}\left(\frac{\partial^2}{\partial s^2} - 6\wp(s + i\hat{\omega}_2) + 6e_2 + \frac{2c}{b\mu}\right). \tag{3.7}$$

This is a constant translate of the Lamé operator (see [51] and [10])

$$\frac{\partial^2}{\partial s^2} - 6\wp.$$

We have the following lemma,

Lemma 3.14. *The Lamé operator*

$$\frac{\partial^2}{\partial s^2} - 6\wp$$

in L^2 has five simple eigenvalues

$$(\lambda_1, \lambda_2, \lambda_3, \lambda_4, \lambda_5) = (\sqrt{3g_2}, -3e_2, -3e_3, -3e_1, -\sqrt{3g_2}),$$

where $g_2 = -4(e_1e_2 + e_2e_3 + e_3e_1)$, *with corresponding eigenfunctions*

$$\begin{aligned}
\phi_1 &= \wp(s) - \sqrt{\tfrac{g_2}{12}} \\
\phi_2 &= cs(s)ds(s) \\
\phi_3 &= ns(s)cs(s) \\
\phi_4 &= ns(s)ds(s) \\
\phi_5 &= \wp(s) + \sqrt{\tfrac{g_2}{12}}.
\end{aligned}$$

The rest of the spectrum consists of a decreasing sequence of negative double eigenvalues $\{\lambda_j\}_{j=6}^{\infty}$, *which tend to negative infinity as* j *gets larger. The eigenfunctions form a complete basis for* $L^2([0,T])$ *where* T *is the real period of* $\wp$.

The above applies equally well to H^1, where H^1 denotes the Sobolev space with index one of functions on the unit circle with square integrable derivatives. In particular, H^1 contains $\bar{H}^1$ as a subspace of codimension one.

Proof: See Magnus and Wrinkler [51], Ince [40] and Birnir [10]. $\square$

Using the fact that $e_1 + e_2 + e_3 = 0$ and $e_1 \geq e_3 \geq e_2$ one quickly verifies that $\lambda_j \geq \lambda_{j+1}$. We need to determine how much the spectrum of the Lamé potential is shifted by the constant $6e_2 + \frac{2c}{b\mu}$. It has already been shown that $\varphi = \sqrt{\mu}ns(\omega\eta + i\hat{\omega}_2, k)$ satisfies the equation

$$0 = \nu\frac{\partial^2}{\partial\eta^2}\varphi - b\varphi^3 + c\varphi.$$

Differentiating this equation once with respect to η, we get

$$0 = (\nu\frac{\partial^2}{\partial\eta^2} - 3b\varphi^2 + c)\varphi'$$

and thus, $\varphi' = Cns' = \tilde{C}csds$ is an eigenfunction of equation (3.6) with zero eigenvalue. This happens also to be an eigenfunction of the Lamé operator with eigenvalue $-3e_2$. This implies that the spectrum of the operator given by equation (3.7), is the spectrum of the Lamé potential shifted by $3e_2 < 0$, i.e. the spectrum is

$$(\tilde{\lambda}_1, \tilde{\lambda}_2, \tilde{\lambda}_3, \tilde{\lambda}_4, \tilde{\lambda}_5) = \frac{b\mu}{2}(\sqrt{3g_2} + 3e_2, 0, -3(e_3 - e_2), -3(e_1 - e_2), -\sqrt{3g_2} + 3e_2),$$

and

$$\mu = -\frac{2c}{3be_2}.$$

We conclude, that when we consider only equation (2.6) and ignore its average term and linearize it with respect to disturbances in H^1, we get one-dimensional unstable and one-dimensional center spaces and a stable eigenspace of codimension two.

We now need to consider the full system (2.6-2.8) linearized about the stall solution. Its right hand side is

$$E\begin{bmatrix} \varphi \\ \Phi \\ \Psi \end{bmatrix} = \begin{bmatrix} \nu\frac{\partial^2}{\partial\eta^2} + \psi_c' - \overline{\psi_c'} & \psi_c' - \overline{\psi_c'} & 0 \\ \frac{1}{l_c}\overline{\psi_c'} & \frac{1}{l_c}\overline{\psi_c'} & -\frac{1}{l_c} \\ 0 & \frac{1}{4l_cB^2} & -\frac{\gamma}{4l_cB^2}(F_T^{-1})' \end{bmatrix}\begin{bmatrix} \varphi \\ \Phi \\ \Psi \end{bmatrix}, \tag{3.8}$$

where ψ_c' and $\overline{\psi_c'}$ denote the Fréchet derivatives of ψ_c and $\overline{\psi_c}$ respectively.

Proposition 3.15. *The stall solution (Φ, Ψ, φ) is an asymptotically orbitally stable periodic orbit if the real parts of the eigenvalues of the restriction of the operator E to the subspace span$\{(\wp - \overline{\wp}, 0, 0), (0, 1, 0), (0, 0, 1)\}$ have negative real parts. Here $\overline{\wp}$ denotes the average of $\wp$. If there exists an eigenvalue of the restricted operator with a positive real part then the stall solution is unstable.*

Proof: If the spectrum of the linearized Poincaré map lies in a closed subset of the open unit disk, then the periodic orbit is asymptotically orbitally stable. If on the other hand there exists an eigenvalue outside the unit disk, then the orbit is unstable. Before we find the spectrum of the linearized Poincaré map associated with the stall solution, we need to determine the spectrum of the operator E given by equation (3.8).

Let $\phi \in H^1 \backslash \mathrm{span}\{\phi_1, \phi_5\}$. Since eigenspaces corresponding to different eigenvalues are orthogonal and $\mathrm{span}\{\phi_1, \phi_5\} = \mathrm{span}\{\wp, 1\}$, we know that $\langle \phi, 1 \rangle = 0$ and thus $\phi \in \bar{H}^1$. Furthermore, since $\psi_c' \in \mathrm{span}\{\phi_1, \phi_5\}$, we have $\overline{\psi_c'}\phi = \langle \psi_c', \phi \rangle = 0$. We can now conclude that if ϕ lies in an eigenspace of the translated Lamé potential corresponding to the eigenvalue λ, then $(\phi, 0, 0)$ lies in an eigenspace of E corresponding to the same eigenvalue. Let $\mathcal{Q}$ be the subspace spanned by all such functions and notice that we have $E\mathcal{Q} \subset \mathcal{Q}$.

For any $\phi \in H^1 \backslash \mathrm{span}\{\phi_1, \phi_5\} \subset \bar{H}^1$, we have $(\phi, 0, 0) \in \mathcal{Q}$ and we can conclude that $\mathrm{codim}(\mathcal{Q})$ in $H^1 \times \mathbb{R}^2$ is 4. Since $\mathcal{Q} \subset \bar{H}^1 \times \mathbb{R}^2$, we can also conclude that $\mathrm{codim}(\mathcal{Q})$ in $\bar{H}^1 \times \mathbb{R}^2$ is 3. The orthogonal complement of $\mathcal{Q}$ is $\mathcal{Q}^\perp = \mathrm{span}\{(\wp - \overline{\wp}, 0, 0), (0, 1, 0), (0, 0, 1)\}$ and one quickly verifies that $E\mathcal{Q}^\perp \subset \mathcal{Q}^\perp$. From all of the above we conclude that the spectrum of E is

$$\sigma(E) = \sigma(E|_{\mathcal{Q}}) \cup \sigma(E|_{\mathcal{Q}^\perp}).$$

We know that $\mathcal{Q}$ contains a one dimensional center subspace corresponding to direction of propagation of the stall solution and the rest of $\mathcal{Q}$ belongs to the stable subspace of E. Furthermore, $\mathcal{Q}$ has a complete basis of eigenvectors. If λ_n is a non-zero eigenvalue of E with an eigenvector χ_n, then $\mathrm{e}^{\lambda_n t}\chi_n(\eta)$ is a solution of the full linearized system in the rotating reference frame. Then $\mathrm{e}^{\lambda_n t}\chi_n(\theta - \frac{1}{2}t)$ is a solution of the full linearized system in the fixed reference frame. This solution gives us an eigenvalue of the linearized Poincaré map $\mu_n = \mathrm{e}^{4\pi\lambda_n}$ with the corresponding eigenvector χ_n.

If the 3×3 matrix $E_{\mathcal{Q}^\perp}$ has three eigenvectors, then we have the complete spectrum of the linearized Poincaré map. In particular, if $E_{\mathcal{Q}^\perp}$ has an eigenvalue with a positive real part, then the linearized Poincaré map will have an eigenvalue outside the unit disk and the periodic orbit is unstable. Let us now assume that all eigenvalues of $E_{\mathcal{Q}^\perp}$ have negative real parts. If one of these eigenvalues has algebraic multiplicity not equal to its geometric multiplicity, then there exist solutions with initial conditions in $\mathcal{Q}^\perp$ that have the growth $p(t)\mathrm{e}^{\lambda t}$, where $p(t)$ is a polynomial of degree at most 2. The exponential decay will win over the polynomial growth in time. Thus, if the linearized Poincaré map turns out to have an eigenvalue that lies outside the open unit disk, we can instead consider the m-th iterate of the Poincaré map and for m large enough it will have all eigenvalues in a closed subset of the open unit disk. We conclude that the stall solution is asymptotically orbitally stable. $\square$

Above we carried out the stability analysis for the first traveling wave solution. We can do the same for the other traveling wave solutions and it turns out that their stability again depends on the eigenvalues of $E|_{\mathcal{Q}^\perp}$. Note, however, that we are abusing the notation slightly because $\mathcal{Q}^\perp$ changes from one traveling wave solution to the next, as does E.

Let us now calculate the entries of the 3×3 matrix $E|_{\mathcal{Q}^\perp}$ for the j-th traveling wave solution. By the proof of Proposition 3.15 we know that $\mathcal{Q}\subset Ker(\overline{\psi_c'})$, so we only need to calculate the action of $\overline{\psi_c'}$ on $\mathcal{Q}^\perp$. To this end consider

$$\begin{aligned}\overline{\psi_c'}(\wp-\bar{\wp},0,0) &= \tfrac{\mu_j}{2\pi}\int_0^{2\pi}(-3b(\wp-e_2)+c)(\wp-\bar{\wp})d\theta\\ &= \tfrac{\mu_j}{2\pi}\int_0^{2\pi}-\tfrac{b}{2}(\wp^2-\tfrac{1}{2}g_2)-\tfrac{b}{4}g_2+3b\wp\bar{\wp}d\theta\end{aligned}$$

where we have added and subtracted $\frac{b}{4}g_2$ and integrated out a constant multiple of $\wp - \bar{\wp}$. By using the identity $\wp'' = 6\wp^2 - \frac{1}{2}g_2$ and the fact that $\wp'$ is periodic, we get

$$\begin{aligned} &= \frac{\mu_j}{2\pi}\int_0^{2\pi} -\frac{b}{2}\wp'' - \frac{b}{4}g_2 + 3b\wp\bar{\wp}d\theta \\ &= \frac{b\mu_j}{4}(12\bar{\wp}^2 - g_2). \end{aligned}$$

Operating on the other two vectors is simpler

$$\begin{aligned} \overline{\psi_c'}(0,1,0) &= \mu_j(3be_2 + c - 3b\bar{\wp}) \\ \overline{\psi_c'}(0,0,1) &= 0. \end{aligned}$$

We now calculate

$$\begin{aligned} (\nu\frac{\partial^2}{\partial\eta^2} + \psi_c')(\wp - \bar{\wp}, 0, 0) &= \frac{b\mu_j}{2}(\frac{\partial^2}{\partial\eta^2} - 6\wp + 6e_2 + \frac{2c}{b\mu_j})(\wp - \bar{\wp}) \\ &= \frac{b\mu_j}{2}(\wp'' - 6\wp^2 + 6\wp\bar{\wp}) + \frac{b\mu_j}{2}(6e_2 + \frac{2c}{b\mu_j})(\wp - \bar{\wp}) \\ &= \frac{b\mu_j}{2}(-\frac{1}{2}g_2 + 6\wp\bar{\wp} + (6e_2 + \frac{2c}{b\mu_j})(\wp - \bar{\wp})). \end{aligned}$$

This allows us to write down the 3×3 matrix

$$E|_{\mathcal{Q}^\perp} = \begin{bmatrix} 3b\mu_j(\bar{\wp} + e_2) + c & -3b\mu_j & 0 \\ \frac{b\mu_j}{4l_c}(12\bar{\wp}^2 - g_2) & \frac{\mu_j}{l_c}(c - 3b(\bar{\wp} - e_2)) & -\frac{1}{l_c} \\ 0 & \frac{1}{4l_cB^2} & -\frac{\gamma}{4l_cB^2}(F_T^{-1})' \end{bmatrix}.$$

Note here that $e_1 \geq e_3 \geq e_2$ are the stationary values of $\wp(\cdot, k_j)$. Because the real period of $\wp$ scales in a simple way with j, one can show that if $e_i(1)$ are the stationary values of $\wp(\cdot, k(\bar{c}_1))$ then $e_i = \frac{e_i(1)}{j}$. Thus, we see that the stationary values e_i and g_2 change in a very simple way with j. Once the constants of integration $\bar{c}_j$ have been determined, the matrix is fully determined and its eigenvalues can be readily calculated.

Figure 3.5 shows a plot of the largest real part of the eigenvalues of the matrix $E|_{\mathcal{Q}^\perp}$ as a function of the parameter B. Here we have chosen the eddy viscosity constant in such a way that there exist exactly three stall solutions. Notice how their stability becomes marginal as the constant B is increased. This could indicate that their basins of attraction are shrinking because the basin of attraction for the surge component is growing.

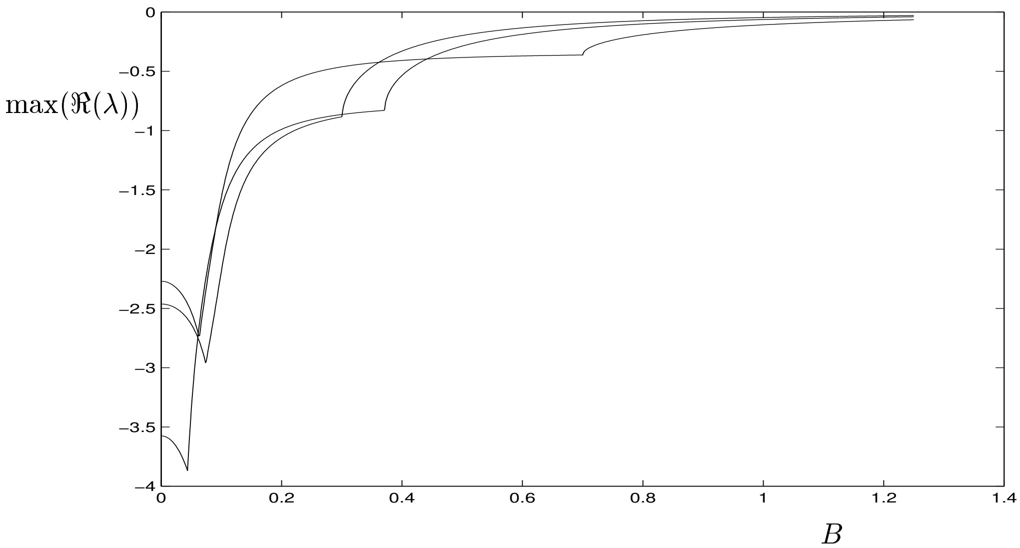

Figure 3.5: *The largest real part of the eigenvalues of the matrix* $E|_{\mathcal{Q}^\perp}$ *plotted for the three stall cell solutions as a function of the parameter* B.

Remark 3.16 The fact that the dynamics close to the stall solution decouple into a 3×3 system and a stable system as described in Proposition 3.15 has some interesting implication for control as we shall see in Chapter 5.

3.3.5 Comparison with KL Analysis

Proposition 3.15 implies that if one wants to try to capture the dynamics of the vMG equation by a Galerkin truncation, then a good choice of basis would include the stall solutions as well as the eigenvector which couples the linear flow near the stall solution to the two ODEs, namely $\chi = (\wp - \bar{\wp}, 0, 0)$.

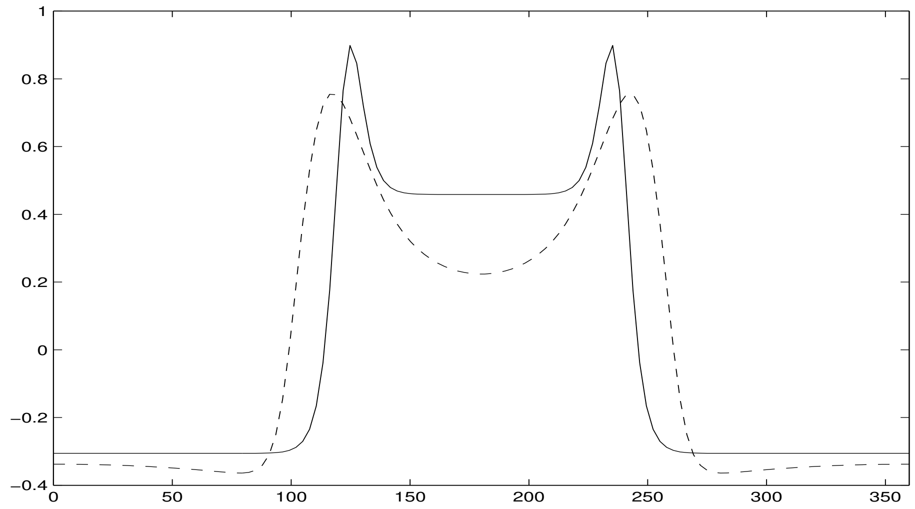

Figure 3.6: *The first KL mode with the dashed line and a linear combination of the stall solution and* χ *with the solid line.*

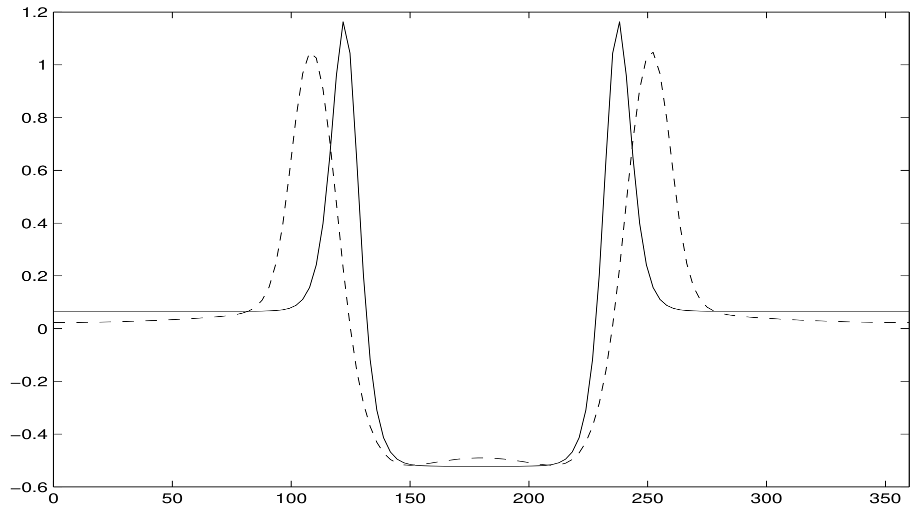

Figure 3.7: *The second KL mode with the dashed line and a linear combination of the stall solution and* χ *with the solid line.*

A considerable research effort has been focused on finding good model reductions of complicated dynamical systems. Karhunen-Loève decomposition or KL analysis is a method that has been frequently applied to the problem of finding a good set of basis functions to make a Galerkin projection onto. It picks out from data the modes which are statistically most important. The data can originate from either simulations or empirical measurements. Since the basic attractor attracts all solutions with initial conditions in a prevalent set, these modes typically capture a component of the basic attractor and how the spatial structure of that component can vary.

The data, to which we want to apply the KL analysis, can be represented by a set of points $x(t) \in \mathbb{R}^n$, where $t \in \{t_0, t_1, t_2, ..., t_N\}$. Then $x(t_i)$ represents the i-th measurement of the system or its value at the i-th timestep. One then performs a principal component analysis of this data to find how well it may be approximated by a projection onto a k-dimensional subspace of the original n-dimensional state space.

A subspace $S \subset \mathbb{R}^n$ can be characterized by the projection operator P mapping $\mathbb{R}^n$ onto S. The object then becomes to find P to minimize the functional

$$H(P) = \sum_{i=1}^{N} \langle x(t_i) - Px(t_i), x(t_i) - Px(t_i) \rangle$$

which measures the total square perpendicular distance of the points from the k-plane S. The following result is well known

Theorem 3.17. (Total Least Squares) *Let R be the correlation matrix of the data, defined by*

$$R = \sum_{i=1}^{N} x(t_i)x(t_i)^*$$

and let $\lambda_1 \geq \lambda_2 \geq ... \geq \lambda_n$ be the ordered eigenvalues of R. Then

$$\min_P H(P) = \sum_{i=n-k+1}^{n} \lambda_i$$

where the minimum is over all rank k projections P.

Now let $s = \text{rank}R$ and let $\phi_1, \phi_2, ..., \phi_s$ denote the orthonormal eigenvectors of R corresponding to nonzero eigenvalues λ_i. Each $x(t_i)$ can be written as

$$x(t_i) = \sum_{j=1}^{s} a_{ij}\phi_j$$

where $a_{ij} = \langle x(t_i), \phi_j \rangle$. The optimal k-dimensional subspace approximant is given by

$$\hat{x}(t_i) = \sum_{j=1}^{k} a_{ij}\phi_j.$$

Let us denote by Q the $k \times n$ matrix whose rows are $\phi_1, ..., \phi_k$, so that $QQ^* = I$. The projected approximant to x is given by $Q^*Qx \in S$, and $y = Qx$ is a representation in terms of the new coordinates ϕ_i on S. This subspace approximant is then optimal, in the sense that the total energy (2-norm) in the subspace is given by

$$\sum_{i=1}^{N} \langle Qx(t_i), Qx(t_i) \rangle = \sum_{j=1}^{k} \lambda_j$$

and this is the maximum achievable by a k-plane. $\phi_1, ..., \phi_k$ span this optimal subspace S and we refer to ϕ_i as the i-th KL mode.

Sonja Glavaski [28] has done KL analysis on a PDE simulation of the vMG equation and calculated the first two modes for a solution that starts near design flow and converges to stall. One would expect the linear span of these two modes to be close to the span of the stall solution and χ. Indeed this is the case as can be seen in Figure 3.6 and Figure 3.7, which show the KL modes along with a rough fit by a linear combination of the stall solution and the mode χ.

The first two KL modes represent 92 percent of the energy. In this comparison one must bear in mind that the KL modes are meant for representing the solution throughout all of the transient whereas one would expect the stall solution and χ to represent the solution well when it is close to the stall solution. This explains why the span of the two KL modes does not match the span of φ and χ exactly. However, the agreement is quite good.

3.3.6 Relaxing the Assumptions $K = I$ and $\gamma = \gamma_*$

Our goal in this section is to prove that when $E_{Q^\perp}$ has no eigenvalues on the imaginary axis, then for K close to the identity and γ close to γ_*, there exists a unique stall solution close to the special one already constructed which has the same stability properties. This follows from the Implicit Function Theorem. Recall that by making $am = 0$ we set $K = I$.

Theorem 3.18. *Let $\bar{x}$ be a stall solution given by Proposition 3.13 and assume that the eigenvalues of $E_{Q^\perp}$ lie off the imaginary axis. There exists a neighborhood V of $(\gamma_*, 0) \in \mathbb{R}^2$ and a neighborhood U of $\bar{x} \in X$ such that for any $(\gamma, am) \in V$ there exists a unique periodic solution $x \in U$. Furthermore, x is asymptotically stable (unstable) if $\bar{x}$ is asymptotically stable (unstable).*

Proof: We already showed in [15] that the solutions of (2.6 -2.8) depend smoothly on the parameters γ and am. We conclude that the Poincaré map will also depend smoothly on these parameters.

Our strategy is now to apply the Inverse Function Theorem to the Poincaré map, P, associated with $\bar{x}$. $\bar{x}$ is a fixed point for P and P linearized about this solution, $DP(\bar{x})$, has a spectrum that is bounded away from the unit circle. In particular it is bounded away from 1 and thus $DP(\bar{x}) - I$ is invertible with a bounded inverse. It now follows from the Implicit Function Theorem that there exists a continuous two parameter family of fixed points of P, $\{x\}_{(\gamma,am)\in V}$. For each $(\gamma, am) \in V$ the fixed point x is a periodic solution of (2.6-2.8).

If $E_Q^\perp$ has eigenvalues with negative real parts then $DP(\bar{x})$, or the linearization of some iterate of P, will be a contraction, i.e. there exists a constant $0 \leq \beta < 1$ such that $\|DP(\bar{x})y_0\| \leq \beta\|y_0\|$ for all y_0. Since P depends smoothly on (γ, am), so does DP. In particular, by taking V small enough we can guarantee that $\|DP(\bar{x}) - DP(x)\| \leq \frac{1-\beta}{2}$. We can now conclude that

$$\|DP(x)y_0\| \leq \beta\|y_0\| + \frac{1-\beta}{2}\|y_0\| < \frac{1+\beta}{2}\|y_0\|,$$

i.e. $DP(x)$ is also a contraction. It follows that the orbit x is asymptotically orbitally stable.

Assume now that $E_Q^\perp$ has an eigenvalue λ with a positive real part. The eigenvalue of $DP(\bar{x})$ corresponding to λ will be an isolated eigenvalue outside the unit disk. Since $DP(x)$ is a relatively bounded perturbation of $DP(\bar{x})$, any isolated eigenvalue will depend continuously on (γ, am) (see Kato [42]). Hence, by making V small enough we guarantee that $DP(x)$ has an eigenvalue outside the unit disk and x is an unstable orbit. □

3.3.7 Numerical Simulations of Stall

In this section we present numerical simulations of stall in four different cases: Figure 3.8 shows $\gamma = \gamma_*, K = I$, Figure 3.9 shows $\gamma = \gamma_*$ and a general K, Figure 3.10 shows a general γ and $K = I$ and finally Figure 3.11 shows both general γ and

K. The pictures on the left show the final stall disturbance as a function of angle and the pictures on the right show how the average flow and pressure rise behave as functions of time. These four different cases give a good indication of how the the two parameters γ and am affect the shape of the traveling wave solution.

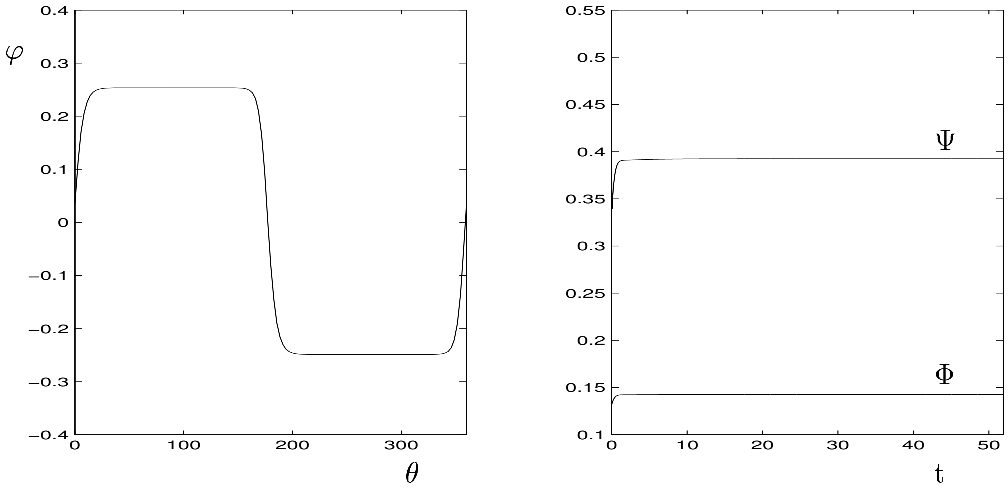

Figure 3.8: *The stall cell when* $\gamma = \gamma_*$ *and* $K = I$.

Note that by choosing the modulus correctly in the Jacobi ns function, one can make it fit the above stall shape well.

These numerical solutions are calculated using a Lax-Wendroff finite difference scheme for equation (2.6) coupled with a Runge Kutta scheme for the equations (2.7) and (2.8). The spatial resolution for the variable φ is 128 points. The initial conditions are set so that φ has the shape of a sinus wave with small amplitude to seed the instability. We let the simulation run for a long time and then take a snapshot of the stall cell when it has settled.

Increasing γ tends to make the trough be deeper and narrower, whereas decreasing it will do the opposite. We only display what happens for $\gamma \geq \gamma_*$, but Remark 4.1 shows that there exists a certain symmetry property for the stall solutions. As a result it suffices to calculate the stall shapes for $\gamma \geq \gamma_*$. Increasing am tends to skew the shape of the traveling wave. The case for $am < 0$ is not of physical interest so we omit it here.

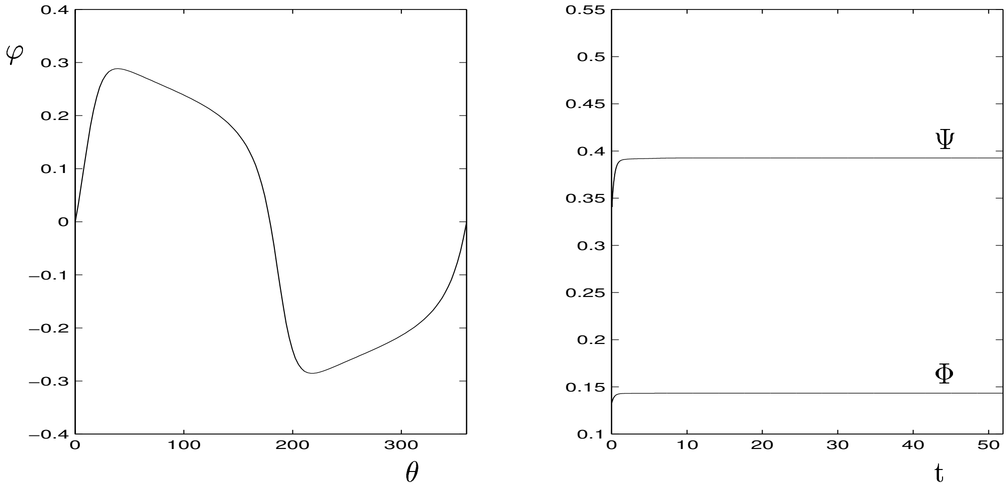

Figure 3.9: *The stall cell when $\gamma = \gamma_*$ and K is not the identity.*

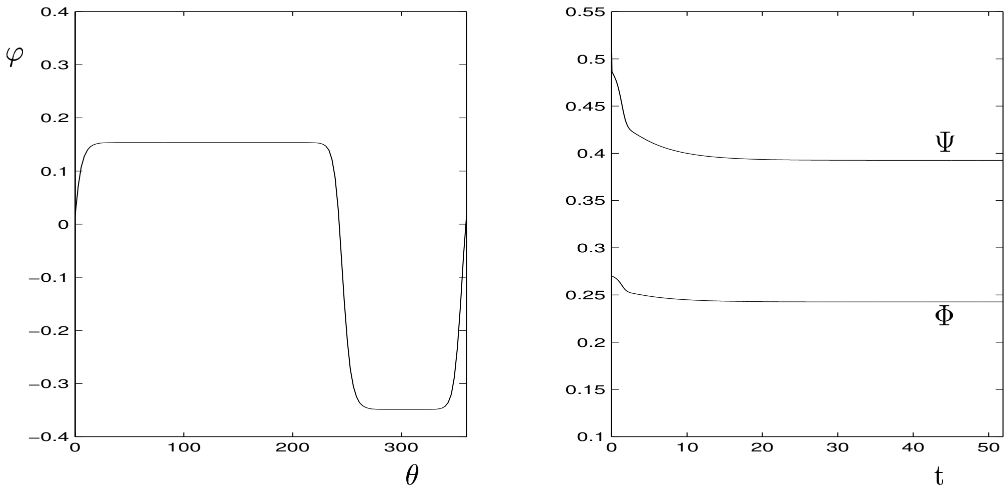

Figure 3.10: *The stall cell when γ is not equal to γ_* but $K = I$.*

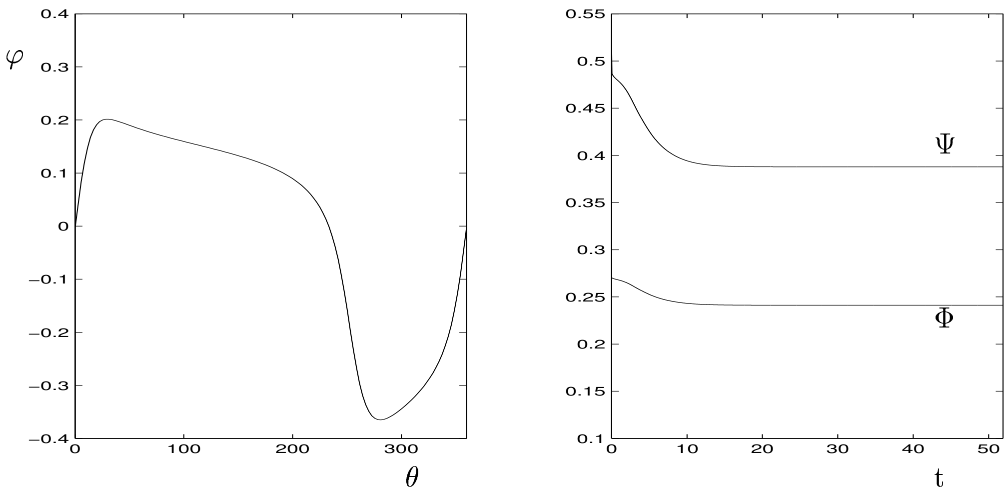

Figure 3.11: *The stall cell when γ is arbitrary and K is not the identity.*

In general the speed of the traveling wave is going to depend on the parameters am and γ. We calculated this speed numerically and Figure 3.12 shows the results of these runs. It indicates that the value of γ has little effect on the propagation velocity, whereas the value of am has a considerable effect on the velocity. The velocity here is measured in revolutions per time unit.

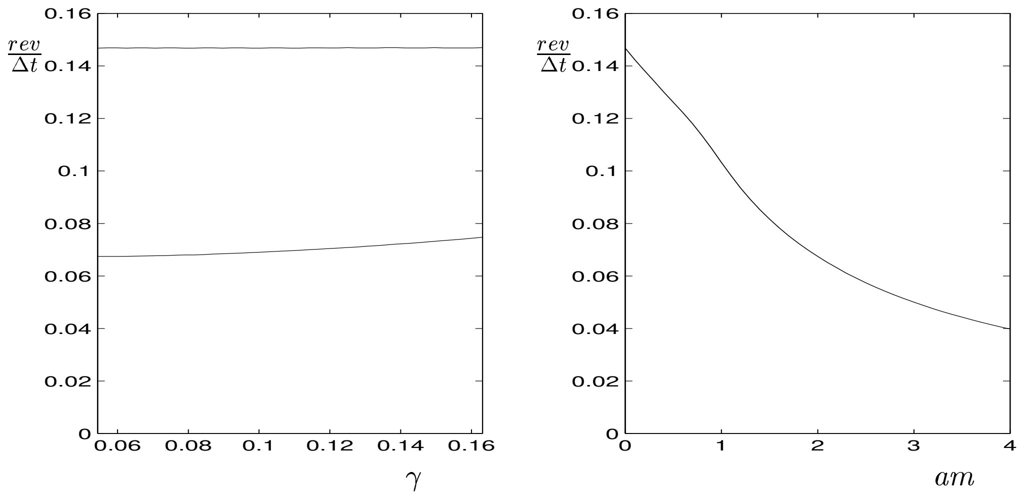

Figure 3.12: *The velocity of the traveling wave as a function of the parameters.*

The left hand picture in Figure 3.12 shows the propagation velocity of the traveling wave as a function of γ first for $am = 0$, i.e. $K = I$, (the higher curve) and then for $am = 2.0$ (the lower curve). This plot indicates that the velocity does not depend strongly on γ for γ close to γ_*. On the right hand side we plotted the propagation velocity as a function of am for $\gamma = \gamma_*$. This shows that the velocity changes considerably with am.

A curious observation is that the value of am also affects the growth rate of the initial disturbance, as it grows into a stall cell. Larger am has a damping effect on the growth.

It is clear from the stability results in the previous section as well as from the numerical simulations here that the operator K^{-1} plays a minor role in the dynamics of the vMG equation. We will therefore ignore it altogether from now on.

3.4 Constructing the Global Attractor

In the special case when $0 < B \ll 1$, we can use the methods of singular perturbation theory to split the system up into a fast system and a slow system. As we have seen, the basic attractor $\mathcal{B}$ has no surge component in this case and it turns out that we can completely construct the global attractor of the slow system $\mathcal{A}_s$. When B is small enough, the slow system attracts all of state space, up to at most a shy set. The basic attractor is therefore contained in $\mathcal{A}_s$ and the analysis of $\mathcal{A}_s$ will give us important information about $\mathcal{B}$ and its bifurcations.

When $\gamma = \gamma_*$, then either design flow is stable and there are no stall solutions or the design flow is unstable and we have one or more stall solutions. One would hope that in this case $\mathcal{A}_s$ contains only the design flow if no stall solutions exist, and when stall solutions do exist, $\mathcal{A}_s$ is composed of the design flow, the stall solutions and the connections between design flow and the stall solutions. As we shall see here below this is indeed the case.

Let $x = (\varphi, \Phi, \Psi)$ be a solution of equation (5.1) and assume that $0 < B \ll 1$. For now we consider just the two ODEs

$$\begin{aligned} \frac{d\Phi}{dt} &= \frac{1}{l_c}(\overline{\psi_c} - \Psi) \\ \frac{d\Psi}{dt} &= \frac{1}{4l_cB^2}(\Phi - \gamma F_T^{-1}(\Psi)) \end{aligned}$$

Since we have a global attractor, we know that $\Phi(t) + \varphi(t)$ will eventually stay bounded and hence $\overline{\psi_c}$ will eventually stay bounded. We can therefore consider the above system as a singular system, see Jones [41]. To a leading order in B we have a fast system

$$\frac{d\Psi}{dt} = \frac{1}{4l_cB^2}(\Phi - \gamma F_T^{-1}(\Psi)) \tag{3.9}$$

where Φ is considered a constant. And a slow system given by

$$\frac{d}{dt}\Phi = \frac{1}{l_c}(\overline{\psi_c} - \Psi) \tag{3.10}$$

$$\Phi = \gamma F_T^{-1}(\Psi). \tag{3.11}$$

If B is small enough, the slow system should be a good approximation to the original system. In other words, $(\Phi(t), \Psi(t))$ will have to lie on the parabolic curve in Figure 3.1. The equations governing the flow will then be

$$\frac{\partial}{\partial t}\varphi = \nu\frac{\partial^2}{\partial\eta^2}\varphi + \psi_c(\Phi + \varphi) - \overline{\psi_c} \tag{3.12}$$

$$\frac{d}{dt}\Phi = \frac{1}{l_c}(\overline{\psi_c} - F_T(\frac{\Phi}{\gamma})). \tag{3.13}$$

Before we go further, let us make the following definition.

Definition 3.19. *An analytic semigroup $T(t) : X \to X$, $t \geq 0$ is said to be a* gradient system *if*

1. *Each bounded trajectory is precompact.*

2. *There exists a Lyapunov function for $T(t)$, i.e. there is a continuous function $V : X \to \mathbb{R}$ such that V is bounded below, $V(x) \to \infty$ as $\|x\| \to \infty$, $V(T(t)x)$ is nonincreasing in t for all $x \in X$ and if $V(T(t)x) = V(x)$ for all t, then x is a stationary solution.*

We want to show that equations (3.12) and (3.13) form a gradient system. Because there exists a global attractor which is compact, each trajectory of the equation will be precompact. A Lyapunov function for this system is given by

$$V(\varphi, \Phi) = \frac{\nu}{2}\langle \varphi_\eta, \varphi_\eta \rangle - \int_0^{2\pi} \int_0^{\Phi+\varphi} \psi_c(s) ds d\theta + \gamma \int_0^{\Phi/\gamma} F_T(s) ds$$

The second term is a fourth order polynomial in $(\Phi + \varphi)$ with a positive leading coefficient. The third term behaves like a cubic polynomial and is dominated by the second term, hence $V \to \infty$ as $\|\Phi + \varphi\| \to \infty$. Furthermore, V is bounded from below. The time derivative of V is given by

$$\begin{aligned}
\dot{V} &= \nu\langle \varphi_\eta, \varphi_{\eta t} \rangle - \langle \psi_c(\Phi + \varphi), \frac{d}{dt}\Phi + \frac{\partial}{\partial t}\varphi \rangle + F_T(\frac{\Phi}{\gamma})\frac{d}{dt}\Phi \\
&= -\nu\langle \varphi_{\eta\eta} + \psi_c(\Phi + \varphi) - \overline{\psi_c}, \varphi_t \rangle - \frac{d}{dt}\Phi(\overline{\psi_c} - F_T(\frac{\Phi}{\gamma})) \\
&= -\|\varphi_t\|^2 - (\frac{d}{dt}\Phi)^2
\end{aligned}$$

and hence it is negative semi-definite. Furthermore, if $\dot{V}(\varphi, \Phi) = 0$, then φ must satisfy the equation

$$0 = \nu \frac{\partial^2}{\partial \theta^2}\varphi + \psi_c(\Phi + \varphi) - \overline{\psi_c} \tag{3.14}$$

and Φ must be constant. In the special case when $\gamma = \gamma_*$ we have already analyzed this equation and its solutions are the design flow (zero) solution and the stall cell solutions. These solutions are stationary solutions in this rotating frame of reference and hence equations (3.12) and (3.13) form a gradient system.

We recall a Theorem that can be found in Hale [34],

Theorem 3.20. *Let $T(t)$ be a gradient system and let $\mathcal{E} = \{x \in X | \dot{V}(x) = 0\}$ is bounded, then the global attractor of T consists of $\mathcal{E}$ and its unstable manifold, i.e. $\mathcal{A}_s = \mathcal{E} \cup W^u(\mathcal{E})$.*

Using the above Theorem we can deduce the following

Corollary 3.21. *Assume that $0 < B \ll 1$ and $\gamma = \gamma_*$. Then the global attractor $\mathcal{A}_s$ of the slow system consists of design flow if $c < \nu$ and if $n < [\sqrt{\frac{c}{\nu}}]n + 1$ it consists of design flow, n stall solutions and the connections between the design flow and the stall solutions.*

Proof: Recall that $c = \max_{s \in \mathbb{R}} \psi_c'(s)$. According to Proposition 3.13 there exist exactly n stall solutions when n is an integer such that

$$n < \sqrt{\frac{c}{\nu}} \leq n + 1.$$

Furthermore, these stall solutions are all stable. If $n = 0$, then design flow is the only solution of equation (3.14) and it is stable. Hence the global attractor is just the design flow. If $n > 0$ then design flow is unstable and it is the only unstable solution of equation (3.14). The unstable eigenspace is spanned by $\{(\sin(j\eta), 0, 0), (\cos(j\eta), 0, 0) | j = 1, ..., n\}$. Let us now take a shooting manifold starting at design flow, which is parallel to $span\{(\sin(j\eta), 0, 0), (\cos(j\eta), 0, 0)\}$. The subspace of $2\pi/j$ periodic solutions is invariant under the flow and hence the shooting manifold must remain within that space. It can therefore only connect with stall solutions which are $2\pi/k$ periodic, where $k = jm$ for some natural number m.

Consider now equation (3.12) for a given $\Phi(t)$. This is a nonlinear parabolic equation which has the property that the number of local maxima and local minima is nonincreasing as a function of time. From this we can conclude that $m = 1$ and hence the shooting manifold must connect with the j-th stall solution.

By Theorem 3.20 we have now that the global attractor consists of design flow if $n = 0$ and of design flow and n stall solutions and the connections from design flow to these stall solutions if $n > 0$. $\square$

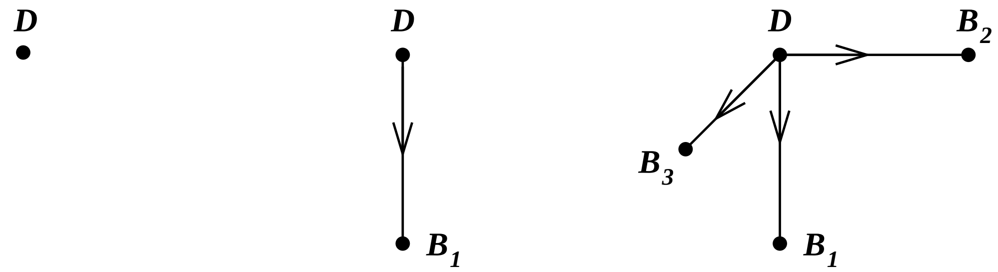

Figure 3.13: *The global attractor for small B and $\gamma = \gamma_*$.*

Figure 3.13 shows what the global attractor looks like schematically in the case $0 < B \ll 1$, $\gamma = \gamma_*$. $\mathcal{B}_1$, $\mathcal{B}_2$ and $\mathcal{B}_3$ represent the first three stall solutions and $\mathcal{D}$ represents design flow. When the eddy viscosity coefficient ν is large, design flow is stable and no stall solutions exist. This is depicted to the left in Figure 3.13. When ν gets smaller one ore more stall solutions emerge and are stable. Design flow becomes unstable and the global attractor contains these solutions and the connections between design flow and stall, see the middle and right of Figure 3.13.

Chapter 4

The Flow on the Basic Attractor

A primary goal of the current jet engine research is to be able to control the flow through the engine. In order to facilitate good control design, a meaningful model reduction is needed. Galerkin approximations using the first Fourier harmonic mode have been able to describe the flow qualitatively, but not quantitatively, see [59] and [56]. Some results have also been obtained using multiple Fourier modes, see Humbert and Krener [38] and Mansoux *et al.* [53], but it is clear from these studies that a better reduced order model is needed. It has been suggested to make a Galerkin approximation with a more general basis than the Fourier basis. This basis could for example be composed of the stall solution we have calculated here along with its first eigenvectors.

The disadvantage of making a Galerkin truncation onto a function with a fixed spatial shape is that such projections do not describe properly how the stall cells seem to grow and decay in simulations. What one observes there is that the stall cell quickly develops a square like spatial structure with a fixed depth. This square structure then widens until it stabilizes at a fixed width or it fills the whole annulus of the compressor which goes into surge. Furthermore, one would want this low order model to capture the dynamics for various throttle settings γ, but the shape of the stall cell depends strongly on the throttle setting. To capture this behaviour with modes of fixed spatial shape one needs to include many modes and the behaviour of the amplitudes of these modes can be very complicated, see Humbert and Krener [38].

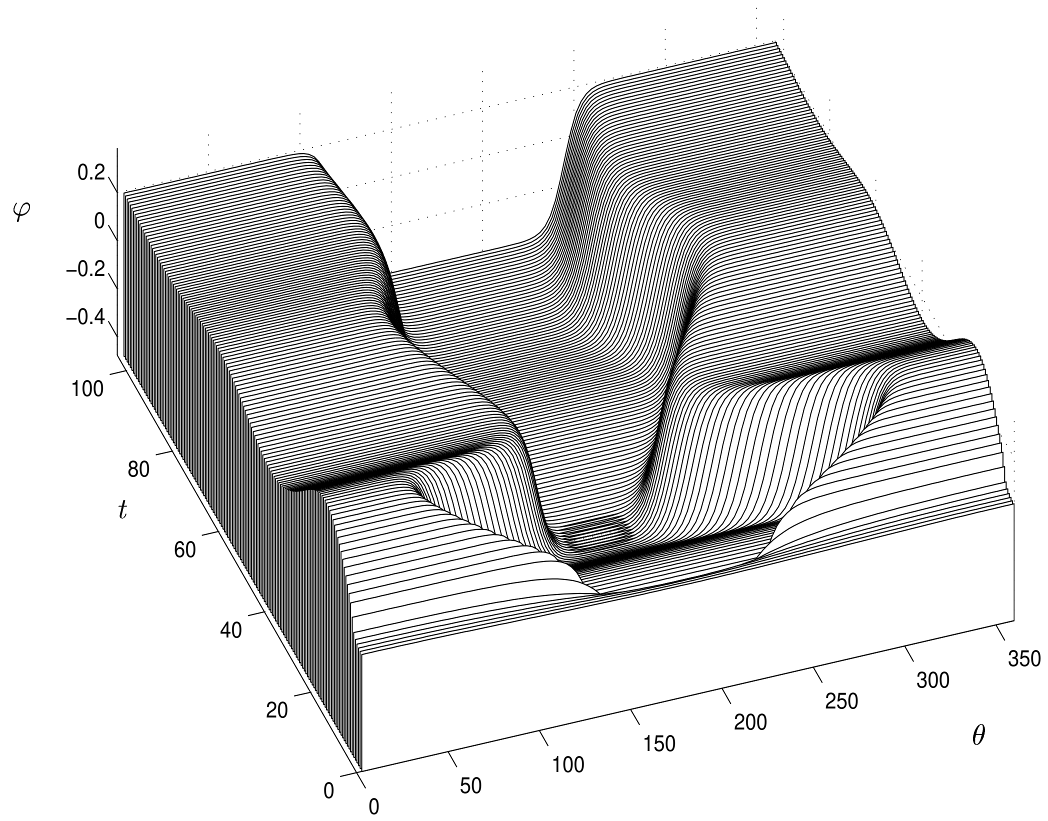

Figure 4.1: *The transient behavior of the deviation, φ, of the flow from the angular averaged flow, Φ, as the system goes into stall. Notice how the spatial structure of the deviation changes; there is a square like dip which widens or shrinks, but its depth stays the same.*

The remedy we want to propose here, is to try to capture the dynamics with a one parameter family of curves. The parameter then determines not only the amplitude, as it does in usual Galerkin truncations, but also the shape of the stall cell.

In Section 4.1 we find explicitly the general stall shape which can be represented as a rational function of the Jacobi elliptic function ns. In fact we find a one parameter family of stall shapes. Section 4.2 constructs a third order model based on the one parameter family of stall shapes found in the previous section. This lower order model is obtained by projecting the full equation onto the one parameter family. Section 4.2.1 contains numerical simulations of the lower order model and compares it with numerical simulations of the full viscous Moore-Greitzer equation. An algebraic reduced order model is presented in Section 4.2.2 and in Section 4.2.3 we describe some possible extensions of the work presented here.

4.1 General Stall Solutions

We have already proven that for γ close to γ_* there exists a one parameter family of traveling wave solutions to the system (3.3.3) and that they are stable. Here we extend this analysis for a general γ and again we obtain an explicit formula for the shape of the stall solution. For $\gamma \neq \gamma_*$ the heteroclinic orbit in Figure 3.4 breaks up, but a homoclinic orbit is formed. Inside this homoclinic orbit there exist again the periodic solutions that we seek, see Figure 4.2.

Solving the two algebraic equations in (3.3.3) we get that $\overline{\psi_c} = \Phi^2/\gamma^2$ and the task we are now faced with, is to find all periodic solutions of

$$0 = \nu\varphi'' + \psi_c(\Phi + \varphi) - \Phi^2/\gamma^2$$

with the correct period. The parameters one can vary are Φ and γ. Since we have

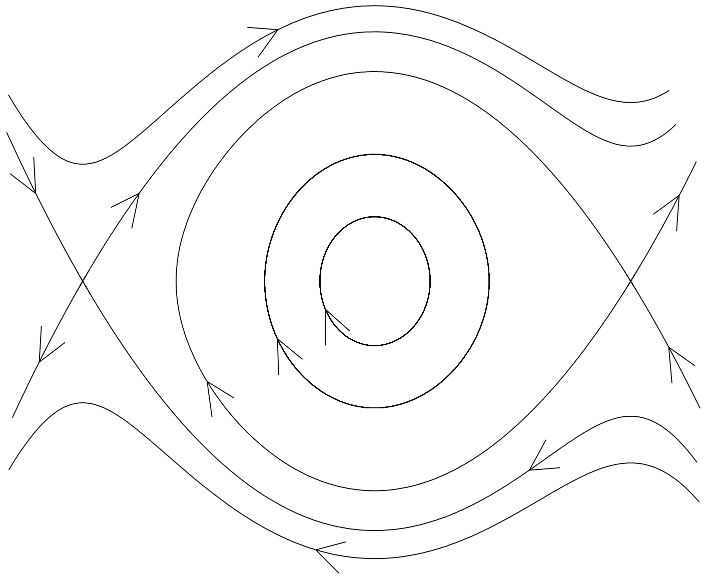

Figure 4.2: *The phase portrait for the Duffing's equation when $\gamma \neq \gamma_*$.*

two parameters and just one constraint we get in general a one parameter family of solutions, which is the same one parameter family that was proven to exist for γ close to γ_* earlier.

Now let us multiply through this equation with φ' and integrate it once to get

$$\frac{1}{2}(\varphi')^2 = \frac{1}{2}(\varphi_0')^2 + \frac{1}{\nu}\int_0^{\varphi} \psi_c(\Phi + s) - \Phi^2/\gamma^2 ds$$

where φ_0' denotes the derivative of the solution at a point where the solution is zero (i.e. the point we started the integration at).

The right hand side will be a general fourth order polynomial in φ. We know that at least for γ close to γ_* this polynomial will have four distinct real roots. There exists a change of coordinates of the form

$$y = \frac{\varphi - p}{\varphi - q} \qquad \text{or} \qquad y = \varphi - p$$

which transforms this equation to

$$\frac{1}{2}(y')^2 = (p-q)^2(A_1 y^2 + B_1)(A_2 y^2 + B_2).$$

Because the original polynomial had real roots the constants can be chosen such that $A_1, A_2 > 0$ and $B_1, B_2 < 0$. The last equation can then be integrated and we get

$$y(\eta) = \sqrt{\frac{-B_2}{A_2}} sn(\eta(p-q)\sqrt{-B_1 A_2}, \sqrt{\frac{B_2 A_1}{B_1 A_2}})$$

or substituting back for y

$$\varphi(\eta) = \frac{p - q\sqrt{\frac{-B_2}{A_2}} sn(\eta(p-q)\sqrt{-B_1 A_2}, \sqrt{\frac{B_2 A_1}{B_1 A_2}})}{1 - \sqrt{\frac{-B_2}{A_2}} sn(\eta(p-q)\sqrt{-B_1 A_2}, \sqrt{\frac{B_2 A_1}{B_1 A_2}})}.$$

When p and q have been determined numerically the shape of the stall cell will be completely determined. We can now make the same transformation as before and translate the argument into the complex plane and substitute ns for sn.

$$\varphi(\eta) = \frac{p - q\sqrt{\frac{-B_2}{A_2}} ns(\eta(p-q)\sqrt{-B_1 A_2} + i\hat{\omega}_2, \sqrt{\frac{B_2 A_1}{B_1 A_2}})}{1 - \sqrt{\frac{-B_2}{A_2}} ns(\eta(p-q)\sqrt{-B_1 A_2} + i\hat{\omega}_2, \sqrt{\frac{B_2 A_1}{B_1 A_2}})}.$$

It turns out that determining the constants p and q numerically is a very sensitive calculation due to the fact that modulus k of the elliptic functions is close to identity. The fronts of the ns function are very sensitive to the modulus when it is close to the identity. A simpler way to calculate this one parameter family is to obtain it from simulations of the full system (2.6)-(2.8). In this way one can calculate the shape of all the stable stall cells. The unstable ones are approximated by scaling down the amplitude of the smallest stable one. The resulting surface for the single cell stall solutions can be seen in Figure 4.3.

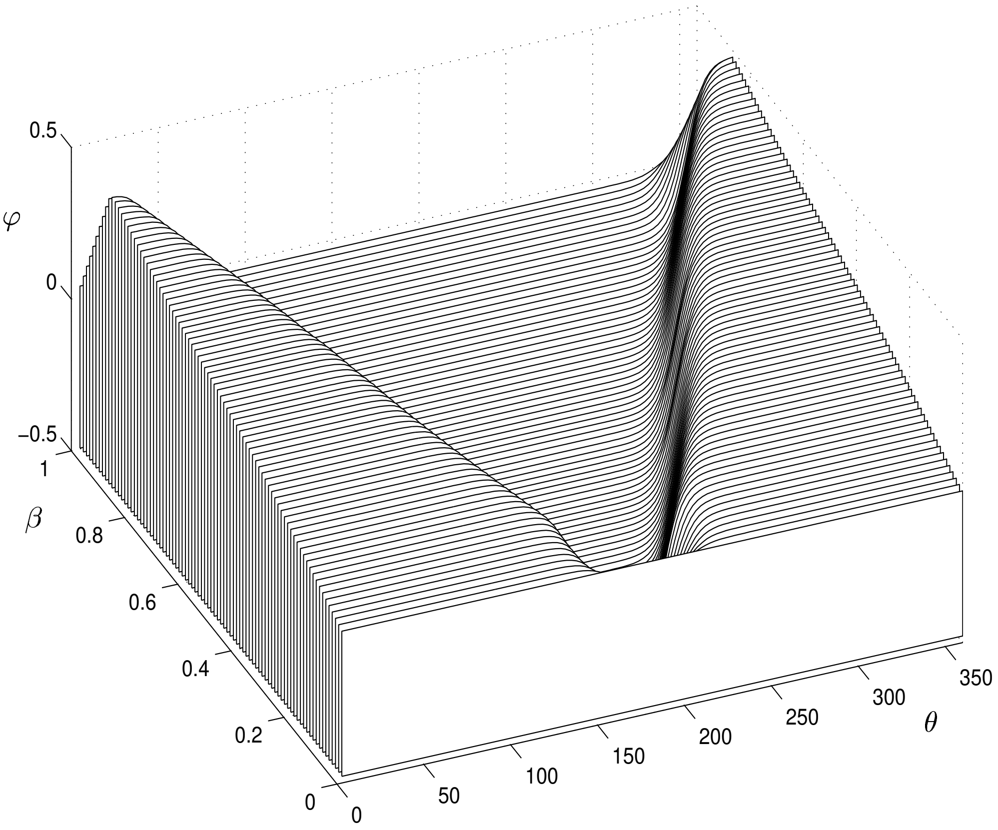

Figure 4.3: *The one parameter family of stall cells. As the parameter β varies from zero to one the stall cells grows from zero to a narrow stall cell that slowly widens until it fills out the annulus and the stall disturbance becomes zero again.*

Remark 4.1 The following observation is helpful when calculating the one parameter family: The family has a certain symmetry property, namely, if (φ, Φ, Ψ) is a stall solution for $\gamma > \gamma_*$, then $(-\varphi, 2\Phi_* - \Phi, 2\Psi_* - \Psi)$ is a stall solution for some $\gamma < \gamma_*$. This is due to the fact that the compressor characteristic ψ_c is a cubic polynomial which is an odd function about the point (Φ_*, Ψ_*). It therefore suffices to calculate the surface for $\gamma > \gamma_*$.

4.2 Model Reduction

We have now determined the one parameter families which describes the stall shape for all stall solutions. Let us for now assume that the union attractor $\cup_{\gamma\geq\gamma_*}\mathcal{B}(\gamma)$ has only one stall component. The next step is to project the solution of (2.6) onto this one parameter family and obtain an evolution equation for the parameter. The parameter determines not only the amplitude, as it does in usual Galerkin truncations, but also the shape of the stall cell. One can describe the stall cell with a one parameter family of curves of the form

$$\varphi(t,\theta) = h(\beta(t), \frac{1}{2}t - \theta) = h(\beta, \eta).$$

Using the differential equation for φ (2.6) a differential equation for the parameter β can be derived. From now on $\frac{d}{dt}$ will be denoted by a dot and partial derivatives by a subscript. First observe that if we denote the second coordinate in h with η then

$$\varphi_t + \frac{1}{2}\varphi_\theta = h_\beta\dot{\beta} + (\frac{1}{2})h_\eta + \frac{1}{2}(-1)h_\eta = h_\beta\dot{\beta}.$$

Using equation (2.6), we can deduce that

$$h_\beta\dot{\beta} = \nu h_{\theta\theta} + \psi_c(\Phi + h) - \overline{\psi_c(\Phi + h)}.$$

Projecting this equation onto h_β and dividing through by the norm of h_β, yields

$$\dot{\beta} = \frac{1}{\|h_\beta\|^2}(\langle h_{\theta\theta}, h_\beta\rangle + \langle\psi_c(\Phi + h) - \overline{\psi_c(\Phi + h)}, h_\beta\rangle)$$

which is just an ordinary differential equation describing the evolution of β.

This last equation can be simplified even further because $\overline{\psi_c}$ does not depend on θ and

$$\int_0^{2\pi} h_\beta d\theta = \frac{\partial}{\partial\beta}\int_0^{2\pi} h d\theta = 0.$$

We can conclude that

$$\int_0^{2\pi} \frac{\partial h}{\partial \beta} \overline{\psi_c(\Phi + h)} d\theta = 0.$$

Assembling the above we have three ordinary differential equations that determine the flow on the basic attractor

$$\begin{aligned}
\dot{\beta} &= \frac{1}{\|h_\beta\|^2}(\langle h_{\theta\theta}, h_\beta\rangle + \langle \psi_c(\Phi + h), h_\beta\rangle) && (4.1)\\
\dot{\Phi} &= \frac{1}{l_c}(\overline{\psi_c(\Phi + h)} - \Psi) && (4.2)\\
\dot{\Psi} &= \frac{1}{4l_c B^2}(\Phi - K_T(\Psi)). && (4.3)
\end{aligned}$$

These equations give a complete description of the flow on the basic attractor in the parameter region where only one stall cell exists, i.e. when $[\sqrt{\frac{c}{\nu}}] = 1$ in Proposition 3.13.

Remark 4.2 If instead of using the one parameter family of stall cells one uses the family given by

$$h(\beta(t), \eta) = \beta(t) \sin(\frac{1}{2}t - \theta),$$

the usual one mode projection is recovered [59].

This one parameter family of stall cells has only been defined for $\beta \in [0, 1]$ and a meaningful way of extending it to the whole axis is needed here. To this end, notice that the surface both starts and ends in a zero solution. We can therefore extend the it as a periodic surface in β with period 1. This is equivalent to thinking of the evolution equation (4.1)-(4.3) as an evolution equation on $S^1 \times \mathbb{R}^2$, i.e. the unit circle times the two dimensional plane.

4.2.1 Simulations of Reduced Order Model

One can simulate numerically the system (4.1)-(4.3) to explore its behavior. Since the one parameter family was generated by a simulation of the full system (2.6)-(2.8) we only have a numerical representation of it. It is therefore necessary to use a numerical look-up table for valuating the right hand side of equation (4.1). This is however not very complicated and we can simulate this system using MATLAB.

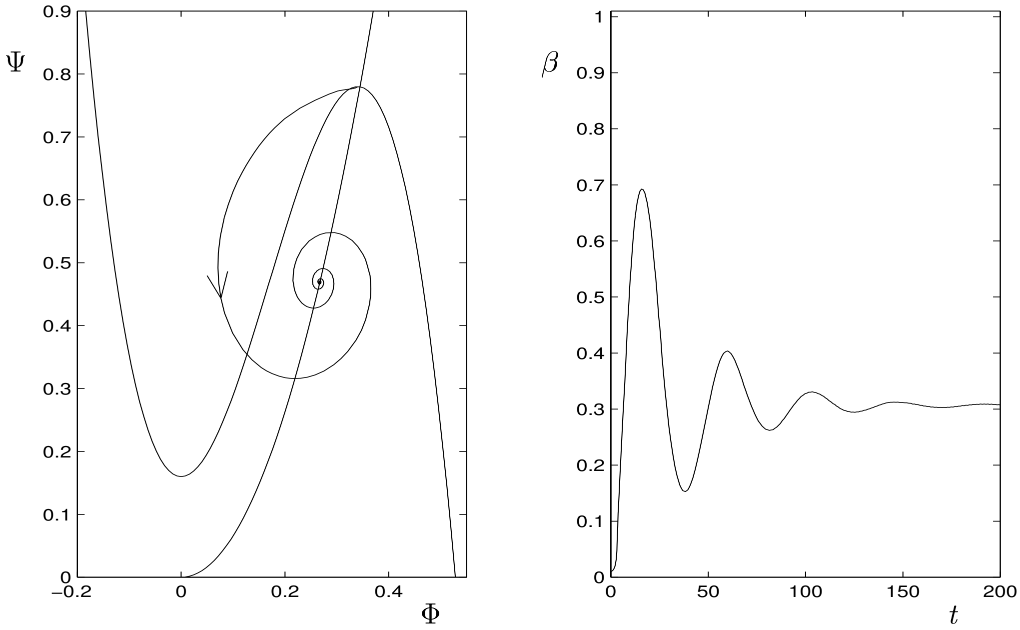

Figure 4.4: *A simulation showing how the reduced order model goes into stall. On the right is the phase plane* (Φ, Ψ) *and on the left we see how the parameter* β *behaves as a function of time.*

Figure 4.4 shows a simulation for a stalling compressor. The left hand side shows the (Φ, Ψ) phase plane. The right hand side shows how the parameter β settles to a constant value in the open interval $(0, 1)$. The final shape the stall cell settles at is shown in Figure 4.5.

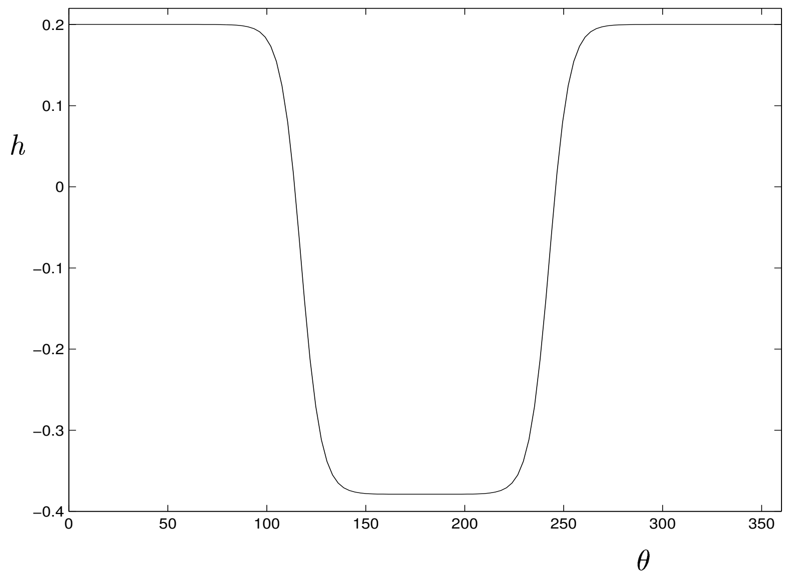

Figure 4.5: *The final stall shape the disturbance φ settles on in the lower order model.*

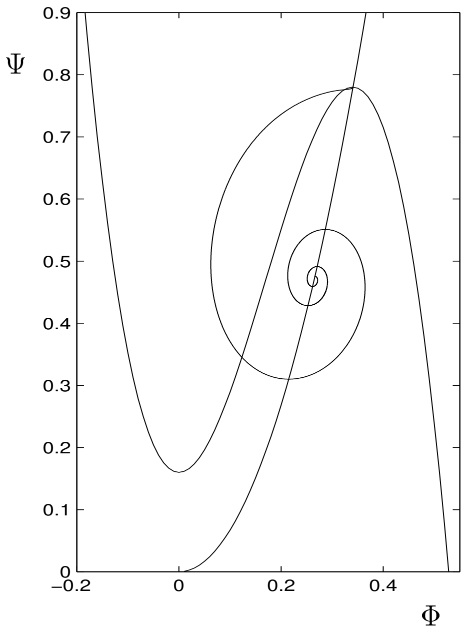

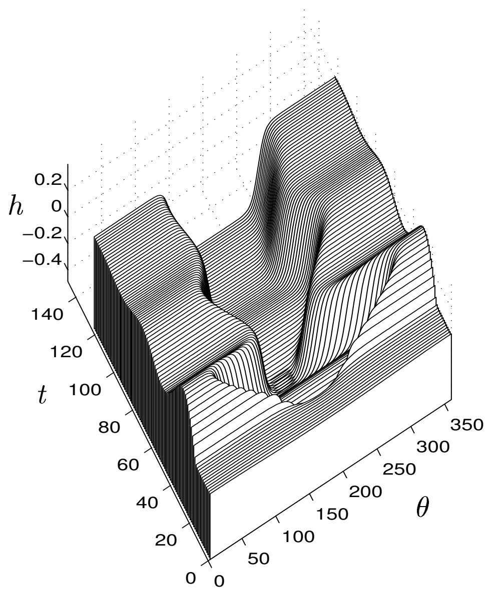

Figure 4.6: *The same phenomenon as in Figure 4.4, but simulated by the PDE model. On the right we have the time evolution of the stall disturbance, φ, as a function of time and angle.*

One should compare this simulation with the same type of calculation done for the full system. The results of these simulations are presented in Figure 4.6. These two simulations yield strikingly similar results and to compare them even further we plot the (Φ, Ψ) variables together in the same plot in Figure 4.7. Here one sees clearly that this third order model yields not only qualitative results, but *is also quantitatively accurate.* This applies to both asymptotic behavior as well as transient behavior. This degree of agreement between the full system and a third order model is impossible to achieve with a traditional Galerkin projection, i.e with a fixed spatial structure.

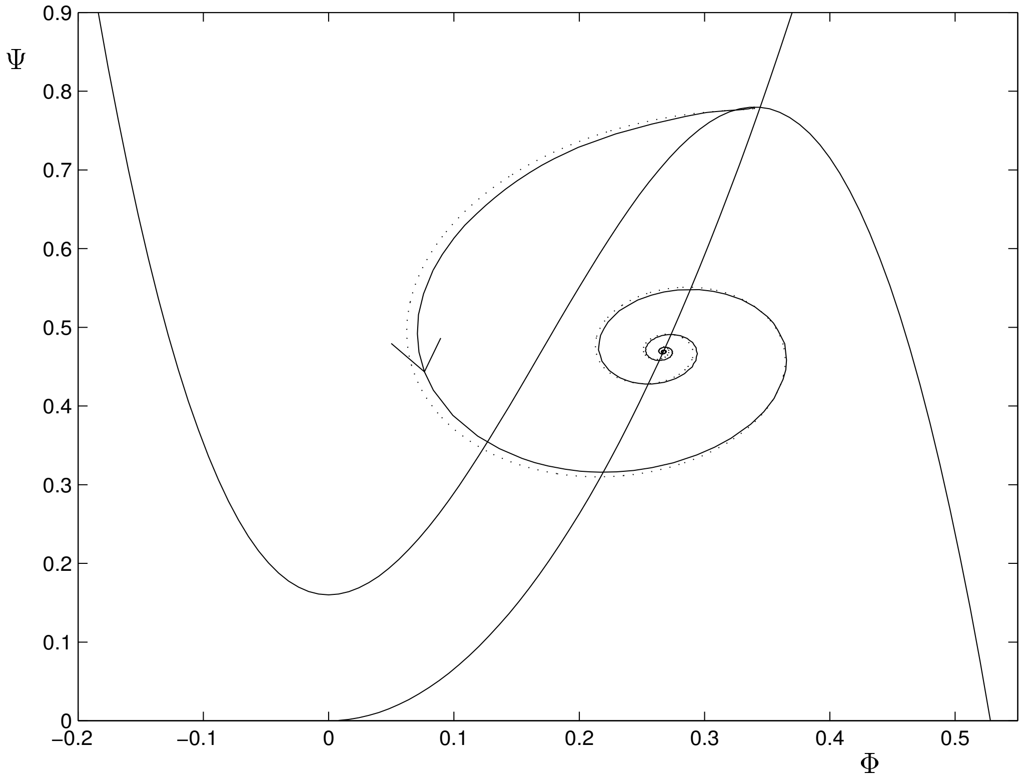

Figure 4.7: *The transient behavior for the reduced order model and the full system are essentially the same. The solid line is the reduced order model simulation and the dotted one is from the PDE simulation.*

To complete the picture we include a simulation which shows that this third order model can also capture surge. This is displayed in Figure 4.8.

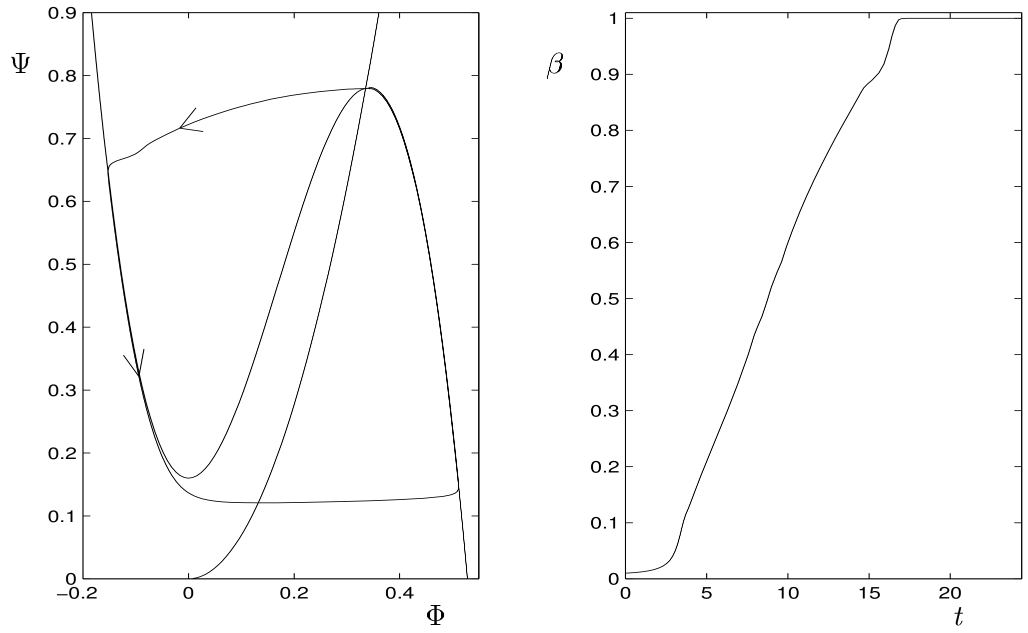

Figure 4.8: *The reduced order model can also capture surge. On the left we see the* (Φ, Ψ) *phase plane and the limit cycle and on the right side we see the transient as the nonaxisymmetric disturbance dies out, i.e.* β *settles onto a value that corresponds to* $\varphi = 0$.

Since we have such a good agreement between the dynamics of the full system and the reduced order model, one can use the third order model to investigate the bifurcations of the full system. Figure 4.9 shows the bifurcation diagram for stall as calculated from the reduced order model. Here one clearly sees how stall comes into existence as a saddle-node bifurcation when the throttle constant γ is reduced. From that bifurcation point we have a branch of stable stall cells that quickly flattens out and a branch of unstable stall cells that connects with the compressor characteristic at the point where design flow becomes unstable to stall disturbances.

Due to the symmetry property of the stall branch, see Remark 2.1, one has another saddle-node bifurcation coming from the other side, i.e. for a negative γ which has an unstable branch connecting to the compressor characteristic and a stable branch that connects to the flat stable characteristic of the other saddle-node bifurcation.

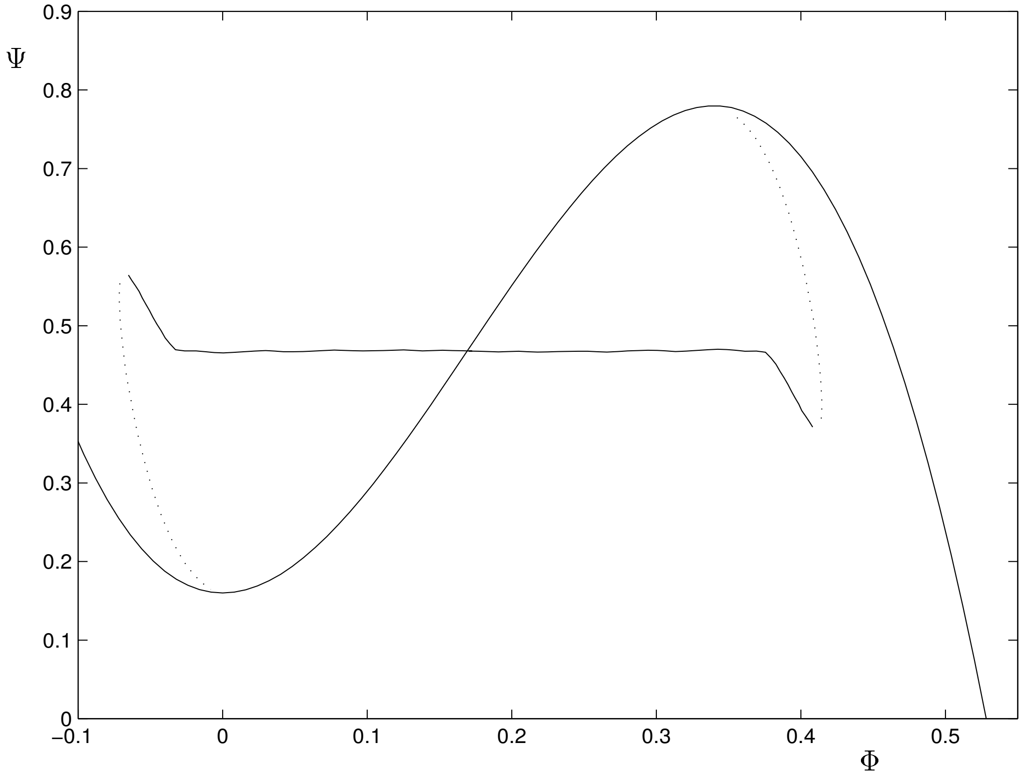

Figure 4.9: *The bifurcation branch for stall. The dotted lines represent unstable branches and the flat solid line represents the stable branch.*

4.2.2 An Approximate Algebraic Model

For some applications it might be more convenient to have an algebraic expression for the three ordinary differential equations rather than a numerically computed table. To avoid having to solve exactly for all the parameters in the one parameter family one could use a piecewise linear approximation of the form given in Figure

4.10. There the parameter β is chosen to represent the width of the dip in the solution and it lives on the interval $[0, 2\pi + 2\epsilon]$.

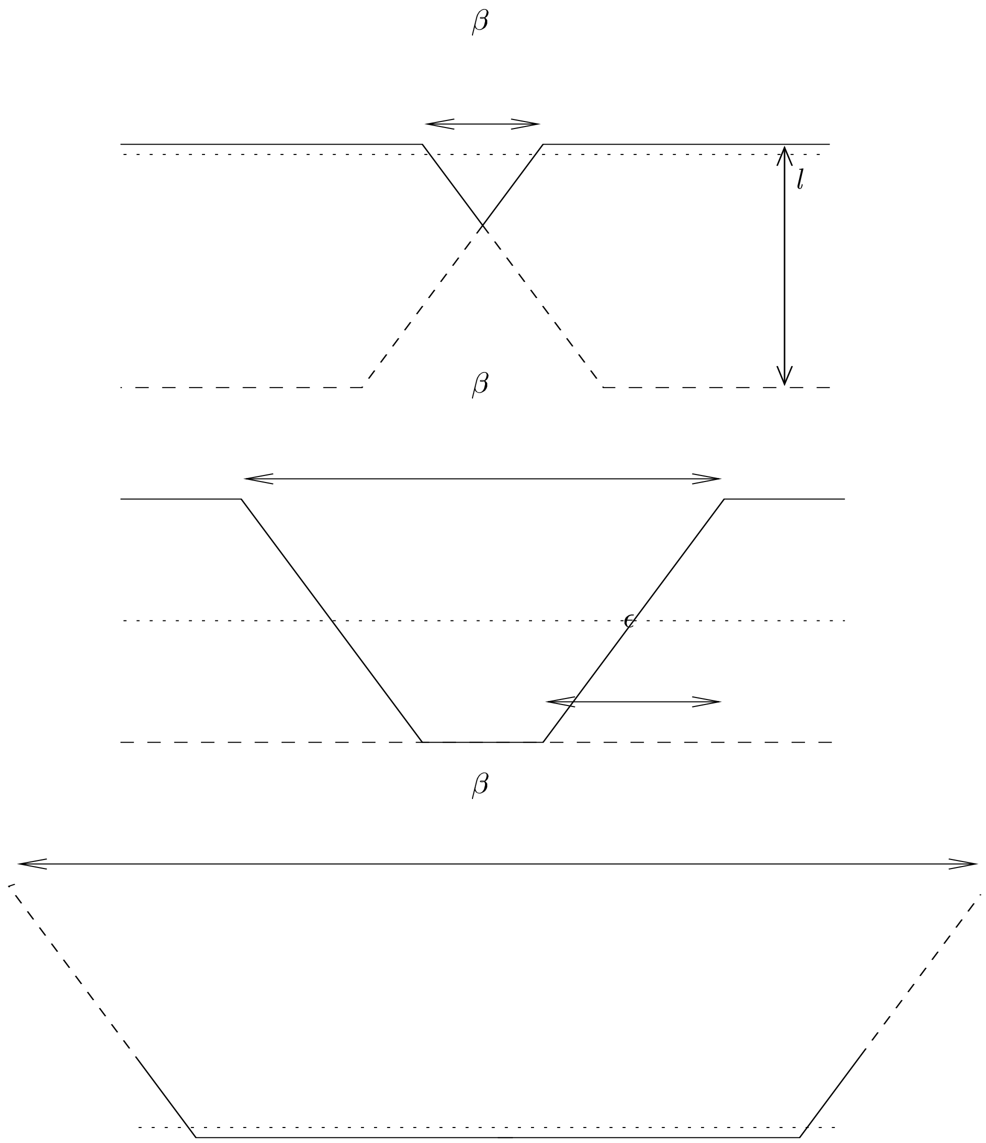

Figure 4.10: *A piecewise linear family of stall cells. The first picture shows the stall cell just after it has formed, the second one shows it after it has developed further and the third just before it vanishes again. The solid line represents the stall solution and the dotted one the zero line. The dashed lines are the continuation of imagined profiles that can move sideways.*

Since the compressor characteristic is a cubic polynomial the integrals in the lower order model can be carried out explicitly and one can obtain an analytic expression for a lower order model that approximates our previous lower order model.

In order to derive the algebraic expression for equation (4.1) with this one parameter family we need to consider three cases: Case 1 is when the stall cell still hasn't reached its full depth as shown in the first picture of Figure 4.10. Case 2 is when the stall has reached its full depth as in the second picture and case 3 is when the stall has filled out almost all of the annulus as in the third picture.

Let us first denote the integral of the compressor characteristic by

$$P(y) = \int_0^y \psi_c(x)dx$$

After some calculation one arrives at the following system of equations

$$\dot{\beta} = \begin{cases} \dfrac{\frac{\sigma_1}{4\pi}(2\pi-\beta)\psi_c(\Phi+\sigma_2)-(1-\frac{\beta}{2\pi})(P(\Phi+\sigma_2)-P(\Phi-\frac{\sigma_1}{2}+\sigma_2))}{(\frac{l}{2\epsilon})^2\beta-2\pi(\frac{l\beta}{4\pi\epsilon})^2}, & \\ & \text{if} \quad \beta \in [0, 2\epsilon] \\ \dfrac{\frac{l}{2\pi}((2\pi-\beta)\psi_c(\Phi+\sigma_1)+(\beta-2\epsilon)\psi_c(\Phi+\sigma_1-l))-(1-\frac{\epsilon}{\pi})(P(\Phi+\sigma_1)-P(\Phi+\sigma_1-l))}{\frac{l^2}{2}(\frac{1}{\epsilon}-\frac{1}{\pi})}, & \\ & \text{if} \quad \beta \in [2\epsilon, 2\pi] \\ \dfrac{\frac{\sigma_1}{4\pi}(\beta-2\epsilon)\psi_c(\Phi-\sigma_2)-(\frac{\epsilon}{\pi}+\frac{\beta}{2\pi})(P(\Phi+\frac{\sigma_1}{2}-\sigma_2)-P(\Phi+\sigma_2))}{-\frac{l^2}{8\pi\epsilon^2}\beta^2+(\frac{l^2}{4\epsilon^2}+\frac{l^2}{2\pi\epsilon})\beta-\frac{l^2}{2\pi}}, & \\ & \text{if} \quad \beta \in [2\pi, 2\pi+2\epsilon] \end{cases}$$

$$\dot{\Phi} = \frac{1}{l_c}(\overline{\Psi_c(\Phi+h)} - \Psi)$$

$$\dot{\Psi} = \frac{1}{4l_cB^2}(\Phi - K_T(\Psi))$$

Here we have made the following definitions

$$\sigma_1 = \begin{cases} \frac{l\beta}{\epsilon} & ,\text{if} \quad \beta \in [0, 2\epsilon] \\ l\frac{\beta-\epsilon}{2\pi} & ,\text{if} \quad \beta \in [2\epsilon, 2\pi] \\ \frac{l}{\epsilon}(2\pi + 2\epsilon - \beta) & ,\text{if} \quad \beta \in [2\pi, 2\pi + 2\epsilon] \end{cases}$$

and

$$\sigma_2 = \frac{\epsilon}{8\pi l}\sigma_1^2.$$

4.2.3 Higher Order Models

In general the basic attractor contains of more than one stall component. These solutions are solitons with different number of pulses. The shape of each pulse is essentially that of the one-pulse solution. It is important to be able to extend the reduced order model to also capture the higher order stall solutions. This could be done by using the ansatz that

$$g(t, \theta) = h_1(\beta_1(t), \eta) + ... + h_N(\beta_N(t), \eta),$$

recall that $\eta = \frac{1}{2}t - \theta$.

We can however be a bit more general. The need might arise if one also wanted to include in the model connections between the different parts of the basic attractor. Let us make the ansatz that the stall disturbance is of the form

$$g(t, \theta) = h(\beta_1(t), ..., \beta_N(t), \eta).$$

Then by equation (2.6)

$$\sum_{n=1}^{N} h_{\beta_n}\dot{\beta}_n = \nu h_{\eta\eta} + \psi_c(\Phi + h) - \overline{\psi_c(\Phi + h)}.$$

Taking the inner product with the different partial derivatives of h, one obtains a system of ODE's of order $N+2$ which is of the form

$$\sum_{n=1}^{N} \langle h_{\beta_n}, h_{\beta_p} \rangle \dot{\beta}_n = \nu \langle h_{\eta\eta}, h_{\beta_p} \rangle + \langle \psi_c(\Phi + h), h_{\beta_p} \rangle, \quad p = 1, ..., N$$

$$\dot{\Phi} = \frac{1}{l_c}(\overline{\psi_c(\Phi + h)} - \Psi)$$

$$\dot{\Psi} = \frac{1}{4 l_c B^2}(\Phi - K_T(\Psi)).$$

Here again we have used the fact that the partial derivatives of h have vanishing average. One also needs to make the assumption that the span of the partial derivatives of h is N dimensional for all s.

In particular, when one assumes that the flow disturbance can be described by a linear combination $g = \beta_1(t)\varphi_1 + ... + \beta_N(t)\varphi_N$ of N orthogonal functions $\varphi_1, ..., \varphi_N$ with norm one, the classical Galerkin truncation is recovered and the equations

$$\dot{\beta}_n = \nu \langle g_{\eta\eta}, \varphi_n \rangle + \langle \psi_c(\Phi + g), \varphi_n \rangle, \quad n = 1, ..., N$$

give the evolution of the amplitudes.

4.3 The Global Attractor Revisited

Armed with the knowledge of the bifurcations of the stall cells we can now construct the slow global attractor $\mathcal{A}_s$ of the slow system (3.10)-(3.11) for all γ values in the case $0 < B \ll 1$. Recall that it contains the basic attractor $\mathcal{B}$.

When γ is increased from γ_*, then as we move along the design flow branch we will encounter the bifurcation points which gave rise to the stall solutions. When we have moved γ just past the first bifurcation point, counting from γ_*, then there will be two stall solutions which are $2\pi/n$ periodic. One of them is stable and the other one unstable. Furthermore, design flow will be stable with respect to small disturbances which are $2\pi/n$ periodic. By Theorem 3.20, the global attractor will therefore be composed of the stall components, the design flow and its connections to the first $n-1$ stall components and the connections from the unstable $2\pi/n$ periodic stall solution to the stable $2\pi/n$ periodic stall solution and to the design flow.

Consider for now only the $2\pi/n$ periodic stall solutions and let us increase γ further. As we increase γ the stable and the unstable stall solutions will get closer to each other until they collide and vanish, see Figure 3.2.

Other stall solutions have the same fate and we have now given a complete description of the global attractor for $0 < B \ll 1$.

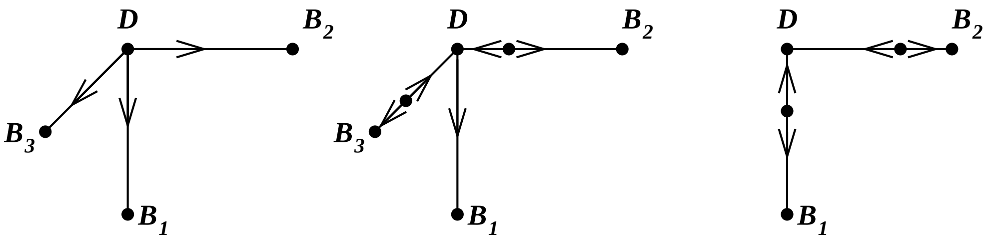

Figure 4.11: *The global attractor for small B.*

Figure 4.11 shows how the global attractor behaves as a function of γ. To the left we have the global attractor for $\gamma = \gamma_*$. In the center we have increased γ past the first two bifurcation points, counting from $\gamma = \gamma_*$. Here two new stall solutions have been created, both of which are unstable. Their unstable manifolds connect them with the corresponding stable stall solutions and to the design flow. On the right we have moved γ past all three bifurcation points. Furthermore, we have moved γ past the point where the third stall component was created in a saddle-node bifurcation, see Figure 3.2, and thus it has vanished. We are left with the 2π and π periodic stall components, the design flow and the connections between these solutions.

Chapter 5

The Basic Control of the vMG Equation

Control of PDEs has traditionally been approached by linearizing the equation about a specific solution. From here researchers have applied optimal control theory [6] [18] or tried to analyze the spectrum of the equation and find ways of influencing it. Frequently the problem is here made finite dimensional via a Galerkin truncation to a large number of modes.

The general approach we want to propose is different. Dissipative PDEs typically have finite dimensional global attractors and hence finite dimensional basic attractors. While this fact justifies the use of Galerkin truncations, the number of modes needed is usually quite large. On the other hand, in the cases when a complete description of the basic attractor has been given, see [12] [29] [17] and the previous two chapters, the dimension of the basic attractor turns out to be relatively small. One can therefore expect that the problem of constructing a good control for a dissipative PDE can be reduced to a low dimensional problem which can be handled with techniques from control theory for ODEs, or simple modifications thereof.

There is, however, a subtle problem here one must be aware of. So far the basic attractor has only been analyzed for constant control parameters. The implementation of active feedback control requires one to allow the control parameters to vary and furthermore they must depend on the state of the system. The relationship between the equation and the inputs and outputs, i.e. actuators and sensors, has therefore not been incorporated into the analysis of the basic attractor. To circumvent this problem we propose to move the control parameters in a piecewise adiabatic fashion. That is, the control parameters change adiabatically, except for that they can have isolated jump discontinuities that are sufficiently far apart in time. This allows one to draw conclusions about the solutions of the equation with inputs and outputs from the previous analysis.

There have been numerous control related results reported for Galerkin truncations of the Moore-Greitzer equation, see [5] [7] [26] [35] [43] [44] [45] [48] [68] and references therein. The first control result for the full system was presented by Banaszuk *et al.* [4]. They constructed a feedback throttle control which made design flow attract all of state space for the inviscid Moore-Greitzer equation. This equation is a hyperbolic equation and the nature of its solutions is quite different from that of the vMG equation. Current results by Mezić [57] indicate that the latter is a better physical model for the flow through the jet engine compression system. Furthermore, the controller constructed by Banaszuk *et al.* is not very cost effective. In particular, it overreacts to small amplitude high frequency disturbances which are naturally damped in the viscous model. Currently Hagen *et al.* [33] have presented some results on control via air injection.

The backstepping control given by Banaszuk *et al.* shows, however, that one can eliminate stall and surge by using throttle control. The question we want to answer in this chapter is how simple can we make the control design and how efficient can the control be? The control philosophy we want to adopt, is to construct a control strategy that can recover design flow operation after large disturbances, but is not necessarily good for regulating the design flow. For that a different strategy would be used.

In the sequel we will allow γ to depend on the state, but we will assume that it does so in a smooth way and that there exists a constant $\tilde{\gamma}$ such that

$$\gamma(\Phi, \Psi, \varphi) \geq \tilde{\gamma} > 0.$$

With these restrictions on γ the results on existence of unique solutions and their regularity still hold. In addition, the system will again have a global attractor whose fractal and Hausdorff dimensions can be bounded by the same bounds as in Theorem 3.7 with γ replaced by $\tilde{\gamma}$.

This chapter is arranged as follows, Section 5.1 defines attractor controllability and basic controllability. Section 5.2 considers the simplest possibility, which is to linearize the system about the design flow and then apply the standard optimal control theory to obtain an optimal control subject to quadratic cost. Here we confirm that stall is uncontrollable in the linearized model. Section 5.3 considers first the case when the throttle is moved adiabatically. We then use our knowledge of the basic attractor of the system to construct a basic control which recovers design flow operation from stall or surge. Numerical simulations are presented in Section 5.3.3. Here we compare the basic control with the backstepping control. In Section 5.4 we prove that the vMG equation with throttle control is not basically controllable. Moreover, it is proven that if one in addition has air injection at ones disposal then the vMG equation is basically controllable.

5.1 Basic Controllability

Let us consider now the issue of controllability. In finite dimensional control theory, a system is said to be controllable if for every two points $x_0, x_1 \in X$ and every two real numbers $t_0 < t_1$, there exists a control function u such that the unique solution of the equation

$$\dot{x} = F(x, u), \quad x(t_0) = x_0 \tag{5.1}$$

satisfies $x(t_1) = x_1$.

This notion of controllability has been extended for linear infinite dimensional systems as exact controllability and approximate controllability, see Banks [6]. In general, this notion of controllability is much too strong for nonlinear infinite dimensional systems with finite dimensional control input and systems with infinite dimensional control input are in many cases not very realistic.

If an evolution equation has an attractor and a basic attractor its solutions will converge asymptotically to the attractor for all initial conditions and to the basic attractor for almost all initial conditions. The simplest thing one could ask of the control is that it make all or almost all initial conditions give rise to solutions that converge to a given component in the basic attractor. A more stringent requirement on the control would be that it make all or almost all initial conditions give rise to solutions that converge to a given solution in the global attractor. This requires us to have enough control authority over the local unstable manifolds of the hyperbolic trajectories in the attractor to make them attractive. We make the following definitions

Definition 5.1. *We say that the equation (5.1) is* basically controllable *if there exists a prevalent set $Y \subset X$ such that for all $x_0 \in Y$ and all components $\mathcal{B}_i$ of the basic attractor $\mathcal{B}$ there exists a control function u such that the solution $x(t)$ with $x(t_0) = x_0$ converges to the component $\mathcal{B}_i$.*

We say that the equation (5.1) is attractively controllable *if there exists a prevalent set $Y \subset X$ such that for all $x_0 \in Y$ and all trajectories z in the attractor $\mathcal{A}$ there exists a control function u such that the ω-limit set of the solution x of (5.1) equals the ω-limit set of z, i.e. $\omega(x) = \omega(z)$.*

We will also speak of basic controllability as b-controllability and attractor controllability as a-controllability. Clearly a-controllability implies b-controllability. As it turns out, our control construction in Section 5.3 relies heavily on the geometry of the basic attractor. Due to this we shall refer to this control as the *basic control.*

To get stronger results than a-controllability or b-controllability of the form that we could get from an arbitrary initial condition to a point in the attractor in finite time is in general hopeless. Since our control only actuates finitely many dimensions, we will need to wait forever for the part of the solution which, in some sense, is perpendicular to our control action to settle onto the desired point.

5.2 Control of Design Flow for the Linearized Equation

The most important component of the basic attractor of the vMG equation is the design flow component. The goal is to construct a control function that makes all solutions converge to the design flow. The simplest approach one could take would be to linearize the system about design flow, $(\Phi_0, \Psi_0, 0)$, corresponding to a throttle parameter γ_0, and then apply the classical optimal control theory. We define the control parameter $u = \gamma - \gamma_0$ and put ourselves into the rotating frame of reference (t, η) and define the variable $y = (y_1, y_2, y_3) = (\varphi, \Phi - \Phi_0, \Psi - \Psi_0)$. The linearized equations can now be written as

$$\dot{y} = Ay + Bu \tag{5.2}$$

where

$$A = \begin{bmatrix} \nu\partial_\theta^2 + \psi_c'(\Phi_0) & 0 & 0 \\ 0 & \frac{1}{l_c}\psi'(\Phi_0) & -\frac{1}{l_c} \\ 0 & \frac{1}{4l_cB^2} & \frac{-\gamma_0}{4l_cB^2}(F_T^{-1})'(\Psi_0) \end{bmatrix} \tag{5.3}$$

and

$$B = \begin{bmatrix} 0 \\ 0 \\ \frac{1}{4l_cB^2}(F_T^{-1})'(\Psi_0) \end{bmatrix}. \tag{5.4}$$

Since the operator A is sectorial it generates an analytic semigroup in X. We denote by $T(t)$ the semigroup operator on X and the norm and inner product will be denoted by $\|\cdot\|$ and $\langle\cdot,\cdot\rangle$ respectively. In this form the equations can be tackled using the standard optimal control theory in Hilbert spaces, see Lions [50] and Banks [6].

Observe first that this system is block diagonal. It can be split into two parts: a two dimensional part that describes the evolution of the average flow and the pressue rise, and a part of codimension 2 which describes the evolution of stall. This second part does not depend on the control parameter γ and can therefore be integrated separately. In other words, stall does not depend on the control parameter and is therefore uncontrollable. The problem is now reduced to a two dimensional problem.

We seek a feedback control that will minimize the cost functional

$$J(y) = \frac{1}{2}(y_1^2(t_f) + y_2^2(t_f)) + \frac{1}{2}\int_0^{t_f} S(y_1^2(t) + y_2^2(t)) + Ru^2 dt$$

It is a well known result [6] that the optimal feedback control is given by

$$u = -\frac{1}{R}B^T Q(t) y(t)$$

where the symmetric matrix $Q(t)$ satisfies the matrix Riccati equation

$$\dot{Q}(t) = -Q(t)A - AQ(t) + \frac{1}{R}Q(t)BB^T Q(t) - SI, \qquad Q(t_f) = I.$$

Here I is the identity matrix and S and R are positive constants. Solving the Riccati equation is equivalent to solving the following three ordinary differential equations

$$\begin{aligned}
\dot{q}_{11} &= (\tfrac{1}{4l_c B^2}(F_T^{-1})'(\Psi_0))^2 q_{12}^2 - S - 2(a_{11}q_{11} + a_{21}q_{12}), \\
\dot{q}_{12} &= (\tfrac{1}{4l_c B^2}(F_T^{-1})'(\Psi_0))^2 q_{12}q_{22} - a_{12}q_{11} - (a_{11} + a_{22})q_{12} - a_{21}q_{22}, \\
\dot{q}_{22} &= (\tfrac{1}{4l_c B^2}(F_T^{-1})'(\Psi_0))^2 q_{22}^2 - S - 2(a_{12}q_{12} + a_{22}q_{22}), \\
q_{ij}(t_f) &= \delta_{ij},
\end{aligned} \tag{5.5}$$

where δ_{ij} is the Kronecker delta. This system can be solved backwards in time numerically. The optimal feedback control is now given by

$$u = \frac{1}{4l_c B^2}(F_T^{-1})'(\Psi_0)((\Phi - \Phi_0)q_{12}(t) + (\Psi - \Psi_0)q_{22}(t)).$$

Design flow solutions that sit to the right of the peak on the compressor characteristic, see Figure 3.1, have the property that all the uncontrollable modes are stable, so in the linear model the design flow is b-controllable and in fact it is a-controllable. However, the fact that stall is uncontrollable in the linear system renders this control of limited use. It is well known that in the nonlinear system for design flow solutions close to the peak of the characteristic, small nonaxisymmetric disturbances can cause the system to go into stall. On the other hand the result by Banaszuk *et al.* [4] proves that design flow can be globally stabilized by using only throttle control. Their control is, however, not optimal in any sense of the word and it reacts very violently to high frequency disturbances which are damped in the viscous model. The question that now arises is whether there is something in between these two control constructions, i.e. does there exist a control which globally stabilizes the design flow but does not require as much control effort as the control constructed by Banaszuk *et al.* We tackle this problem in the next section.

5.3 Basic Control of Design Flow for the Nonlinear Equation

The union attractor for constant throttle functions has been analyzed completely [13],[16] and one would like to use this knowledge of the asymptotic dynamics when constructiong a control law. However, when γ is no longer constant, but a function of the state variables, the components of the basic attractor may change, altering the asymptotic dynamics.

Let us assume for now that we only consider control strategies that move the throttle in an adiabatic fashion. Restricting the control to this class guarantees that the union attractor is unchanged. The best one can hope to do here is to slide the solution along the union attractor until it reaches the desired operation point. If stall occurs, then one slides the system along the branch of stable stall cells, by increasing γ, until the saddle-node bifurcation point is reached and stall ceases to exist and the flow converges to design flow. This design flow is achived at a very low pressure rise. In order to increase the pressure rise we decrease γ again until the desired operation point is reached. Figure 4.9 shows the bifurcation diagram for the first stall solution.

Remark 5.2 The union attractor will be unchanged if we, in addition, allow γ to have finite discontinuities, as long as the time between the jumps is long enough to let the solution settle.

Within the class of adiabatic controls, this is the optimal control. When one considers the larger class of controls that are not neccesarily adiabatic, this control strategy is no longer optimal. It has however been shown that a reduced order model, which reduces the flow to the basic attractor, captures the dynamics of the full model not only qualitatively, but also quantitatively [16]. Transient behavior, while the flow is going from one component of the basic attractor to another, is also well captured. With this in mind it make sense to modify the adiabatic control construction by tracking trajectories on the basic attractor. If the tracking is done in an optimal fashion one would hope that the resulting control strategy is close to an optimal strategy with respect to some cost functional. We claim that our basic control strategy is in this sense near optimal.

Let $\xi(t)$ be a parameterization of a family of stationary solutions in the union attractor $\cup_{\gamma\geq\bar{\gamma}}\mathcal{B}(\gamma)$. Note that since we are working in a rotating frame of reference, stall will be a stationary solution. Then corresponding to $\xi(t)$ we can find $\bar{\gamma}(t)$ such that for $\gamma = \bar{\gamma}(t)$, $\xi(t)$ is a stationary solution of the equation (2.6-2.8). We denote the solution of the system (2.6-2.8) by $x(t) = (\varphi, \Phi, \Psi)(t) = \xi(t) + y(t)$ and the control parameter by $\gamma = \bar{\gamma}(t) + u(t)$. Let us now linearize the system (2.6-2.8) about the trajectory $\xi(t)$ and write it as

$$\dot{y} = A(t)y + B(t)u - \dot{\xi}(t). \tag{5.6}$$

Here $A(t)$ and $B(t)$ depend on time through the trajectory $\xi(t)$. Our goal is to make y as small as possible with very little control effort. In other words, we want to find a regulator for equation (5.6) which is optimal with respect to the cost function

$$J(u) = \frac{1}{2}\|S_f y(t_f)\|^2 + \frac{1}{2}\int_0^{t_f} \|Sy(t)\|^2 + Ru^2(t)dt$$

where R is a constant and S_f and S are symmetric positive definite linear operators.

This is a well known problem which has been solved, see Sage and White [67] or Banks [6]. The optimal feedback control is given by

$$u(t) = -\frac{1}{R}B^T(t)(Q(t)y(t) - \zeta(t))$$

where the symmetric operator $Q(t)$ satisfies the equation

$$\dot{Q}(t) = -Q(t)A(t) - A(t)Q(t) + \frac{1}{R}Q(t)B(t)B^T(t)Q(t) - S \qquad Q(t_f) = S_f \tag{5.7}$$

and the function $\zeta(t)$ satisfies

$$\dot{\zeta}(t) = -(A(t) - \frac{1}{R}B(t)B^T(t)Q(t))^T\zeta(t) - Q(t)\dot{\xi}(t) \qquad \zeta(t_f) = 0. \tag{5.8}$$

These equations can be solved backwards in time to yield the optimal control u.

It turns out that when we linearize the vMG equation about a solution in the basic attractor, then all but finitely many directions in state space will be uncontrollable. The uncontrolled dynamics are stable and as a result the two equations (5.7) and (5.8) will reduce to finitely many ordinary differential equations.

5.3.1 Construction of the Controller

To make the construction of the controller as simple and intuitive as possible we proceed in the following way. When a disturbance occurs to the system that is large enough that it cannot recover without intervention, we change the control parameter to a setting where the only component in the basic attractor is the design flow. This consists of increasing γ to a level γ_1 so that the throttle characteristic no longer intersects the branch of stall cells. We then wait until the flow is in a small enough neighborhood U of the design flow. This design flow setting is, however, at a low pressure rise level so to increase the pressure rise we now track a trajectory ξ_1 to the desired design flow setting, see Figure 5.1. As we will prove later, if the state is close enough to the starting point of ξ_1 and the cost on the control small enough, this strategy will work for all initial disturbances.

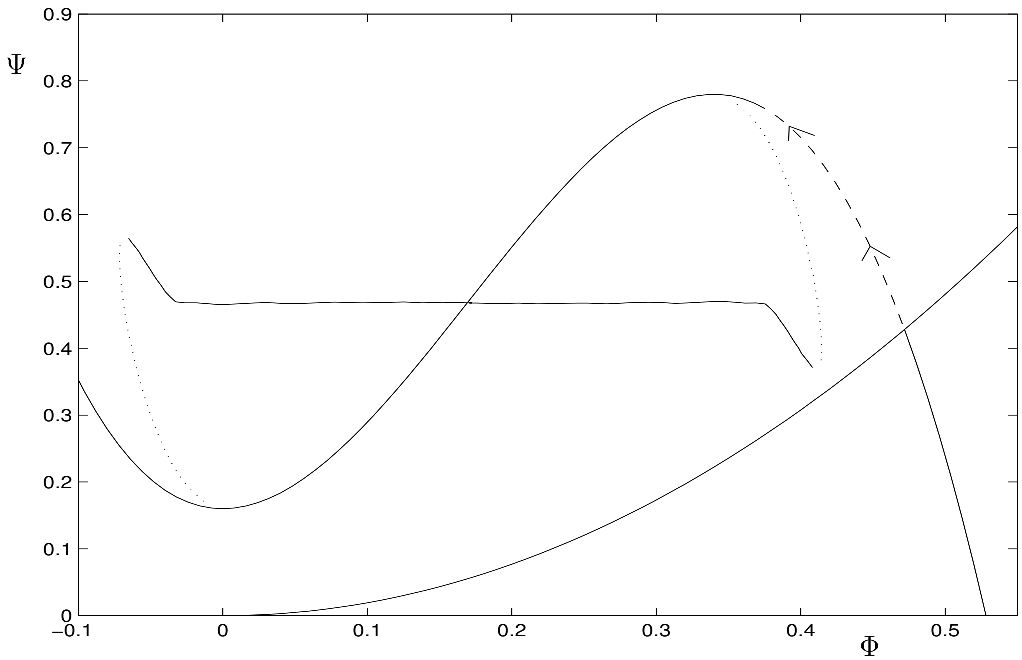

Figure 5.1: *This figure shows the throttle setting $\gamma = \gamma_1$ that defines the start of the trajectory ξ_1 which is shown as a dashed line.*

This control construction will still be very close to the original one as the system will settle into stall or surge very fast and then traverse near the union attractor towards the design flow corresponding to the throttle setting γ_1.

The linearization of the system about the trajectory ξ_1 is exactly that given by equations (5.3) and (5.4), except for that now these operators are time dependent, i.e. instead of (Φ_0, Ψ_0) we have $(\Phi, \Psi)_{\bar{\gamma}(t)}$. Just like before, there is an uncontrollable subspace of codimension 2, but since we are on the right side of the peak of the characteristic, this space is stable and small disturbances will decay in time. We therefore only need to consider the first two modes which describe the flow in the (Φ, Ψ)-plane and it suffices to know q_{11}, q_{12}, q_{22}, ζ_1 and ζ_2. The equations for these coefficients are

$$\begin{aligned}
\dot{q}_{11} &= \left(\tfrac{1}{4l_cB^2}(F_T^{-1})'(\Psi_{\bar{\gamma}(t)})\right)^2 \tfrac{q_{12}^2}{R} - s_{11} - 2(a_{11}(t)q_{11} + a_{21}(t)q_{12}),\\
\dot{q}_{12} &= \left(\tfrac{1}{4l_cB^2}(F_T^{-1})'(\Psi_{\bar{\gamma}(t)})\right)^2 \tfrac{q_{12}q_{22}}{R} - s_{12} - a_{12}(t)q_{11}\\
&\quad -(a_{11}(t) + a_{22}(t))q_{12} - a_{21}(t)q_{22},\\
\dot{q}_{22} &= \left(\tfrac{1}{4l_cB^2}(F_T^{-1})'(\Psi_{\bar{\gamma}(t)})\right)^2 \tfrac{q_{22}^2}{R} - s_{22} - 2(a_{12}(t)q_{12} + a_{22}(t)q_{22}),\\
q(t_f)_{ij} &= s_{fij}
\end{aligned} \tag{5.9}$$

and

$$\begin{aligned}
\dot{\zeta}_1 &= -a_{11}(t)\zeta_1 - (a_{21}(t) - (\tfrac{1}{4l_cB^2}(F_T^{-1})'(\Psi_{\bar{\gamma}(t)}))^2 \tfrac{q_{21}}{R})\zeta_2 - q_{11}\dot{\xi}_1 - q_{12}\dot{\xi}_1,\\
\dot{\zeta}_2 &= -a_{12}(t)\zeta_1 - (a_{22}(t) - (\tfrac{1}{4l_cB^2}(F_T^{-1})'(\Psi_{\bar{\gamma}(t)}))^2 \tfrac{q_{22}}{R})\zeta_2 - q_{12}\dot{\xi}_1 - q_{22}\dot{\xi}_1,\\
\zeta(t_f) &= 0.
\end{aligned} \tag{5.10}$$

The basic feedback control is now given by

$$u(t) = \gamma_1 \tag{5.11}$$

if $x(t)$ has not reached the neighborhood U and

$$u(t) = \frac{1}{4l_c B^2 R}(F_T^{-1})'(\Psi_{\bar{\gamma}(t)})((\Phi - \Phi_{\bar{\gamma}(t)})q_{12}(t) + (\Psi - \Psi_{\bar{\gamma}(t)})q_{22}(t) + \zeta_2) \qquad (5.12)$$

otherwise. This simple control strategy suffices to guarantee that all solutions with initial conditions in some prevalent set will converge to design flow in a near optimal fashion.

Theorem 5.3. *There exists an open set U, a constant R and a prevalent set $Y \subset X$ such that the control strategy given by equations (5.11) and (5.12) make all solutions of the viscous Moore-Greitzer equation, with initial conditions in Y, converge to the desired stable design flow.*

Proof: For $u = \gamma_1$, the only component in the basic attractor is the design flow at the starting point of $\xi_1 = \xi_1(0)$. Hence there exists a prevalent set $Y \subset X$ such that for all initial conditions in Y the solution will converge to $\xi_1(0)$. Let $U \subset X$ be an open neighborhood of $\xi_1(0)$. By making U smaller, we can make sure that the stall disturbance is as small as we please and that (Φ, Ψ) is as close to the starting point of the trajectory ξ_1 as we please before we start tracking the trajectory.

On the other hand, if there is no stall disturbance, i.e. if $\varphi = 0$, then by decreasing R we can track the trajectory ξ_1 as closely as we want. The feedback control is robust with respect to small disturbances, so as long as the stall disturbance stays small we can guarantee that we stay within a small neighborhood of the trajectory. It therefore only remains to show that small stall disturbances will remain small.

The energy method for equation (2.6) gives us that

$$\begin{aligned} \frac{1}{2}\frac{d}{dt}\|\varphi\|_1^2 &\leq -\nu\|\varphi_\eta\|_1^2 + \frac{1}{2\pi}\int_0^{2\pi} \psi_c'(\Phi+\varphi)\varphi_\eta^2 d\theta \\ &\leq \left(-\nu + \frac{1}{2\pi}\max_\theta \psi_c'(\Phi+\varphi)\right)\|\varphi\|_1^2. \end{aligned}$$

Here $\|\cdot\|_1$ is the Sobolev norm in $\bar{H}^1$. The trajectory ξ_1 lies to the right of the peak of the compressor characteristic and on that side the derivative of the characteristic is negative. By making Φ stay close enough to the trajectory and the L^∞ norm of φ small enough we can guarantee that the second term will be less than or equal to zero. The L^∞ norm is bounded by the $\bar{H}^1$ norm and as a result if (Φ, Ψ) stays close to the trajectory then small stall disturbances will decay. $\square$

One can clearly make the trajectory so that the point being tracked by the control will be moving in a smooth fashion. Furthermore, parameterizing the trajectory in a very slow manner approaches the adiabatic control construction which will guarantee that γ will be positive and bounded away from zero. This then guarantees that the control given will be a smooth function and the existence and regularity results mentioned in Chapter 1 still hold.

5.3.2 Modifications of Control Construction

The control construction given above is but one of many possible constructions. It could be beneficial to construct a regulator for the starting point of ξ_1 instead of just setting $u = \gamma_1$ or one could track a trajectory along the stall branch. The first extension is very simple, but the other one is not as trivial and we outline an approach to it here. The hard part lies in linearizing the system in the correct basis so that the problem reduces to a finite dimensional problem.

In Chapter 4 we proved that for specific parameter values when one linearizes the system about a stall solution there is a subspace of codimension 3 which is uncontrollable but stable for a large parameter range. The 3 dimensional subspace which can be influenced by the throttle parameter is spanned by the average flow, the pressure rise and one more vector which is given by $(\varphi^2 - \overline{\varphi^2}, 0, 0)$ where φ is the stall solution and $\overline{\varphi^2}$ represents the angular average of φ^2. One of the key elements of that proof was that a part of the linearized operator, the Lamé operator, given by

$$L = \nu \partial_{\eta\eta} + \psi_c'(\Phi + \varphi),$$

had two eigenvectors given by $\varphi^2 + a_1$ and $\varphi^2 + a_2$ and those two combined to give the vector that interacted with pressure rise and average flow.

Now let (φ, Φ, Ψ) be a general stall solution. Then the corresponding operator L will have one zero eigenvalue corresponding to translations of the soliton.

Proposition 5.4. *Assume that the self-adjoint operator L has two eigenvectors of the form $\chi^+ = \varphi^2 + k_1^+ \varphi + k_2^+$ and $\chi^- = \varphi^2 + k_1^- \varphi + k_2^-$ corresponding to distinct eigenvalues each with one dimensional eigenspace. Assume also that the spectrum has a simple zero eigenvalue and the rest of the spectrum is negative.*

Then the vMG equation linearized about the stall solution has an uncontrollable subspace $\mathcal{Q}$ of codimension 3 which is stable and $\mathcal{Q}^\perp$ is the span of $\{(\chi^+ - \overline{\chi^+}, 0, 0), (0, 1, 0), (0, 0, 1)\}$.

Here the overline represents the angular average as before.

Proof: We know from our previous stability results for the stall solution that the spectrum of the Lamé potential consists of five single eigenvalues and the rest of the spectrum is negative and double and converges to $-\infty$. Changing the Fréchet derivative ψ_c' a bit will be a relatively compact perturbation which will perturb the spectrum only slightly [42]. In particular, we can assume that the spectrum of L converges to $-\infty$.

Because (φ, Φ, Ψ) is a traveling wave solution of (2.6-2.8) and since the characteristic is a cubic polynomial we know that

$$\varphi_{\eta\eta} = a\varphi^3 + b\varphi^2 + c\varphi + d$$

for some constants a, b, c, d which depend on Φ. By completing the quadratures one can also show that φ satisfies the equation

$$\frac{1}{2}(\varphi_\eta)^2 = \frac{1}{4}a\varphi^4 + \frac{1}{3}b\varphi^3 + \frac{1}{2}c\varphi^2 + d\varphi + e$$

for some constant e. Using these two equations one can show that the two eigenvalues λ^+ and λ^- corresponding to the two eigenvectors χ^+ and χ^- are the real roots of

$$(c - \nu\lambda)(\frac{\nu\lambda}{3a} + \frac{c}{a} - \frac{2b^2}{9a^2}) - \frac{2bd}{3a} - 4e = 0$$

and we have

$$\begin{aligned} k_1^+ &= \frac{2b}{3a} = k_1^- \\ k_2^+ &= \frac{1}{c - \nu\lambda^+}(\frac{2bd}{3a} + 4e) \\ k_2^- &= \frac{1}{c - \nu\lambda^-}(\frac{2bd}{3a} + 4e). \end{aligned}$$

Notice that

$$\psi_c'(\Phi + \varphi) = \chi^+ + C = \chi^- + C'$$

for some constants C and C'.

Let $\phi \in H^1 \backslash \mathrm{span}\{\chi^+, \chi^-\}$ and define $\chi = \chi^+ - \overline{\chi^+} = \chi^- - \overline{\chi^-}$. Since eigenspaces corresponding to different eigenvalues are orthogonal and $\mathrm{span}\{\chi^+, \chi^-\} = \mathrm{span}\{\chi, 1\}$, we know that $\langle \phi, 1 \rangle = 0$ and thus $\phi \in \bar{H}^1$. Furthermore, since $\psi_c' \in \mathrm{span}\{\chi^+, \chi^-\}$, we have $\overline{\psi_c'}\phi = \langle \psi_c', \phi \rangle = 0$. We can now conclude that if ϕ lies in an eigenspace of L corresponding to the eigenvalue λ, then $(\phi, 0, 0)$ lies in an eigenspace of A corresponding to the same eigenvalue. Let $\mathcal{Q}$ be the subspace spanned by all such functions and notice that we have $A\mathcal{Q} \subset \mathcal{Q}$.

For any $\phi \in H^1 \backslash \mathrm{span}\{\chi^+, \chi^-\} \subset \bar{H}^1$, we have $(\phi, 0, 0) \in \mathcal{Q}$ and we can conclude that $\mathrm{codim}(\mathcal{Q})$ in $H^1 \times \mathbb{R}^2$ is 4. Since $\mathcal{Q} \subset \bar{H}^1 \times \mathbb{R}^2$, we can also conclude that $\mathrm{codim}(\mathcal{Q})$ in $\bar{H}^1 \times \mathbb{R}^2$ is 3. The orthogonal complement of $\mathcal{Q}$ is $\mathcal{Q}^\perp = \mathrm{span}\{(\chi^+ - \overline{\chi^+}, 0, 0), (0, 1, 0), (0, 0, 1)\}$ and one quickly verifies that $A\mathcal{Q}^\perp \subset \mathcal{Q}^\perp$. From all of the above we conclude that the spectrum of A is

$$\sigma(A) = \sigma(A|_{\mathcal{Q}}) \cup \sigma(A|_{\mathcal{Q}^\perp})$$

and that A is block diagonal. The block corresponding to $\mathcal{Q}$ is orthogonal to the control action and is therefore uncontrollable. We know that $\mathcal{Q}$ contains a one dimensional center subspace corresponding to direction of propagation of the stall solution and the rest of $\mathcal{Q}$ belongs to the stable subspace of A. $\square$

As a result of the above theorem, when one wants to track a parametrized curve of stall solutions, one only has to consider the projection of the linearized system onto the three dimensional space $\mathcal{Q}^\perp$. One therefore only needs to consider a 3×3 projection of the operator $Q(t)$.

Assume now that $0 < B \ll 1$ and that there exists only one stall component in the union attractor. Furthermore, assume that we want to operate the engine at a constant throttle parameter γ_0 for which design flow is stable. If γ_0 is small enough then there will be a unique stable stall solution ξ_0 corresponding to it. We know this by our analysis of the global attractor in Section 4.3. This stall solution is a member of a family of stall solutions and as we increase γ we will come to the value where the stall solution is created in a saddle-node bifurcation, see Figure 3.2. Let $\gamma_0(t)$ be a parameterization from γ_0 to that value. Corresponding to $\gamma_0(t)$ there is a curve of stall solutions $\xi_0(t)$. Now let $Q_0(t)$ and $\zeta_0(t)$ be the solutions of equations (5.7) and (5.8) respectively corresponding to $(\xi_0(t), \gamma_0(t))$ and let

$$\gamma(t) = \gamma_0(t) - \frac{1}{R} B^T(t)(Q_0(t)y(t) - \zeta_0(t)). \tag{5.13}$$

We can implement this control strategy before we implement the strategy constructed in the previous section and the following Theorem is immediate.

Theorem 5.5. *Let the assumptions above and those of Proposition 5.4 hold. Then there exists an open set U, a constant R and a prevalent set $Y \subset X$ such that the control strategy given by equations (5.13), (5.11) and (5.12) make all solutions of the viscous Moore-Greitzer equation, with initial conditions in Y, converge to the desired stable design flow.*

If the engine is operating in design flow with $\gamma = \gamma_0$ when a large disturbance occurs the system will converge to the stall solution ξ_0. It therefore makes sense to track a curve of stall cells that starts there.

Remark 5.6 Proposition 5.4 has some implications for nonaxisymmetric control actuation as well. If we assume control actuation that does not destroy this property of the equation, then the Proposition would indicate that the nonaxisymmetric component of the control action should be shaped like the vector $\chi = \chi^+ - \overline{\chi^+}$. This would move the state along the one parameter family of stall cells as opposed to try to push off of this strongly attracting surface.

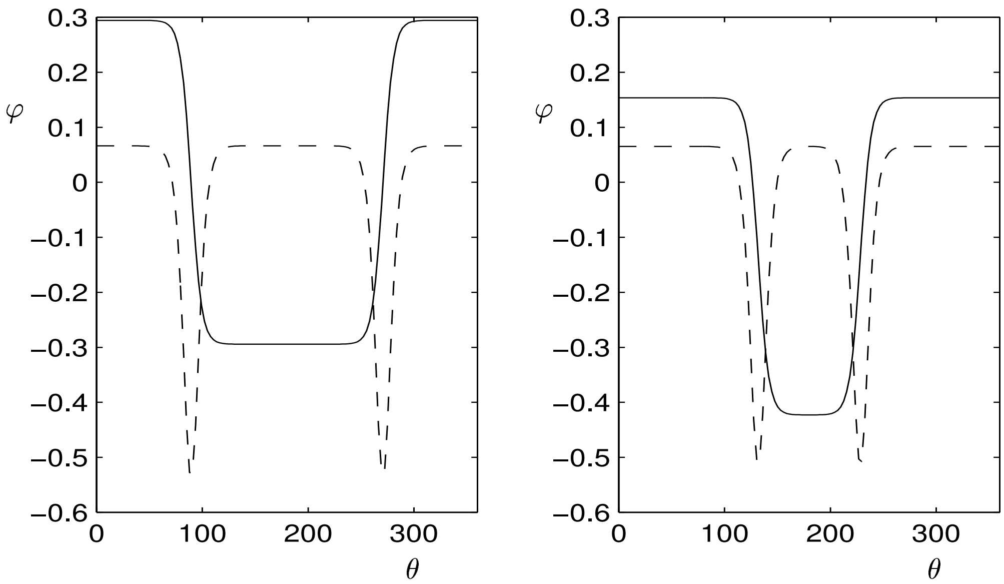

Figure 5.2: *The stall cell with solid line and the vector* χ *with dashed line for* $\gamma = \gamma_*$ *on the left and* $\gamma > \gamma_*$ *on the right.*

Figure 5.2 shows the stall cell and the vector χ for two different parameter settings, on the left for the specific parameter values chosen in [13] and on the right for a general parameter setting. This figure shows that the general characteristics of the vector χ are the same.

5.3.3 Numerical Simulations

Here we present some numerical simultions that display how our control (5.11-5.12) performs and its performance is compared with that of the backstepping control given by Banaszuk *et al.* [4]. For all of the simulations the initial condition is a small disturbance in the average flow and pressure rise, but a large disturbance in the stall direction.

Figure 5.3 shows the trajectory of the solution in the (Φ, Ψ)-plane when the basic controller is used. The large disturbance grows into a fully blown stall, but then design flow is recovered. Figure 5.4 shows the stall disturbance.

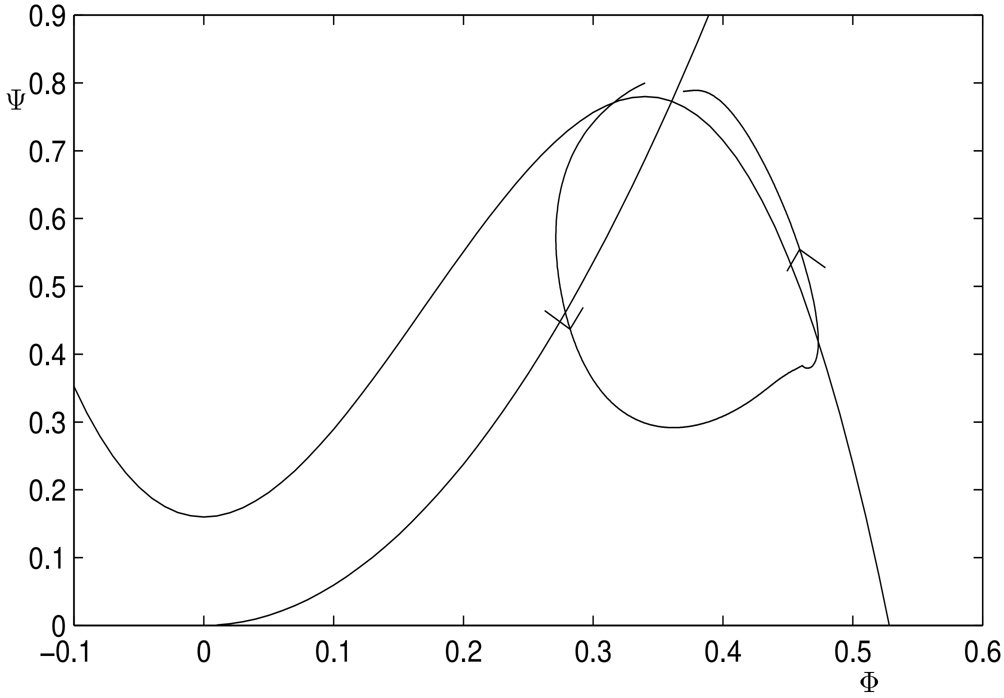

Figure 5.3: *The* (Φ, Ψ)*-phase plane for a stalling compressor under the basic control.*

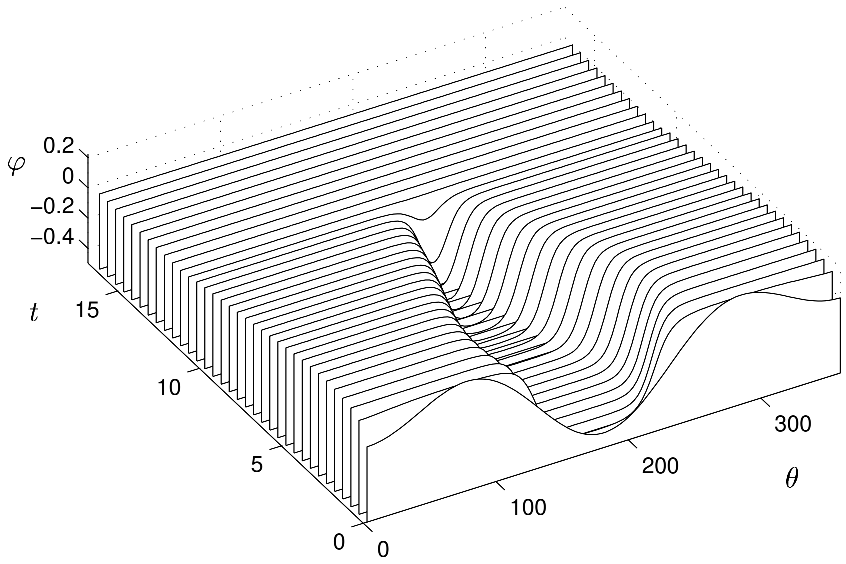

Figure 5.4: *The evolution of the stall disturbance under the basic control.*

The same simulation, but with the backstepping control is shown in Figure 5.5 and Figure 5.6.

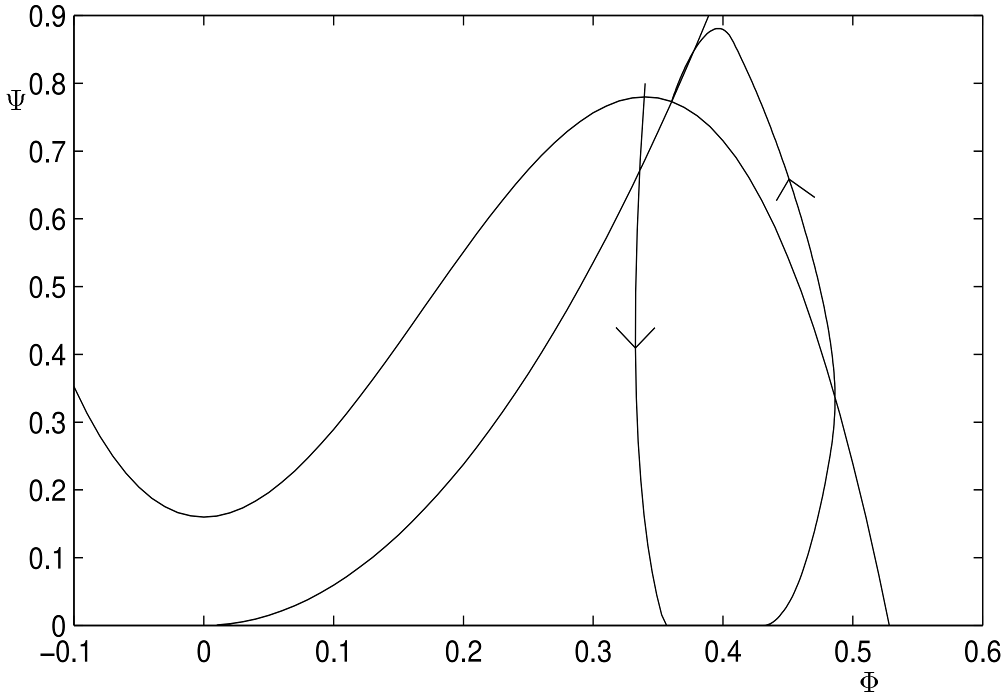

Figure 5.5: *The (Φ, Ψ)-phase plane for a stalling compressor under the backstepping control.*

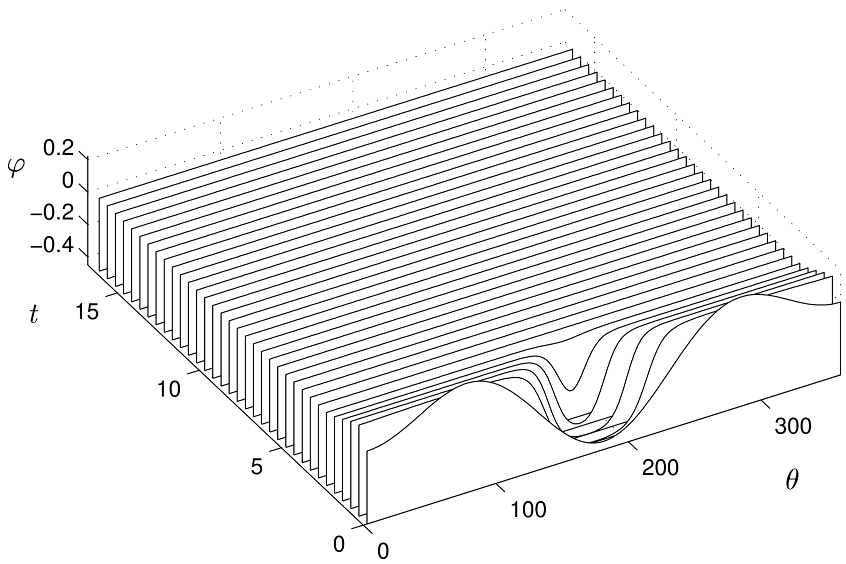

Figure 5.6: *The evolution of the stall disturbance under the backstepping control.*

It is clear from these Figures that the backstepping controller reacts much more forcefully to stall disturbances. It does recover the stall disturbance faster than the basic controller, but at the cost of dropping the pressure rise completely during part of the transient. The fundamental difference between the two control constructions here is that the backstepping controller doesn't take into account long time behavior of the system and tries to reduce the disturbance locally in time at all cost. The basic controller, however, uses the asymptotic dynamics and does not over react to disturbances that may be growing locally in time but will eventually decay. The time it takes the controls to recover design flow can be seen in Figure 5.7 which shows the pressure rise as a function of time for both control strategies.

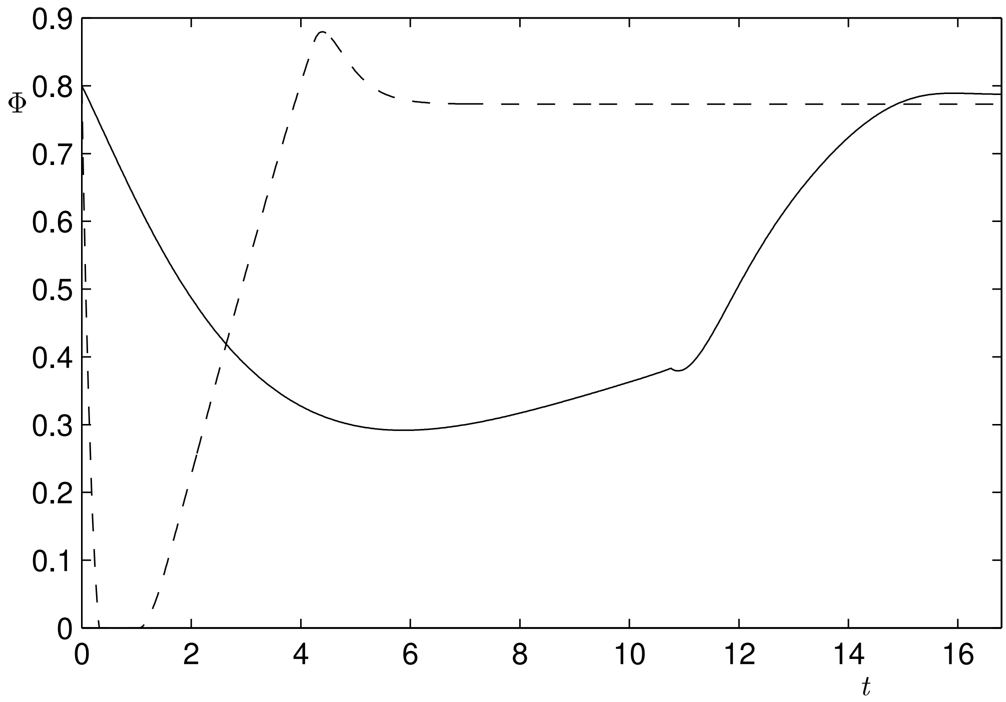

Figure 5.7: *The pressure rise as a function of time under basic control in solid line and backstepping control in dashed line.*

The control effort excerted by the two controllers is shown in Figure 5.8. This Figure shows particularly well that the control effort needed by the backstepping controller is greater than can be asked of physical actuators. The control effort is saturated so that $\gamma \in [0.01, 100]$. On the other hand the control effort needed by the basic control is reasonable. One could argue that the gain chosen for the stall component in the backstepping control construction should be decreased, but here we have set it at its smallest allowed level, or equal to $\sqrt{\pi/6}$ [4].

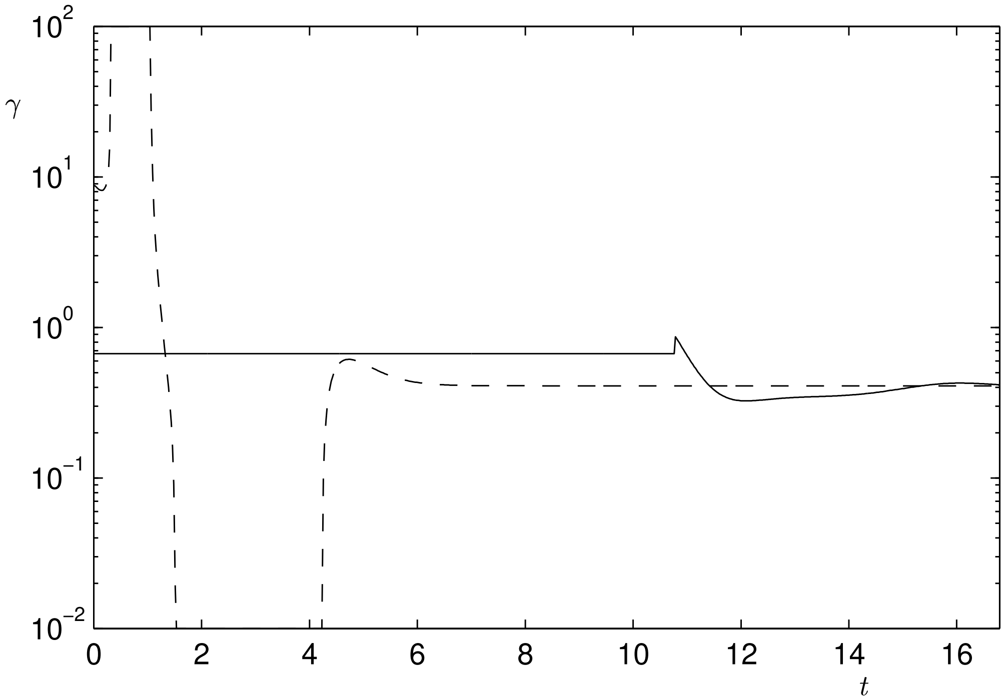

Figure 5.8: *The control effort γ as a function of time under basic control in solid line and backstepping control in dashed line.*

Surge is in general harder to control than stall. It requires more control effort and is a more violent instability. We present here the same sequence of figures as before, but now for a compressor that goes into surge.

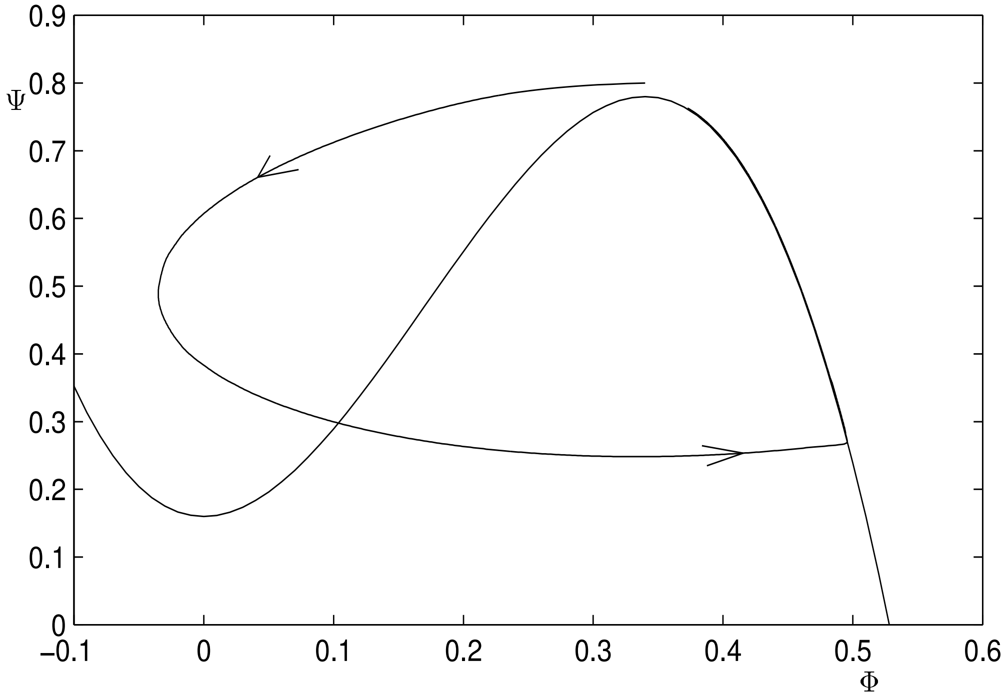

Figure 5.9: *The (Φ, Ψ)-phase plane for a surging compressor under the basic control.*

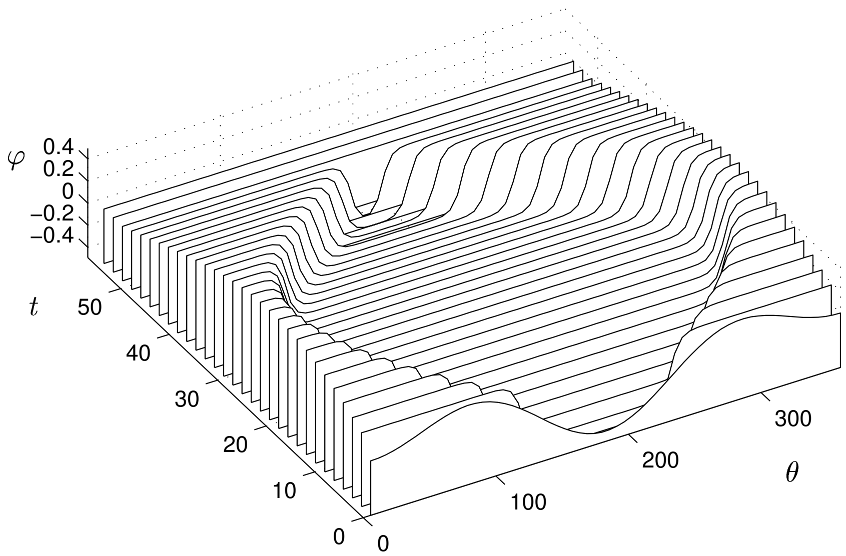

Figure 5.10: *The evolution of the stall disturbance under the basic control.*

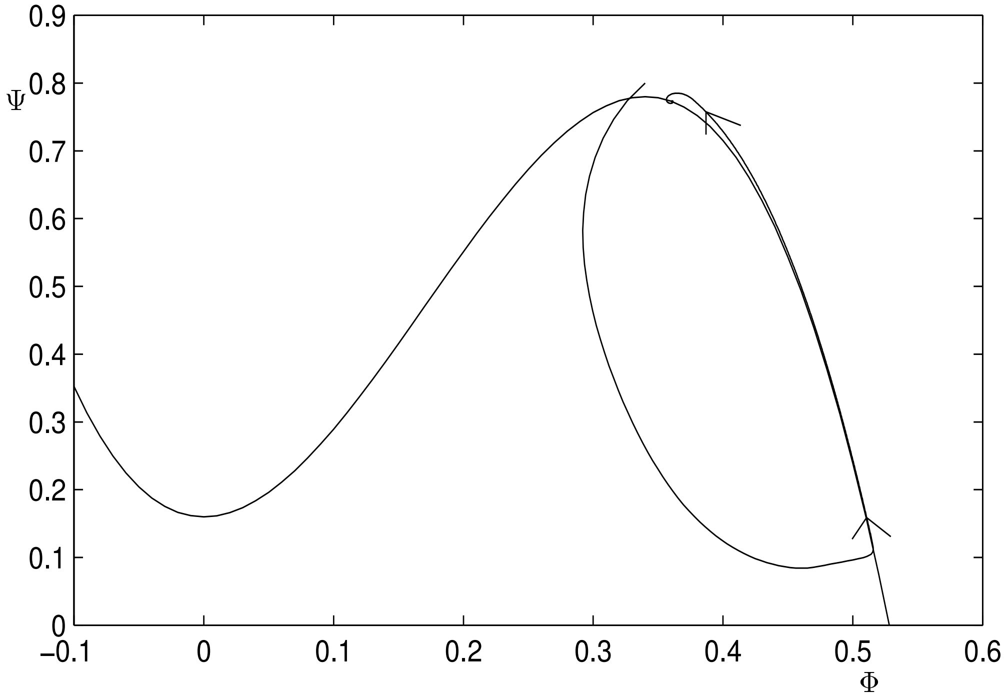

Figure 5.11: *The (Φ, Ψ)-phase plane for a surging compressor under the backstepping control.*

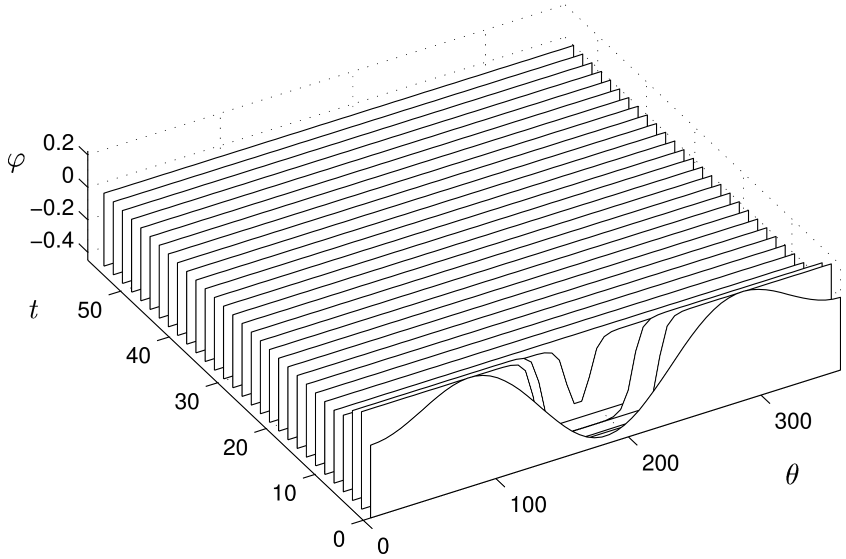

Figure 5.12: *The evolution of the stall disturbance under the backstepping control.*

Again the backstepping control strategy is recovers design flow faster than the basic control strategy as can be seen in Figure 5.13.

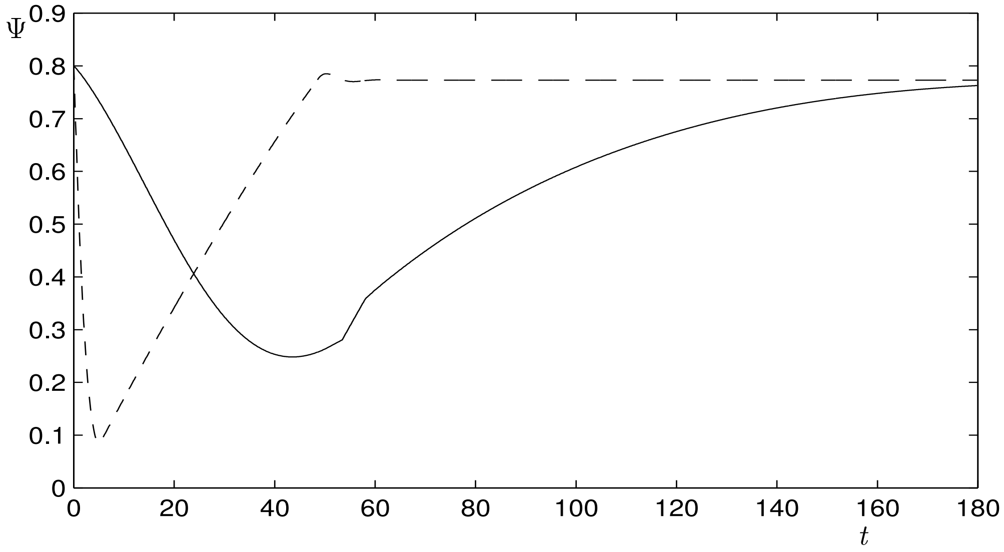

Figure 5.13: *The pressure rise during control of a surging compressor. The basic control is shown in a solid line and the backstepping control in a dashed line.*

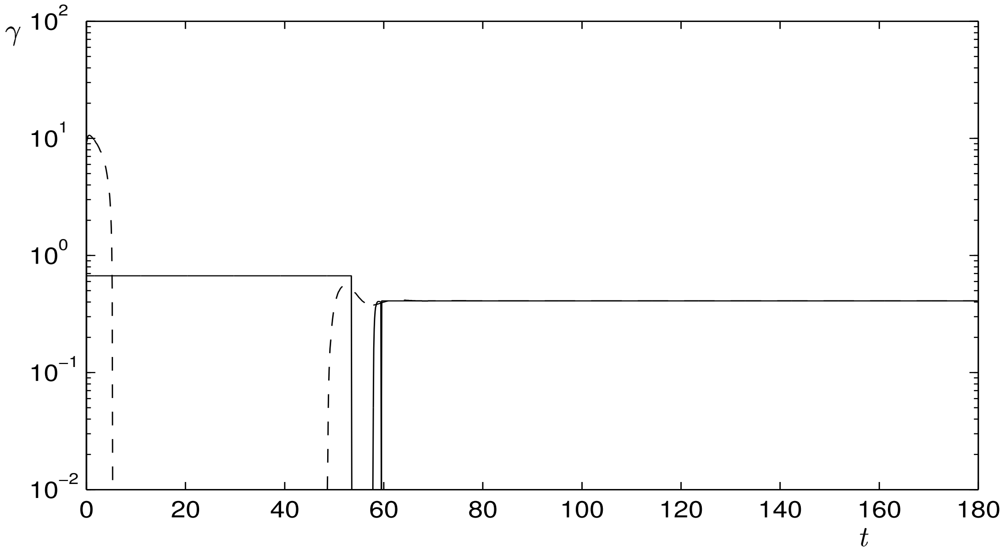

Figure 5.14: *The control effort during control of a surging compressor. The basic control is shown in a solid line and the backstepping control in a dashed line.*

As can be clearly seen on Figure 5.14, both control strategies saturate. This is due to the fact that surging compressors are harder to control and more control effort is needed.

These simulations show that the fundamental difference between the basic control and the backstepping control is that the latter does not take into account the asymptotic dynamics of the system and it reacts violently to all disturbances. The backstepping control does reduce the disturbances faster than the basic control, but at an unacceptable cost. The basic control uses the asymptotic dynamics and allows disturbances to run their course and die out with much less control effort.

5.4 Basic Controllability of the vMG Equation

We consider here the problem of when the vMG Equation is b-controllable. Although this problem is not of great practical importance it is more important theoretically to show that there exists at least one example of a system which is b-controllable.

Here above we have constructed a basic feedback control for design flow, see Theorem 5.3 and Theorem 5.5. In order to have b-controllability it therefore suffices to show that we can get from a small neighborhood of the design flow to any other component in the basic attractor. We have, however, the following Theorem.

Theorem 5.7. *If the global attractor of the vMG equation contains more than one stall component then the vMG equation with throttle control is not b-controllable.*

Proof: With only throttle control at our disposal, the only way we can influence the stall part of the equation is through Φ. Consider now a solution of the vMG equation such that $\varphi(0, \theta) = k \sin\theta$ for some non-zero constant k. If we consider only equation (2.6), then this is a time dependent parabolic equation for which it is well known that the number of local maxima and local minima is non-increasing in time. It is therefore not possible to start with this initial condition and use throttle control to get to a stall component which has more than one local maximum and one local minimum. In fact one can show that this is true for all initial conditions close enough to the one chosen here so the vMG equation is not b-controllable with throttle control. $\square$

From now on we will make the assumption that $0 < B \ll 1$. In this case we have given a complete description of the global attractor and it contains no surge solution. To label the components of the union attractor we denote the design flow component by $\mathcal{B}_0$ and the stall components by $\mathcal{B}_1, ...\mathcal{B}_n$. Further assume that we can influence the flow in a non-axisymmetric way by air injection in addition to throttle control. We will avoid the difficult issue of exactly how to model the air injection, but will instead make the following simple assumption.

Hypothesis I: If the flow at time t is axisymmetric, i.e. $\varphi(t, \cdot) = 0$, then by using the air injectors we can modify it so that for $j = 1, ..., n$ and some $\epsilon > 0$ small $\varphi(t, \cdot)$ will be non-zero, but small, $2\pi/j$ periodic and it will have exactly j local maxima and minima.

Theorem 5.8. *Let* $0 < B \ll 1$. *Given* Hypothesis I *and that we have throttle control, the vMG equation is b-controllable.*

Proof: Let x_0 be the design flow and let $j \in \{1, ..., n\}$. By using the air injectors we can make the solution at time ϵ be $2\pi/j$ periodic with exactly j local maxima and j local minima. Now set $\gamma = \gamma_*$. For this parameter setting, the global attractor consists of the stall components $\mathcal{B}_i$, design flow $\mathcal{B}_0$ and the connections from design flow to the stall solutions. The connection to the i-th stall solution is $2\pi/i$ periodic. Our solution, which is $2\pi/j$ periodic, must settle onto the global attractor and it can only settle onto the design flow or a stall solution which is $2\pi/k$ periodic, where $k = jm$ for some integer m. However, the number of maxima and minima of $\varphi(t, \cdot)$ is nonincreasing in time and thus m cannot be greater than one. Furthermore, the design flow is unstable with respect to $2\pi/j$ periodic disturbances so the solution cannot settle onto design flow. The only possibility remaining is that the solution settle onto the j-th stall solution $\mathcal{B}_j$.

We have now constructed a control which takes the design flow $\mathcal{B}_0$ to $\mathcal{B}_j$, in particular it takes the design flow to an open set U in the basin of attraction of $\mathcal{B}_j$. By continuity this control will take a small neighborhood V of the design flow into U. We have already constructed a throttle control which guarantees that for any initial condition we can get into V in finite time. We can thus get into U in finite time and the proof is complete. $\square$

Chapter 6

Conclusion

The study of the long time behavior of nonlinear partial differential equations has been increasingly popular in the last few decades and many beautiful results have been obtained. Researchers are, however, only just beginning to explore the different applications this theory has.

We have here analyzed the flow through the compression system of a jet engine in the setting of the viscous Moore-Greitzer model. The basic attractor has been constructed and, for a specific parameter range, the global attractor has been completely determined. Furthermore, we have found some practical applications for the knowledge we have gained about the long time behavior of the system. In particular, we have constructed a reduced order model which captures all of the essential dynamics of the original system, quantitatively as well as qualitatively. This applies both to long time behavior as well as transients between components on the attractor. We have also constructed a control law that makes the solutions for almost all initial conditions converge to the desired solution in the attractor. By utilizing the long time dynamics of the system, the control objective can be achieved with minimal control effort. Further extensions of this particular control construction were also suggested.

Like so many other research projects, this thesis raises more questions than it answers and opens up new venues of research. Can flutter and combustion instabilities be analyzed and controlled in a similar fashion? Is it possible to find similar reduced order models for other equations which permit solitary wave solutions? How does one generalize the control ideas here to a more general setting? The story is not completed, and it hopefully never will be.

Bibliography

[1] J.J. Adamczyk, W. Stevans, and R. Jutras. Supersonic stall flutter of high-speed fans. *Journal of Engineering for Power*, 104:675–682, 1982.

[2] R.A. Adomaitis and E.H. Abed. Local nonlinear control of stall inception in axial flow compressors. *29th Joint Propulsion Conference and Exhibit*, 1993. AIAA Paper 93–2230.

[3] A.V. Babin and M.I. Vishik. *Attractors of Evolution Equations.* Elsevier Science Publishers, Amsterdam, 1992.

[4] A. Banaszuk, H.A. Hauksson, and I. Mezić. A backstepping controller for a nonlinear partial differential equation model of compression system instabilities. *SIAM J. of Control and Optimization*, 1998.

[5] A. Banaszuk and A.J. Krener. Design of controllers for MG3 compressor models with general characteristics using graph backstepping. submitted.

[6] S.P. Banks. *State-Space and Frequency-Domain Methods in the Control of Distributed Parameter Systems.* Peter Peregrinus Ltd., 1983.

[7] R. L. Behnken, R. D'Andrea, and R. M. Murray. Control of rotating stall in a low-speed axial flow compressor using pulsed air injection: Modeling, simula-

tions, and experimental validation. In *Proc. 1995 Conference on Decision and Control*, pages 3056–3061, 1995.

[8] O. Bendiksen and P. Friedmann. Coupled bending-torsion flutter in cascades. *AIAA Journal*, 18:194–201, 1980.

[9] O. Bendiksen and P. Friedmann. The effect of bending-torsion coupling on fan and compressor blade flutter. *Journal of Engineering for Power*, 104:617–623, 1982.

[10] B. Birnir. An example of blow-up for the complex KdV equation and existence beyond the blow-up. *SIAM J. of Appl. Math.*, 47(4):710–725, 1987.

[11] B. Birnir. Global attractors and basic turbulence. In K.M. Spatschek and F.G.Mertens, editors, *Nonlinear Coherent Structures in Physics and Biology*, volume 329, New York, 1994. NATO ASI Series.

[12] B. Birnir and R. Grauer. The global attractor of the damped and driven sine-Gordon equation. *Comm. Math. Phys.*, 162:539–590, 1994.

[13] B. Birnir and H.A. Hauksson. The basic attractor of the viscous Moore-Greitzer equation. *To appear*, 1998.

[14] B. Birnir and H.A. Hauksson. The basic control of the viscous Moore-Greitzer equation. *To appear*, 1998.

[15] B. Birnir and H.A. Hauksson. Finite dimensional attractor of the Moore-Greitzer PDE model. *SIAM J. of Appl. Math.*, 1998.

[16] B. Birnir and H.A. Hauksson. The low-dimensional flow on the basic attractor of the viscous Moore-Greitzer equation. *To appear*, 1998.

[17] B. Birnir and K. Nelson. Attractors of nonlinear wave equations. *Preprint*, 1995.

[18] J.A. Burns and Y.R Ou. Feedback control of the driven cavity problem using LQR designs. In *Proceedings of the 33rd Conference on Decision and Control*, pages 289–294, 1994.

[19] B.D. Coller. Hopf/hopf interaction in compressor models. *Preprint*, 1996.

[20] P. Constantin and C. Foias. Global Lyapunov exponents, Kaplan-Yorke formulas and the dimension of the attractors for 2D Navier Stokes equations. *Comm. Pure Appl. Math.*, 38(1):1–27, 1985.

[21] P. Constantin, C. Foias, B. Nicolaenko, and R. Temam. *Integral Manifolds and Inertial Manifolds for Dissipative Partial Differential Equations*. Springer, 1989.

[22] F.E.C. Culick. Some recent results for nonlinear acoustics in combustion chambers. *AIAA Journal*, 32(1), 1994.

[23] I.J. Day. Axial compressor performance during surge. *Journal of Propulsion and Power*, 10(3):329–336, 1994.

[24] A. Debussche and R. Temam. Inertial manifolds and the slow manifolds in meteorology. *Differential and Integral Equations*, 4(5):897–931, 1991.

[25] J.F. Escuret and V. Garnier. Numerical simulations of aerodynamic flow instabilities in axial compressors. *Von Karman Institute for Fluid Dynamics: 1995-1996 Lecture Series*, 1996.

[26] K. M. Eveker, D. L. Gysling, C. N. Nett, and O. P. Sharma. Integrated control of rotating stall and surge in aeroengines. In *Sensing, Actuation, and Control in Aeropropulsion; SPIE 1995 International Symposium on Aerospace/Defense Sensing and Dual-Use Photonics*, 1995.

[27] H. Försching. Aeroelastic stability of cascades in turbomachinery. *Prog. Aerospace Sci.*, 30:213–266, 1994.

[28] S. Glavaski. *KL analysis of the vMG equation - personal communication*, 1998.

[29] R. Grauer and B. Birnir. The center manifold and the bifurcations fo the sine-Gordon breather. *Physica D*, 56:165–184, 1992.

[30] E.M. Greitzer. Surge and rotating stall in axial flow compressors, Part II. *Trans. ASME, Journal of Engineering for Power*, pages 199–217, 1976.

[31] J. Guckenheimer and P. Holmes. *Nonlinear Oscillations, Dynamical Systems, and Bifurcations of Vector Fields.* Springer, 1983.

[32] D.L. Gysling, M.R. Myers, and C.N. Nett. *Private communication*, 1995.

[33] G. Hagen, K. Zhang, B. Bamieh, and I. Mezić. Control of axial compressors via air injection. *Preprint*, 1998.

[34] J.K. Hale. *Asymptotic Behavior of Dissipative Systems.* American Mathematical Society, 1988.

[35] J.M. Haynes, G.J. Hendricks, and A.H. Epstein. Active stabilization of rotating stall in a three- stage axial compressor. *ASME Journal of Turbomachinery*, 116:226–239, 1994.

[36] D. Henry. *Geometric Theory of Semilinear Parabolic Equations.* Springer, 1981.

[37] C. Hermite. *Oeuvres de Charles Hermite*, volume 3. Paris: Gauthier-Villar, 1912.

[38] J.S. Humbert and A.J. Krener. Analysis of higher order Moore-Greitzer compressor models. *IEEE Conference on Control Applications*, 1997.

[39] B.R. Hunt, T. Sauer, and J.A. Yorke. Prevalence: A translation-invariant "almost every" on ininite-dimensional spaces. *Bull. of the Am. Math. Soc.*, 27(2):217–238, 1992.

[40] E.L. Ince. *Ordinary Differential Equations.* Dover, 1956.

[41] C.K.R.T. Jones. *Geometric Singular Perturbation Theory.* C.I.M.E. Lectures, Session on Dynamical Systems, 1994.

[42] T. Kato. *Perturbation Theory for Linear Operators.* Springer, 1980.

[43] A.J. Krener. The feedbacks that soften the primary bifurcation of mg3. preprint.

[44] M. Krstic, J.M. Protz, J. D. Paduano, and P. Kokotovic. Backstepping design for jet engine stall and surge control. In *Proc. 1995 Conference on Decision and Control*, pages 3049–3055, 1995.

[45] M. Krstic and H. Wang. Modeling and control of deep-hysteresis aeroengine compressors. preprint.

[46] O.A. Ladyzhenskaya. *The Mathematical Theory of Viscous Incompressible Flow.* Gordon and Breach, New York, 1969.

[47] D.F. Lawden. *Elliptic Functions and Applications.* Springer, 1989.

[48] D.C Liaw and E.H. Abed. Active control of compressor stall inception: a bifurcation theoretic approach. *Automatica*, 32:109–115, 1996.

[49] E. Lieb. On characteristic exponents in turbulence. *Comm. Math. Phys.*, 92:473–480, 1984.

[50] J.L. Lions. *Optimal Control of Systems Governed by Partial Differential Equations.* Springer, 1971.

[51] W. Magnus and W. Wrinkler. *Hill's Equation.* Willey-Interscience, 1966.

[52] R. Mane. In D.A. Rand and L.S. Young, editors, *Dynamical Systems and Turbulence*, New York, 1980. Springer.

[53] C. A. Mansoux, D. L. Gysling, J. D. Setiawan, and J. D. Paduano. Distributed nonlinear modeling and stability analysis of axial compressor stall and surge. In *Proc. American Control Conference*, pages 2305–2316, 1994.

[54] M. Marion and R. Temam. Nonlinear galerkin methods. *Journal of Numerical Analysis*, (5):1139–1157, 1989.

[55] F.E. McCaughan. Numerical results for axial flow compressor instability. *ASME Journal of Turbomachinery*, 111:434–441, 1989.

[56] F.E. McCaughan. Bifurcation analysis of axial flow compressor stability. *SIAM Journal of Applied Mathematics*, 50:1232–1253, 1990.

[57] I. Mezić. A large-scale theory of axial compression system dynamics. *preprint*, 1998.

[58] J. Milnor. On the concept of attractor. *Communications in Mathematical Physics*, 99:177–195, 1985.

[59] F.K. Moore and E.M. Greitzer. A theory of post-stall transients in axial compression systems:Part 1 - Development of equations. *ASME Journal of Engineering for Gas Turbines and Power*, 108:68–76, 1986.

[60] AGARD Manual on. *Aeroelasticity in Axial-Flow Turbomachines, Volume 1(1987); Unsteady Turbomachinery Aerodynamics, Volume 2(1988).* AGARDograph No. 298, 1988.

[61] V.A. Pliss and G.R. Sell. Approximation dynamics and the stability of invariant sets. *IMA preprint series #1393*, 1996.

[62] G. Raugel and G.R. Sell. Navier-Stokes equations on thin 3d domains i: Global and local attractors. *IMA volumes in Mathematics and its applications*, 55:137–163, 1993.

[63] G. Raugel and G.R. Sell. Navier-Stokes equations on thin 3d domains i: Global attractors. *AHPCRC preprint 90-04, J. Amer. Math. Soc.*, 6:503–568, 1993.

[64] G. Raugel and G.R. Sell. Navier-Stokes equations on thin 3d domains i: Global regularity. *AHPCRC preprint 92-062, Proc. College de France*, 1993.

[65] D. Ruelle. "Large volume limit of distribution of characteristic exponents in turbulence". *Comm. Math. Phys.*, 87:287–302, 1982.

[66] D. Ruelle. "Characteristic exponents for a viscous fluid subjected to time-dependent forces". *Comm. Math. Phys.*, 92:285–300, 1984.

[67] A.P. Sage and C.C. White. *Optimum Systems Control*. Prentice Hall, 2 edition, 1977.

[68] R. Sepulchre and P. Kokotovic. Shape signifiers for control of surge and stall in jet engines. preprint.

[69] R. Temam. *"Infinite-Dimensional Dynamical Systems in Mechanics and Physics."*. Springer, 1988.

[70] P. Du Val. *Elliptic Functions and Elliptic Curves*. Cambridge University Press, 1973.

[71] D.S. Whitehead. Bending flutter of unstalled cascade blades at finite deflection. *ARC R&M 3386*, 1962.

[72] D.S. Whitehead. Torsional flutter of unstalled cascade blades at zero deflection. *ARC R&M 3429*, 1964.

[73] A.G. Wilson and C. Freeman. Stall inception and development inan axial flow aeroengine. *Trans. ASME, Journal of Turbomachinery*, 116:216–225, 1994.